CARRIER SYNCHRONIZATION IN A DIGITAL RADIO SYSTEM

CARRIER SYNCHRONIZATION IN A DIGITAL RADIO SYSTEM

by

D. CHEUNG

A Thesis

Submitted to the Faculty of Graduate Studies

in Partial Fulfilment of the Requirements

for the Degree

Master of Engineering

McMaster University

April 1976.

Master of Engineering(1976) McMaster University
(Electrical Engineering) Hamilton, Ontario

TITLE: Carrier Synchronization in a Digital Radio System

AUTHOR: David Cheung
B.Eng.(McMaster University,1974)

SUPERVISOR: Dr. D.P.Taylor

NUMBER OF PAGES: 142

ABSTRACT

The problem of coherent carrier recovery and the effects of phase error on the performance of an offset quadrature-phase-shift-keying (QPSK) duobinary system have been investigated in the thesis. The system of interest is similar to RD-3 digital system that is being developed and installed as an efficient high data-rate digital radio communication system by Bell Northern Research Laboratory (BNR).

Four carrier regeneration loop structures are investigated and analysed in the thesis. These are:

(i) estimate-aided suppressed carrier loop

(ii) decision-directed feedback loop

(iii) shifted decision-directed feedback loop

(iv) half-shifted decision-directed feedback loop

All of these loop structures employ the technique of data-aided carrier synchronization. The estimate-aided loop structure exhibits steady-state behavior similar to that of a conventional Costas loop. The remaining three loop structures differ from the estimate-aided loop in the sense that they require decisions to make on the noisy received signal. These are then fedback to the carrier recovery circuit in such a way as to create a spectral line at carrier frequency. The loop behavior in the presence of additive noise has been investigated in some detail. For each loop, analytical expressions for the phase detector characteristic (S-curve) and the steady-state phase error probability density function (pdf) are derived, and provide a means

of comparing the performance of the different recovery schemes.

ACKNOWLEDGEMENTS

It is a pleasure to acknowledge my gratitude to my research sepervisor, Dr. D.P.Taylor of the Department of Electrical Engineering. Dr. Taylor suggested the problem, and his encouragement and friendly guidance in the way of research made the work a rare educational experience.

I would also like to express my appreciation to others who helped:

To the National Research Council of Canada which provided financial support in the form of scholarships and research grants;

To Dr. Chan of Communication Research Laboratory who gave discussions in computer simulation;

To Mr. P.Hetrakel who gave useful discussions in this work;

To Mr. C.W.Law for proof-reading the thesis.

TABLE OF CONTENTS

LIST OF ILLUSTRATIONS

CHAPTER 1

INTRODUCTION

1.1 Introduction

Since the 1950's, microwave radio has proven to be a very economical system for long distance signal transmission. As a result it has become the most widely used means of long distance point-to point communication. At the present time, microwave radio is primarily operated in the analog mode where the baseband communications signals are modulated in analog form onto a radio-frequency carrier wave for transmission. In North America, such systems operate at carrier frequencies near 4 and 6 GHz. In the modulation process, the amplitude, frequency or phase angle of the carrier is continuously varied as a function of the instantaneous value of the modulating signal. At the receiving end this signal is recovered by the reverse process of demodulation. In this continuous or analog mode the receiver output signal may be regarded as an estimate of the original transmitted signal.

Today, however, there is a trend toward the use of digital microwave radio transmission [12]. Two of the main reasons for this trend are the cost advantages realizable using digital hardware and multiplexing, and the ease with which digital systems can be expanded to accomodate future communications traffic growth. In digital transmission discrete valued digital signals are used to modulate the high-frequency carrier, and at the receiver, after demodulation the output may be regarded as a sequence of decisions.

In addition there are several other reasons why digital radio communication is attractive. First, we can regenerate noiseless digital signals at every repeater site along the route thus avoding cumulative performance

degradation due to a large number of amplifiers, each of which contributes noise and distortion. Second, digital multiplexing allows some electronic circuits to be shared by several channels, and thus cost less than equivalent analog multiplexing arrangements. Third, baseband digital transmission systems are seeing increasing usage in short haul connection between telephone central offices. Digital radio offers a great advantage in facilitating the interconnection of these digital systems with the long haul (trans-Canada) transmission network. Because the baseband digital signals can be transmitted without conversion to analog form, they do not need to be demultiplexed and converted to analog signals first and then multiplexed again for transmission on the analog microwave network, but can be modulated directly onto the digital radio carrier.

A further advantage is that signals from different origins, e.g. television signals, data signals and audio signals, can be mixed using the digital facilities [23][26]. The interface between the digital system and the analog system is made by digital terminals which convert the incoming analog signals to a digital form suitable for use on a digital transmission facility. Digital multiplexers then form the interface between digital transmission facilities of different rates. They combine signals from many digital lines by the process of interleaving, or time-division multiplexing and bring all signals to a synchronous rate. The advantage is that it is relatively easy to have a hierachical multiplexing structure. The receiving portion of the terminal just performs the inverse of the transmitting portion functions, and in many respects is a duplicate of the transmitter portion.

1.2 The Canadian Digital Radio System

The digital radio system we are investigating here is the one that will operate in Canada starting in 1978. The system will, for economic reasons, be overbuilt on the analog radio network in order to utilize the existing repeater sites which are spaced about every 30 miles and cover most of the country. The digital system will operate in a 500 MHz band at a carrier frequency of approximately 8 GHz. The choosing of this frequency range is dictated by the fact that the radio frequency bands from 7.725 to 7.975 GHz and from 8.025 to 8.275 GHz are available and the existing microwave antennas (horn reflector attennas with circular waveguide which are usable from 3.5 to over 11 GHz) can be used to decrease the requirement on new equipment. The complete planned digital system will carry six two-way radio channels, each using about 41MHz of bandwidth.

In order to maximize the available channel capacity and to be economically competitive with existing analog systems, the digital system is designed to transmit two DS3 carrier groups in a 45 MHz bandwidth. A DS3 carrier group is a 44.7 Mbit/sec digital signal. The transmission will be achieved using a technique which is called duobinary coding. In this code each transmitted data symbol is made dependent not only on the present data bit but on the previous one as well. This deliberate correlation of symbols has the effect of concentrating the signal power in a narrower frequency range closer to the carrier frequency. It has been shown that the use of duobinary coding approximately doubles the efficiency of use of the available frequency spectrum [24]. This allows one 44.7 Mbit/sec DS3 signal to be accomodated in less than a 45 MHz

bandwidth. By combining the duobinary encoding which can be done at baseband with the use of 4 phase coherent phase-shift-keying (CPSK) modulation it is then possible to put 2 DS3 signals or approximately 90 Mbits/sec into a 45 MHz bandwidth. The resulting system thus has an available capacity of 1344 voice circuits corresponding to an overall bit rate of 91.040 Mbits/sec.

The particular combination of duobinary encoding and 4-phase CPSK modulation results in a transmitted signal which is partially amplitude and partially phase modulated. This is due to the fact that the duobinary encoder produces 3-level symbols (nominally +2,0,-2) with a nonrectangular pulse shape. To accomplish the 4-phase modulation the input data is split into two streams, each at approximately 45 Mbits/sec. These two streams are separately differentially encoded, duobinary encoded and finally used to amplitude modulate two carrier signals which are in phase quadrature with each other. In addition the signals in the two streams are offset by 1/2 bit (at 45 Mbits/sec) with respect to each other. The resulting system is thus an offset quaternary, phase-shift-keying, duobinary (Offset QPSK duobinary) system.

At the receiver the signal is, as with virtually all high speed data signals, coherently detected. To successfully transmit information through a phase-coherent communication system, the receiver must be capable of determining and tracking the instantaneous phase of the received signal with as little error as possible. The transmitted data-bearing signal can be modulated onto a carrier in such a way that a residual carrier component exists in the overall signal power spectrum. This component can be tracked at the receiver with a narrowband phase-locked loop (PLL) and used to provide the desired reference

signal for coherent demodulation. This situation has been analyzed in some detail (e.g. Viterbi [22], Stiffler [21], and Lindsey [19]). However, the power contained in this residual carrier component contains only information about the phase and frequency of the carrier, and thus represents transmitter power which is not available for the transmission of data. In order to maximize the data power and therefore minimize the receiver probability of error, the data are often modulated onto a carrier in such a way that the transmitted signal has zero average power at the carrier frequency. Coherent demodulation of such a signal then requires some type of suppressed-carrier recovery circuit or tracking loop for establishing a coherent carrier reference for use in demodulating the data.

A number of methods [19-21] have been proposed for generating a reference carrier from a suppressed carrier received signal. One of these methods involves the principle of a decision-directed feedback loop [28]. Recently, a tracking loop utilizing this principle for establishing an accurate phase reference at the receiver has been developed and analyzed by Lindsey and Simon [9], and is known as a data-aided carrier tracking loop. In their loop structure, the outputs of data detectors are fed back and used to remove the data modulation from the received signal in such a way as to leave a carrier component which can be tracked by a phase-locked loop structure.

The offset QPSK duobinary system being considered in this thesis utilizes suppressed carrier modulation. In order to recover a coherent carrier component from this signal, a number of suppressed-carrier tracking loop structures which utilize the principle of data(estimate or decision) feedback are

suggested for use in generating coherent quadrature reference signals for use in data demodulation. The data-aided carrier tracking loop proposed by Lindsey and Simon has been considered without including the effects of inter-symbol interference (ISI) (caused by bandlimiting and /or data correlation) in the analysis of its operation. In [5], ISI is included in the analysis of loop operation, but a residual carrier component is assumed to be present, so the carrier could also be tracked with a conventional phase-locked loop. Following these applications which consider only binary phase modulated carriers, Lindsey and Simon have proposed decision-feedback loops which reconstruct coherent carrier references for the detection of polyphase signals [10]. Later, the decision-feedback loop which tracks a quaternary-phase-shift-keying (QPSK) signal was modified to accomodate a quaternary-amplitude-shift-keying (QASK) signal[6] and offset QPSK signal [7]. In this thesis, we will investigate the problem of carrier synchronization for the offset QPSK duobinary system proposed for use in digital microwave radio. Specifically, we will consider the design of data (estimate or decision) feedback loop structures to recover a coherent carrier from the offset QPSK duobinary signal.

1.3 Scope of the Thesis

The outline of the thesis is as follows. In chapter 2, we perform a basic performance analysis of the offset QPSK duobinary system. An expression for the average probability of system error conditioned on a fixed carrier phase error, namely $P_e(\phi)$, is derived. An upper bound on $P_e(\phi)$ and an approximation technique are also developed. Simulation results for the system performance as a function of steady state phase error are presented and comparisons are made. In chapter 3, we propose an estimated data feedback loop structure

for carrier recovery and investigate its steady-state loop phase detector characteristic. In chapter 4, we investigate a decision-directed feedback loop. In chapter 5, we investigate two modified decision-directed feedback structures which yield improved performance compared to the basic structure described in chapter 4. In chapter 6, we draw conclusions from the study, and make some suggestions for further work.

CHAPTER 2

DIGITAL RADIO SYSTEM

2.1 Introduction

The system under study is an offset duobinary quaternary-phase-shift-keying (QPSK) system which may be used for digital radio communication [23]. A block diagram of this system in a radio communication environment is shown in Fig 1. The transmitter consists of a precoder which differentially encodes the data, a balanced quadrature modulator and a duobinary [illegible] filter. The receiver consists essentially of a coherent demodulator and decoder. The advantages of choosing a duobinary filter are studied in this chapter. Two possible system models, which specify how the duobinary pulse-shaping filters are apportioned between the transmitter and the receiver are considered. Model 1 is arranged so that the shaping is optimally [1] distributed between the transmitter and the receiver for a wideband additive noise channel. Model 2 is a more realistic arrangement where the transmitter filter completely determines the duobinary pulse shape and hence the shape of the overall frequency response and the receiver filter merely bandlimits the noise, and has no effect on the signal component. The two system models are shown in Fig 2. The differential encoder used in this system is for precoding purposes. It allows the error propagation phenomenon common to all partial response systems to be avoided and hence leads to a simplification of the decoder structure.

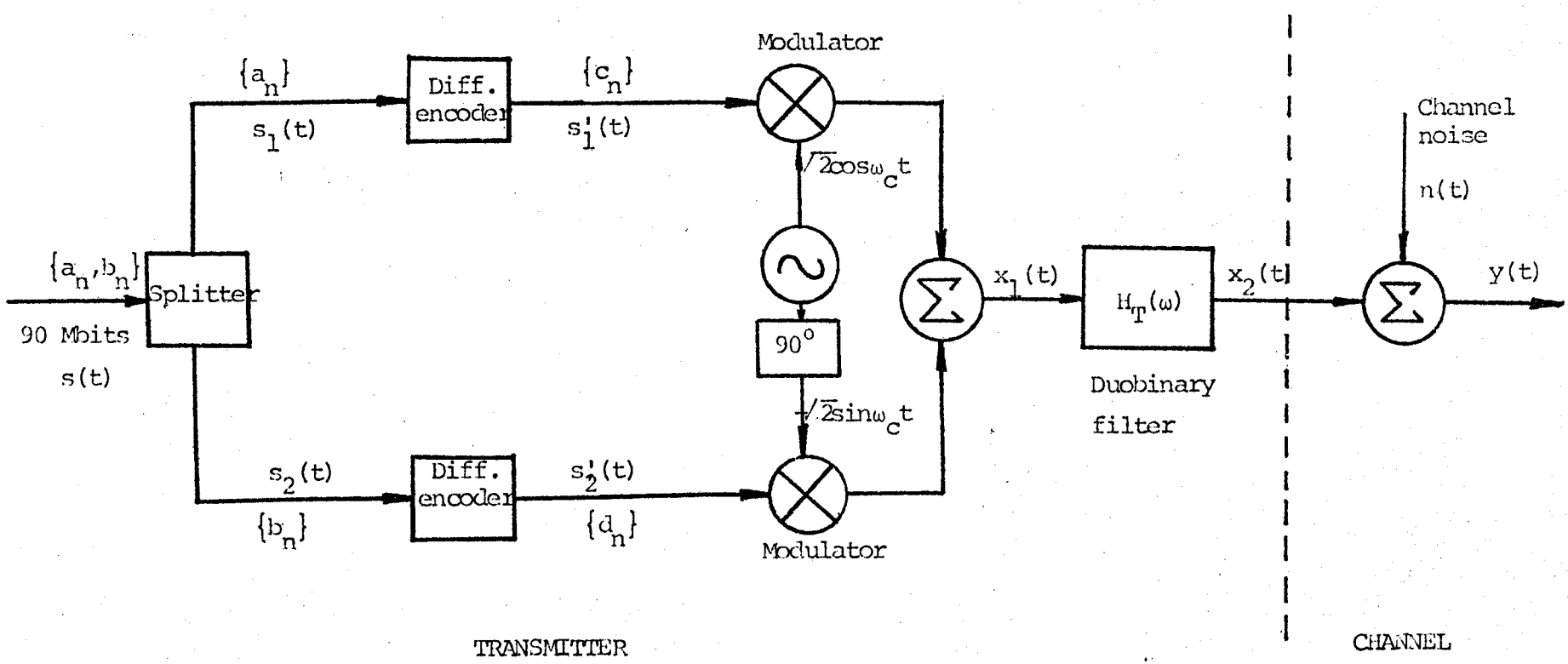

Fig. 1a Offset QPSK duobinary system model

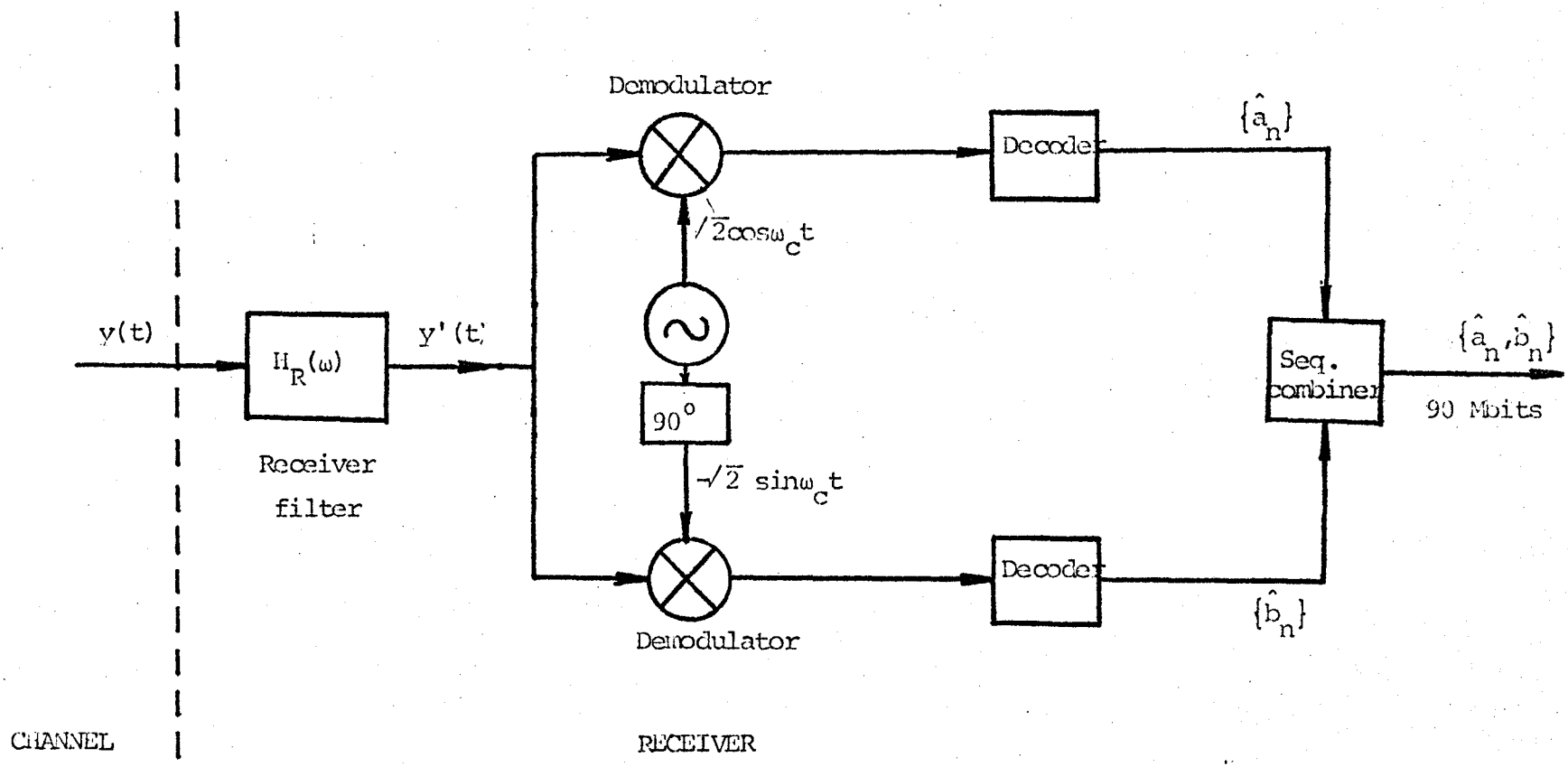

Fig.1b Offset QPSK duobinary system model.

Because of the frequency instabilities in high-frequency radio, it is sometimes difficult to obtain carrier synchronization with sufficiently low jitter to preclude significant detection loss. This problem has been investigated by Rhodes [4] for offset quaternary-phase-shift-keying (offset QPSK) signals. Gitlin and Ho [11] later investigated the same problem for staggered quadrature amplitude modulation (SQAM) system. The degradation due to carrier phase error for the offset QPSK duobinary system is studied in the last part of this chapter. A general expression for an upper bound on the average probability of symbol error is obtained. also system performance in the presence of a steady-state phase error and additive Gaussian noise is simulated on the computer.

2.2 System Model

2.2.1 Duobinary concept

The duobinary technique is an encoding technique which permits signalling at twice the Nyquist rate. "Duo" indicates that the bit capacity of a straight-binary system can be doubled. This concept was first introduced by Lender [24].

The coding technique is illustrated by the following example. Consider two sequences of digits. The first sequence a_n can be +1 or -1 with $p(+1)=p(-1)=1/2$ where p denotes probability. The second sequence b_n can be +2, 0, or -2. To transform the a_n into the b_n sequence, we form each b_k by adding each a_k to the previous digit a_{k-1} as shown below

a_n	(-1)	-1	-1	-1	1	1	-1	-1	1	1
b_n		-2	-2	-2	0	2	0	-2	0	2

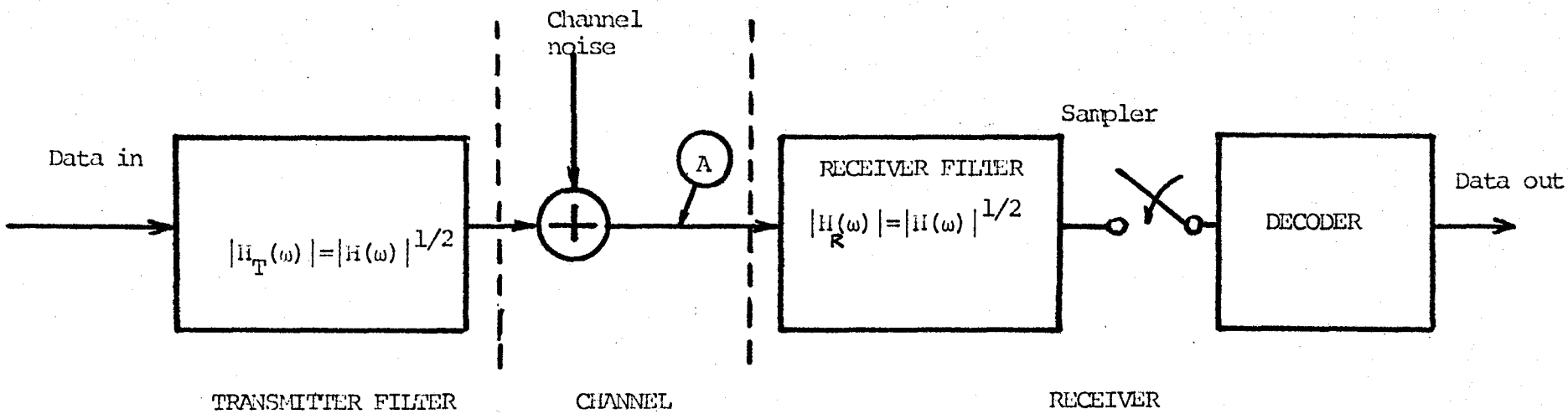

(a)

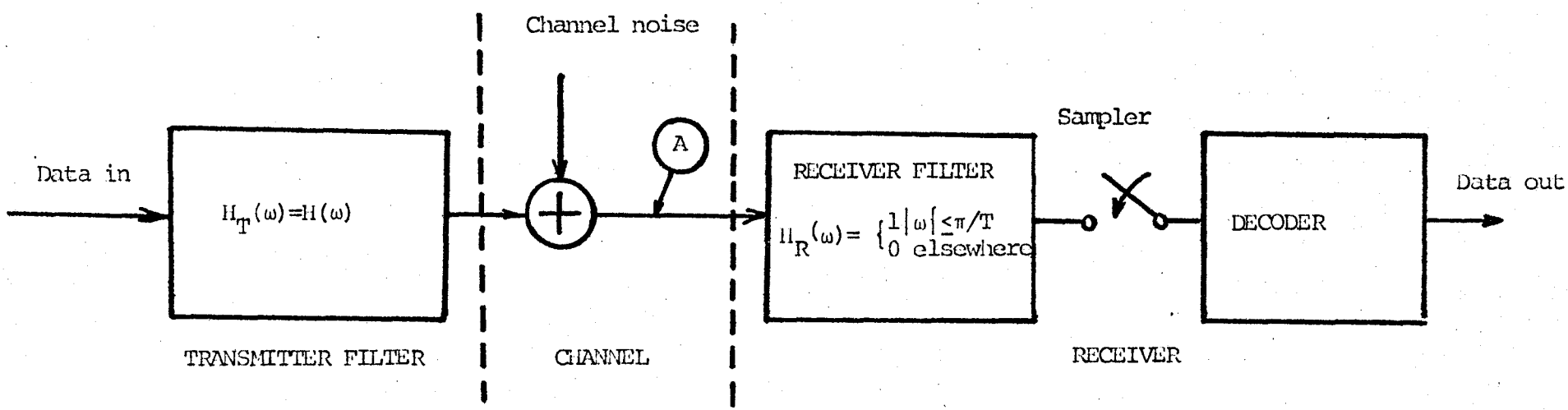

(b)

Fig.2 Partial-response system models

(a) Model 1 (b) Model 2

We note that in two successive time slots, it is impossible for the b_n sequence to transit from +2 to -2, or vice versa. This coding technique compresses the bandwidth of the sequence a_n by a factor of 2. This transformation or encoding can also be accomplished by a kind of filter, known as a duobinary filter. The duobinary pulse-shaping filter has the impulse response

$$h(t) = \frac{4}{\pi} \left(\frac{\cos(\pi t/T)}{1 - 4t^2/T^2} \right) \qquad (2.1a)$$

with the corresponding transfer function

$$H(\omega) = \begin{cases} 2T\cos(\omega T/2) & |\omega| \leq \pi/T \\ 0 & \text{elsewhere} \end{cases} \qquad (2.1b)$$

as illustrated in Fig 3, where T^{-1} is the signalling rate. It may observed that if this impulse response is sampled at time $t=-T/2$, then

$$h_n = h(t+nT) = \begin{cases} 1 & n=0,1 \\ 0 & \text{otherwise} \end{cases}$$

and thus intersymbol interfenence can arise only from the preceding symbol, that is in the absence of noise

$$b_k = a_k + a_{k-1} \qquad (2.2)$$

If a_k can assume the two possible values ± 1 as stated previously, then b_k has the three values ± 2 and 0. Thus the binary input to the system has been converted to a three-level output. Equation (2.2) can also be used to decode the data. Once a_{k-1} is decided, its effect on b_k can be eliminated by subtraction, and a_k can be decided. The details and advantages of this encoding technique have been discussed in [18][24]. In the next section, we will perform the basic system analysis, and the coding process

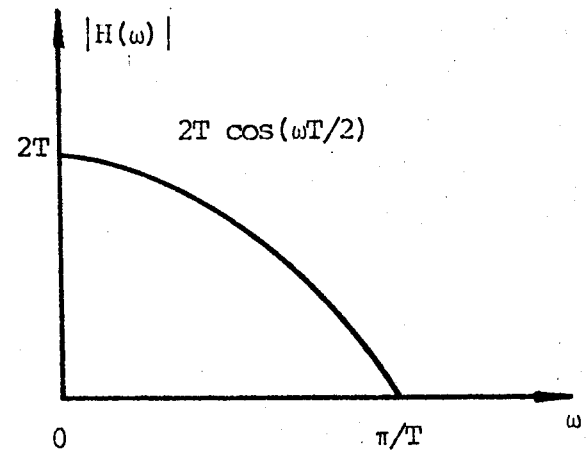

(i) TRANSFER FUNCTION

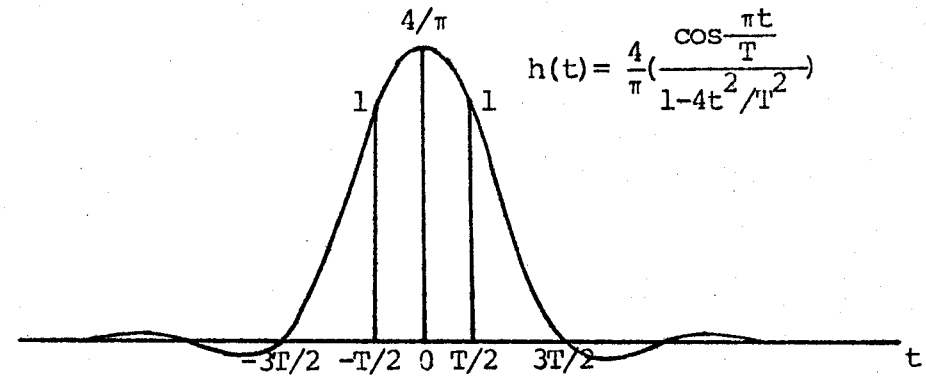

(ii) IMPULSE RESPONSE

Fig.3 Duobinary filter transfer function and impulse response

using a duobinary pulse shaping filter will be discussed in more detail.

2.2.2 Basic analysis

The complete system is shown in Fig 1. The input message s(t) is periodic and consists of a random sequence of binary bits. Each bit is spaced T seconds apart, corresponding to a signalling speed of 1/T baud. The 90 Mbit signal, which is the signalling speed we are interested in, is fed into the signal splitter (cf Fig.1) and is divided into two separate bit streams or signals, $s_1(t)$ and $s_2(t)$. This separation is done by assigning the "odd" and "even" bits to separate channels, as shown in Fig 4. We can denote the even bit stream as a sequence of binary data bits $\{a_n\}$ and the odd bit stream as sequence of binary data bits $\{b_n\}$ n=0,1,2,3,····. The sequence $\{b_n\}$ is delayed by T sec with respect to the sequence $\{a_n\}$. The signals $s_1(t)$ and $s_2(t)$ hence may be represented by a train of amplitude modulated pulses,

$$s_1(t) = \sum_n a_n g(t-2nT) \qquad \text{(even bit stream)}$$

$$s_2(t) = \sum_n b_n g(t-(2n+1)T) \qquad \text{(odd bit stream)} \qquad (2.3)$$

where $a_n = \pm 1$, $b_n = \pm 1$ depending on the input message and g(t) is a rectangular pulse of width 2T centered at t=0. The data pairs $a_n b_n$ are transmitted alternately in time as a_0b_0, a_1b_1, a_2b_2, ·····. The precoding operation is performed, using a differential encoder, on both sequences of binary input digits $\{a_n\}$ and $\{b_n\}$ in the I-channel (in-phase channel) and the Q-channel (quadrature-phase channel) respectively. The sequences $\{a_n\}$ and $\{b_n\}$ are converted by the differential encoding to the binary sequences $\{c_n\}$ and $\{d_n\}$ using the following rule:

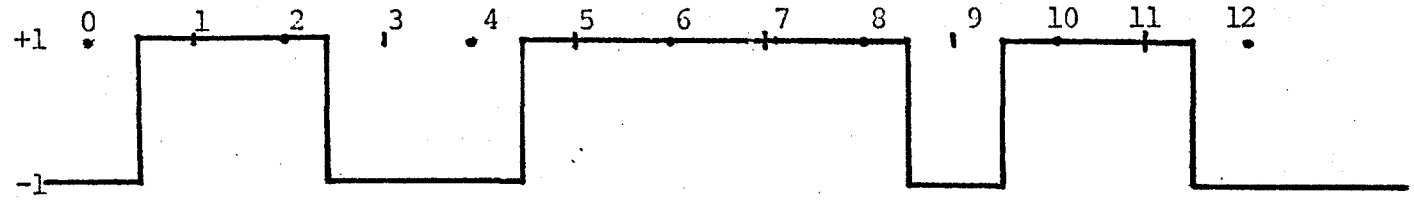

(i) Input message s(t)

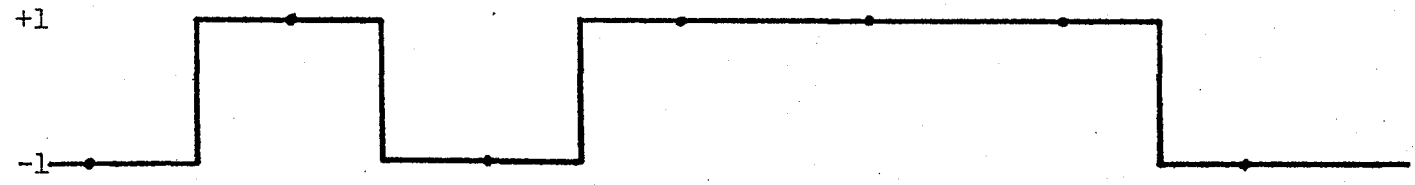

(ii) $s_1(t)$ (the "even" bit stream)

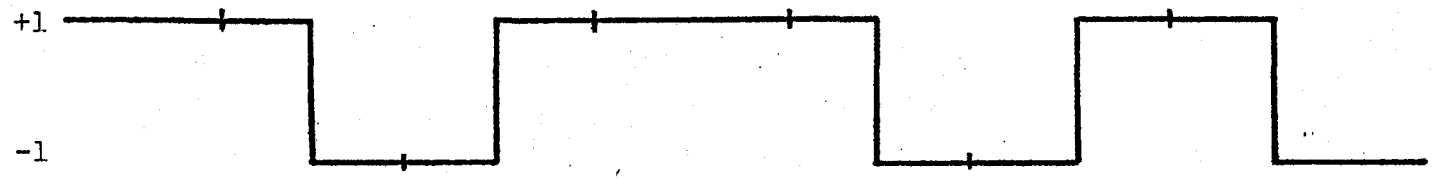

(iii) $s_2(t)$ (the "odd" bit stream)

Fig. 4 $s(t)$, $s_1(t)$ and $s_2(t)$ input message

$$c_n = a_n \oplus c_{n-1}$$

$$d_n = b_n \oplus d_{n-1}$$

where the symbol $\oplus$ represents modulo-2 summation of the binary digits and is defined in this case by

$\oplus$	-1	+1
-1	-1	+1
+1	+1	-1

The output of the differential encoders $s_1'(t)$ and $s_2'(t)$ may be written as

$$s_1'(t) = \sum_n c_n g(t-2nT) \qquad \text{(even bit stream)}$$

$$s_2'(t) = \sum_n d_n g(t-(2n+1)T) \qquad \text{(odd bit stream)} \qquad (2.4)$$

The staggered sequences $\{c_n\}$ and $\{d_n\}$ amplitude modulate their respective carriers $\sqrt{2}\cos \omega_c t$ and $-\sqrt{2}\sin \omega_c t$ and the results are summed to produce the bandpass signal $x_1(t)$ which may be written as

$$\begin{aligned} x_1(t) &= \sqrt{2}[s_1'(t)\cos\omega_c t - s_2'(t)\sin\omega_c t] \\ &= \sqrt{2}\mathrm{Re}\{\,[s_1(t)+js_2(t)]e^{j\omega_c t}\,\} \\ &= \sqrt{2}\mathrm{Re}[\gamma_1(t)e^{j\omega_c t}] \end{aligned} \qquad (2.5)$$

where $\gamma_1(t)=s_1'(t)+js_2'(t)$, and Re indicates real part of . To represent $x_1(t)$ in the frequency domain, we note that since $x_1(t)$ can be rewritten as

$$x_1(t) = \sqrt{2}/2[\,\gamma_1(t)e^{j\omega_c t}+\gamma_1^*(t)e^{-j\omega_c t}\,] \qquad (2.6)$$

we obtain

$$X_1(f) = \sqrt{2}/2[\;\Gamma_1(f-f_c)+\Gamma_1^*(-f-f_c)\;] \qquad (2.7)$$

where f_c is the carrier frequency.

The duobinary pulse-shaping filter has the impulse response given in equation (2.1a) as

$$h(t) = \frac{4}{\pi} \left(\frac{\cos(\pi t/T)}{1 - 4t^2/T^2} \right) \tag{2.8}$$

with the corresponding transfer function in equation (2.1b) as

$$H(\omega) = \begin{cases} 2T\cos(\omega T/2) & |\omega| \leq \pi/T \\ 0 & \text{elsewhere} \end{cases} \tag{2.9}$$

If we consider the duobinary filtering as a baseband process, as we may in this particular application, then since the signals $s_1'(t)$ and $s_2'(t)$ are at the rate 1/2T bits/sec, and the pulses g(t) have width 2T, we must replace T by 2T in the duobinary filter equations to obtain

$$h(t) = \frac{4}{\pi} \left(\frac{\cos(\pi t/2T)}{1 - t^2/T^2} \right) \tag{2.10}$$

The corresponding transfer function is then

$$H(\omega) = \begin{cases} 4T\cos\omega T & |\omega| \leq \pi/2T \\ 0 & \text{elsewhere} \end{cases} \tag{2.11}$$

It may be easily shown that the equivalent bandpass filter has the impulse response

$$\begin{aligned} z(t) &= h(t)\cos\omega_c t \\ &= \mathrm{Re}[h(t)e^{j\omega_c t}] \end{aligned} \tag{2.12}$$

with corresponding transfer function

$$\begin{aligned} Z(f) &= \tfrac{1}{2} [\, H(f-f_c) + H^*(-f-f_c) \,] \\ &= 2T\, [\cos 2\pi(f-f_c)T + \cos 2\pi(f+f_c)T] \end{aligned} \tag{2.13}$$

This, however does not represent the filter which we wish to use. Rather it represents the response which we wish the filter to have to the rect-

angular pulse signals of duration 2T. Therefore let us define the so called duobinary filter shown in Fig 3. by the transfer function

$$F(f) = \tfrac{1}{2} [\, D(f-f_c) + D^*(-f-f_c) \,] \tag{2.14}$$

or equivalently the bandpass impulse response

$$f(t) = d(t)\cos\omega_c t \tag{2.15}$$

We may then write the transmitted signal $x_2(t)$ in the frequency domain as

$$\begin{aligned} X_2(f) &= F(f)X_1(f) \\ &= \tfrac{\sqrt{2}}{4}[\, D(f-f_c)\Gamma_1(f-f_c) + D^*(-f-f_c)\Gamma_1^*(-f-f_c)\,] \\ &= \tfrac{1}{2}\{\tfrac{\sqrt{2}}{2}[\, \Gamma_2(f-f_c) + \Gamma_2^*(-f-f_c)\,]\} \end{aligned} \tag{2.16}$$

where $\Gamma_2(f) \overset{\sqrt{2}}{=} D(f)\Gamma_1(f)$ or

$\gamma_2(t) \overset{\sqrt{2}}{=} \gamma_1(t) \circledast d(t)$ where $\circledast$ is the convolution operation symbol.

In the time domain,

$$\begin{aligned} X_2(t) &= \int_{-\infty}^{\infty} x_1(\tau) f(t-\tau)\, d\tau \\ &= \sqrt{2}\int_{-\infty}^{\infty} \mathrm{Re}[\gamma_1(\tau)e^{j\omega_c\tau}]\,\mathrm{Re}[d(t-\tau)\,e^{j\omega_c(t-\tau)}]\,d\tau \\ &= \sqrt{2}\,\mathrm{Re}[\, e^{j\omega_c t}\int_{\infty}^{\infty} \gamma_1(\tau)\,d(t-\tau)\,d\tau\,] \end{aligned} \tag{2.17}$$

Since $\gamma_1(t)=s_1'(t)+js_2'(t)$ and $g(t)$ is real, therefore we can write

$$X_2(t) = \sqrt{2}\,\mathrm{Re}\,[\, e^{j\omega_c t}\int_{-\infty}^{\infty}(s_1'(\tau)+js_2'(\tau))\,d(t-\tau)\,d\tau\,] \tag{2.18}$$

which may readily be written in the form:

$$\begin{aligned} X_2(t) = \sqrt{2}\,[\, \sum_n c_n \int_{-\infty}^{\infty} g(\tau-2nT)\,d(t-\tau)\,d\tau\,]\cos\omega_c t \\ -\sqrt{2}\,[\, \sum_n d_n \int_{-\infty}^{\infty} g(\tau-(2n+1)T)\,d(t-\tau)\,d\tau\,]\sin\omega_c t \end{aligned} \tag{2.19}$$

We note that except for different delay factors, the two integrals in the above expression are identical.

To find the form of the impulse response d(t) of Fig 1, we note that we want the transmitted signal $x_1(t)$ to have duobinary pulse shaping imposed on it. This implies

$$\int_{-\infty}^{\infty} g(\tau)\, d(t-\tau)\, d\tau = h(t)$$

where h(t) is the duobinary impulse response defined in equation (2.1a). This equation is best solved in the frequency domain where it may be written as

$$G(\omega)D(\omega) = H(\omega)$$

Since

$$H(\omega) = \begin{cases} 4T\cos\omega T & |\omega| \leq \pi/2T \\ 0 & \text{elsewhere} \end{cases}$$

and

$$\begin{aligned} G(\omega) &= \int_{-\infty}^{\infty} g(t) e^{-j\omega t} dt \\ &= \int_{-T}^{T} e^{-j\omega T} dt \\ &= \frac{2T\sin\omega T}{\omega T} \end{aligned}$$

which has zeros at $\omega T = k\pi$ (or $\omega = k\pi/T$) $k=1,2,3,\cdots\cdots$, so that G(ω) is not zero anywhere in the range $-\pi/2T \leq \omega \leq \pi/2T$. It is therefore possible to find the transfer function D(ω) by simple division as

$$\begin{aligned} D(\omega) &= H(\omega)/G(\omega) \\ &= \frac{4T\cos\omega T}{2T\left(\frac{\sin\omega T}{\omega T}\right)} \qquad |\omega| \leq \pi/2T \end{aligned} \tag{2.20}$$

Thus

$$D(\omega) = \begin{cases} 2\omega T\cot\omega T & |\omega| < \pi/2T \\ 0 & \text{elsewhere} \end{cases} \tag{2.21}$$

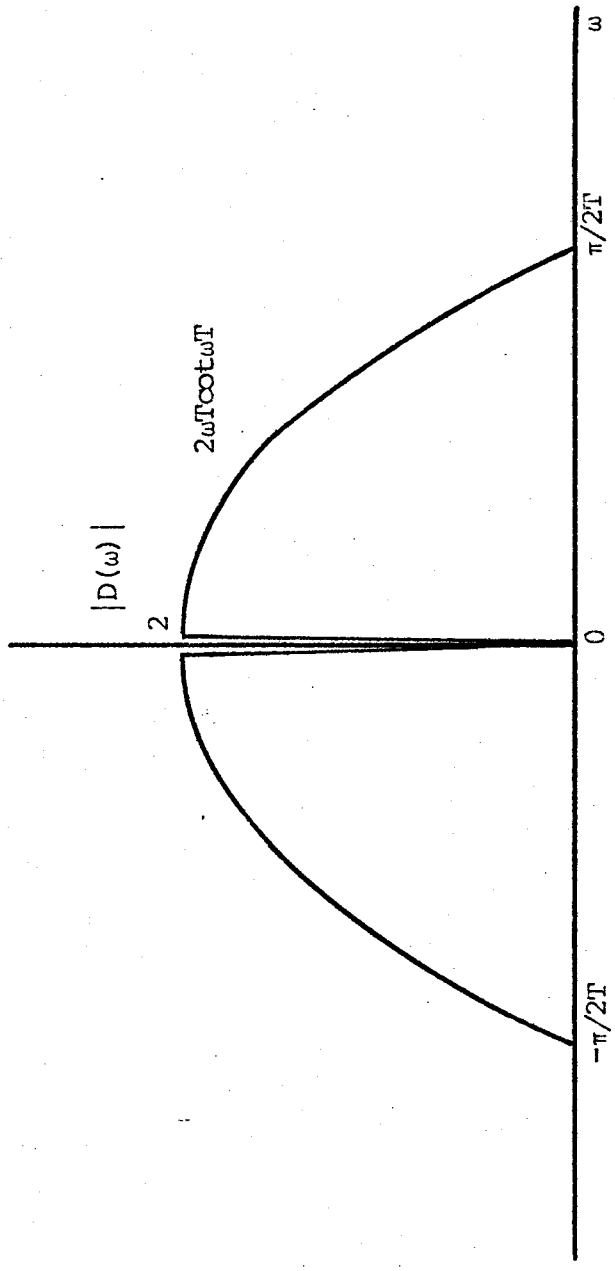

Fig. 5 Transfer function D(ω)

$D(\omega)$ is plotted in Fig 5. By using the filter $D(\omega)$ we may write $x_2(t)$ in the desired duobinary shaped form as

$$x_2(t) = \sqrt{2} \sum_n c_n\, h(t-2nT)\, \cos\omega_c t - \sqrt{2} \sum_n d_n\, h(t-(2n+1)T)\, \sin\omega_c t \tag{2.22}$$

where $h(t)$ is the duobinary pulse shape for a rate of $1/2T$ baud as defined in equation (2.10). In this chapter we consider that $x_2(t)$ is transmitted over a purely additive noise channel, where the noise may be represented in narrowband form as

$$n(t) = \sqrt{2}\, [\, n_1(t)\cos\omega_c t - n_2(t)\sin\omega_c t\,] \tag{2.23}$$

where $n_1(t)$ is the in-phase noise component and $n_2(t)$ is the quadrature-phase noise component. We assume it to be white over the bandwidth of interest, namely $1/2T$ Hz with two-sided power spectral density $N_o/2$ watts/Hz. We also assume it to be Gaussian with mean zero and variance

$$\sigma_n^2 = \sigma_{n_1}^2 = \sigma_{n_2}^2 = \frac{2No}{4T} = \frac{No}{2T} \qquad \text{(bandwidth=1/2T)}$$

which is equal to the total noise power. The received signal $y(t)$ may then be written as

$$y(t) = \sqrt{2}[\, \sum_n c_n h(t-2nT) + n_1(t)\,]\cos\omega_c t$$
$$-\sqrt{2}[\, \sum_n d_n h(t-(2n+1)T) + n_2(t)\,]\sin\omega_c t \tag{2.24}$$

The receiver consists of a demodulator and decoder as shown in Fig 1. For the moment, we assume that an ideal coherent demodulator is used. The signal $y(t)$ is then multiplied by the two locally generated quad-

rature reference signals

$$m_I(t) = \sqrt{2}\cos\omega_c t$$

$$m_Q(t) = -\sqrt{2}\sin\omega_c t \qquad (2.25)$$

The results of these multiplications (neglecting double frequency terms) are

$$r_I(t) = \sum_n c_n\, h(t-2nT) + n_1(t)$$

and

$$r_Q(t) = \sum_n d_n\, h(t-(2n+1)T) + n_2(t) \qquad (2.26)$$

from which we wish to decode the binary symbols $\{c_n\}$ and $\{d_n\}$ and ultimately the original data $\{a_n\}$ and $\{b_n\}$.

Apart from a relative delay of T sec the signals $r_I(t)$ and $r_Q(t)$ are identical and their behavior will be statistically the same. Therefore if we compute the error probability in decoding say $\{c_n\}$, it will be the same as in decoding $\{d_n\}$. Additionally, because of the wide sense stationary nature of the noise the average probability of error will be the same regardless of which symbol is detected.

Thus let us consider the signal $r_I(t)$ and the detection process at time $t=2kT$. First consider only the signal component

$$\sum_n c_n\, h(t-2nT)$$

For illustrative purposes we have assumed $c_0=c_1=c_2=c_{-1}=c_3=1$ and plotted the signals in Fig 6. Examination of the figure reveals that if the signal is sampled at $t=2T$ to detect c_1, there is then intersymbol interference

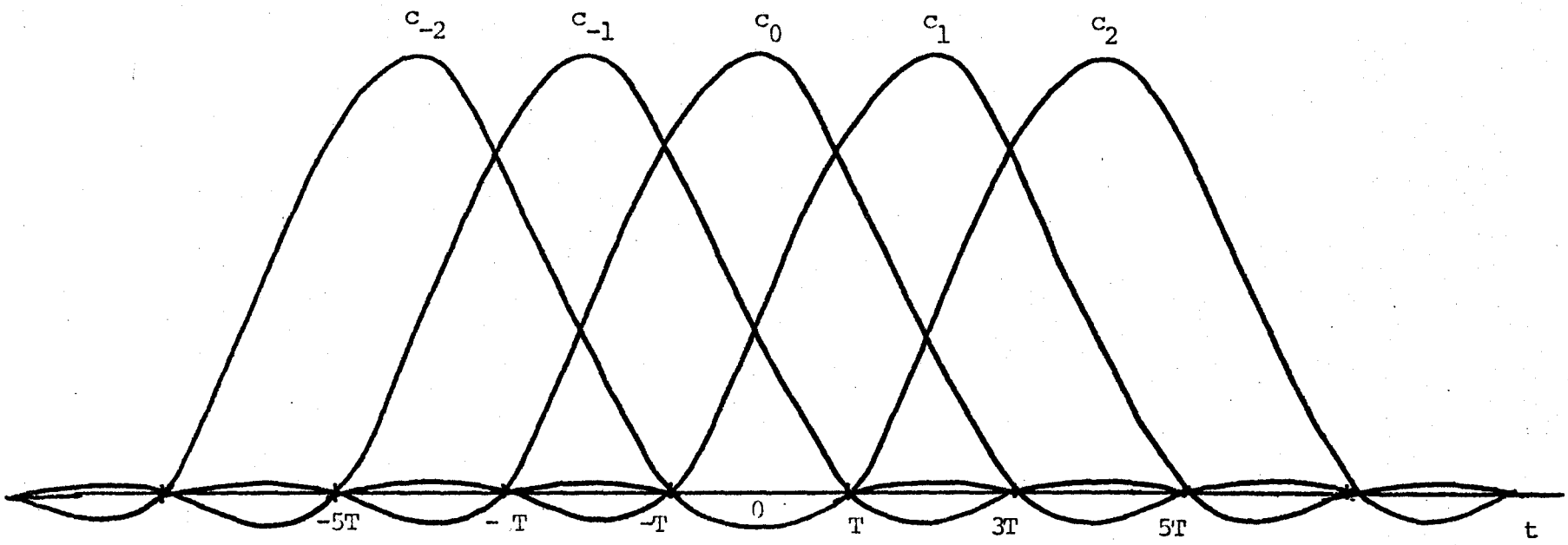

Fig. 6 The duobinary shaping pulses .
(signaling speed = 1/2T baud)

due to c_0, c_2, c_{-1}, and c_{-2}. However, if the signal is sampled at t=T, there is then ISI only from the preceding symbol c_0 and the sample has the value

$$c_1+c_0$$

It is not hard to see that this is the best time to sample in order to detect c_1. Moreover, this is generally true. In order to detect c_k at t=2kT for any k the optimum time to sample is at t=2kT-T at which point the sample will have the value

$$c_k+c_{k-1}$$

This sample can have only the 3 values ± 2 and 0 or more generally $\pm 2d$ and 0 where d is the actual level separation in volts. Because of the differential encoding which has been applied to the original data the decoding turns out to be very simple and is illustrated in the following table

Table 1

Original data			Received Sample	
a_k	c_{k-1}	$c_k=a_k \oplus c_{k-1}$	$c_k+c_{k-1}=\rho_{2k}$	
-1	-1	-1	-2	
+1	-1	+1	0	(d=1)
-1	+1	+1	+2	
+1	+1	-1	0	

We therefore see that if the received sample c_k+c_{k-1} has value $\pm 2d$, then

the original transmitted bit a_k was a 1. Hence the decoder for these precoded signals is quite simple and consists of a 3 level slicer only. The outputs of the decoders in the two channels can now be combined to recover the original data stream by alternately gating the even and odd channels at the original bit rate such that the proper phase relation between the gate signal and the data timing in each channel is maintained.

It is worthwhile to examine the possible symbol values, $\pm 2d$ and 0. We can see that a direct transition between +2d and -2d is impossible. These three levels signals are highly correlated [24]. In fact the duobinary coding technique has the effect of changing the uncorrelated binary symbol sequence into a correlated 3-level sequence. The consequence of this process is the redistribution of the spectral density of the original binary sequence into a highly concentrated spectral density near zero frequency (equivalently the carrier frequency) [23][24]. Fig 7 illustrates the 2:1 bandwidth compression property of the duobinary sequence compared to the original binary symbol spectrum. Note that the large concentration of energy in the vicinity of zero frequency has no significance in high speed data transmission since a carrier must be employed due to the bandpass characteristics of most transmission media. Thus we can see that the available channel capacity is doubled by employing the duobinary coding technique. On the other hand, if we wish to double the capacity per radio channel using the multilevel phase modulation technique, we have to go to 16 level phase modulation. This greatly increases the equip-

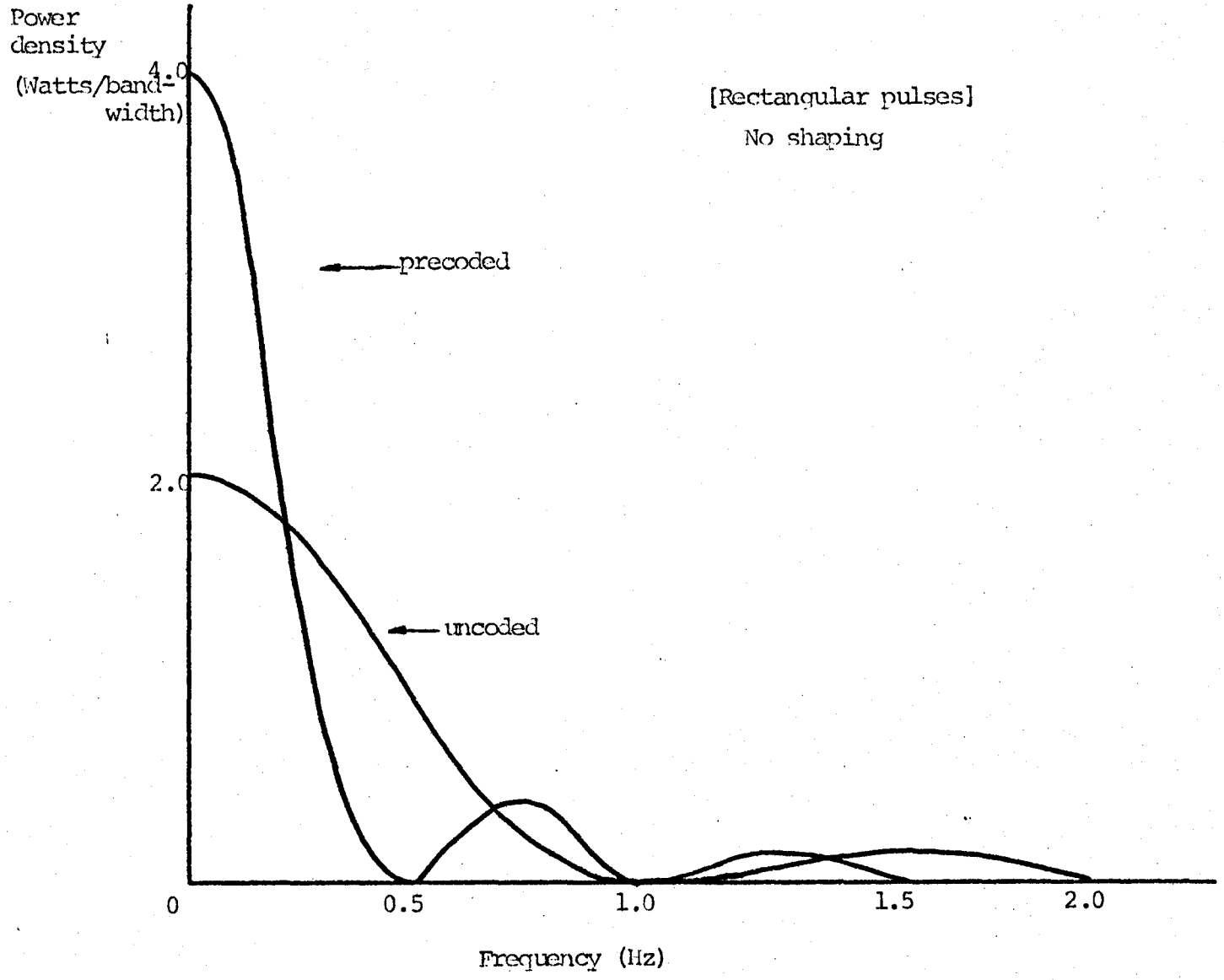

Fig 7. Power spectral density for duobinary precoded signals and uncoded binary digital signals.

ment complexity and causes a fairly heavy performance penalty in terms of error-rate versus signal to noise ratio. Using duobinary coding, the capacity per radio channel is doubled with only a moderate performance penalty. More important is that the equipment complexity is much simpler, and hence the cost is lower.

Most systems are quite intolerant of timing perturbations in the receiver sampler when the transmission rate is close to the channel Nyquist rate [29]. For the duobinary system, it has been shown that the speed tolerance, which measures the sensitivity of a system to changes in the signalling rate, is 42.5% [1]. This figure indicates the insensitivity of the duobinary system to receiver sampler timing perturbations. Also, another performance index, eyewidth as indicated by Kabal[1], shows that the system is quite insensitive to changes in the sampler phase. We may, therefore conclude that bit timing in the duobinary system is not critical, provided coherent demodulation has been achieved. In the remaining of this chapter, we shall consider the degradation due to the unavoidable frequency instabilities in the high frequency radio channel. These instabilities lead to errors in the demodulating carrier phase and the effect of this phase error must be examined.

2.2.3 System modulation type

Since duobinary coding is used in the system, the type of modulation is no longer simply a 4-level PSK system. The duobinary coding is combined with the four level phase modulation and results in a complex

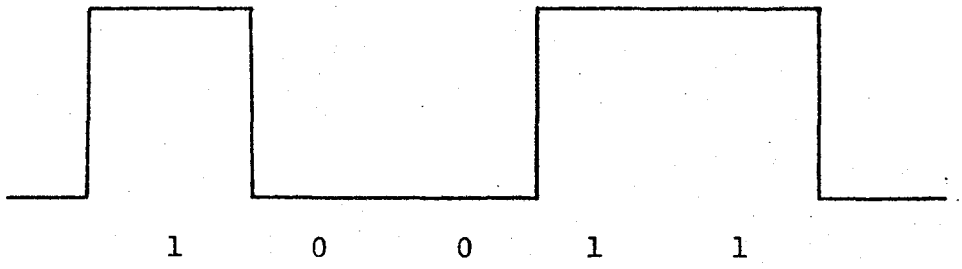

(a) Binary signal

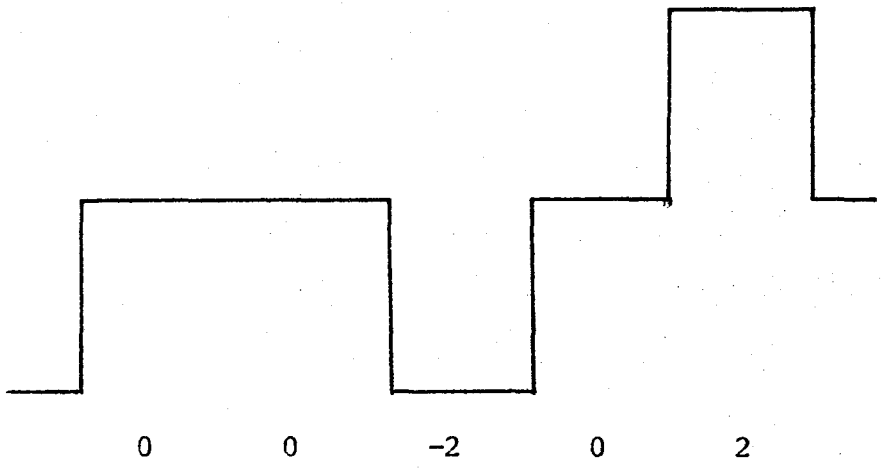

(b) Partial response coding

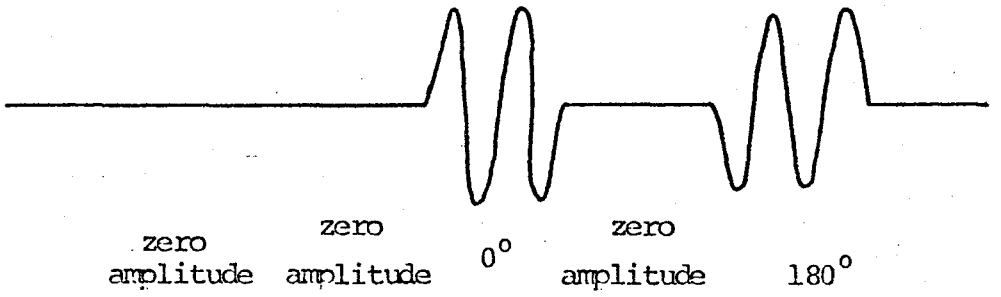

(c) Carrier wave phase modulated by partial response signal

Fig. 8 Modulation process

modulation process which is partly phase and partly amplitude modulation. The process is illustrated in Fig. 8 where Fig. 8a is simply a binary symbol sequence (differentially encoded) or series of pulses with amplitude -1 (logical 0) or +1. The duobinary coded signal will then be a series consisting of -2,0 and +2 as shown in Fig 8b. Once the signal has undergone duobinary coding, it is used to modulate the carrier wave by representing the levels -2 and +2 by phases 0 and 180 degree respectively, and the level 0 by zero amplitude. As four level phase modulation is used with duobinary coding, we can combine two similar signals in quadrature, that is, differing in phase by 90 degrees. Fig 8c illustrates the carrier wave phase modulated by a duobinary baseband signal, and two of these are added in quadrature to produce the resultant modulated wave.

2.3 Performance Evaluation

2.3.1 Ideal coherent detection with zero phase error

To evaluate the performance of the duobinary system, we assume that the transmitted binary data $\{a_k\}$ and $\{b_k\}$ have equal probability of having the values ± 1. Referring to table 1 in section 2.2.2, it may be shown that

$$P(\rho_{2k}=2d)=P(\rho_{2k}=-2d)=1/4$$

and

$$P(\rho_{2k}=0) = 1/2$$

where $\rho_{2k}= c_k + c_{k-1}$ is the 3-level duobinary data and $\{c_k\}$ is the differentially encoded binary signal sequence. Let us consider the noisy de-

modulated received signal

$$p(t) = \sum_n c_n\, h(t-2nT) + n_1(t) \tag{2.27}$$

If the signal is sampled at $t=2kT-T$ we have

$$\rho_{2k} = c_k + c_{k-1} + n_{2k}$$

where $c_k+c_{k-1}=2,0$ or -2 and n_{2k} is a Gaussian random variable. This sample is threshold detected using the decision scheme

$$-d < \rho_{2k} < d \Longrightarrow a_k = 1$$
$$\rho_{2k} \leq -d \Longrightarrow a_k = -1$$
$$\rho_{2k} \geq d \Longrightarrow a_k = -1$$

as described above. The average probability of error for this detection process may be written as

$$\begin{aligned} Pe = {} & [\, P(\rho_{2k} \leq -d \,|\, a_k=1) + P(\rho_{2k} \geq d \,|\, a_k=1) \,]\, P(a_k=1) \\ & + [\, P(\rho_{2k} > -d \,|\, a_k=-1) + P(\rho_{2k} < d \,|\, a_k=-1) \,]\, P(a_k=-1) \end{aligned} \tag{2.28}$$

or equivalently on defining $r_k=c_k+c_{k-1}$

$$\begin{aligned} Pe = {} & [\, P(\rho_{2k} \leq -d \,|\, r_k=0) + P(\rho_{2k} \geq d \,|\, r_k=0) \,]\, P(r_k=0) \\ & + P(\rho_{2k} > -d \,|\, r_k=-2)\, P(r_k=-2) + P(\rho_{2k} < d \,|\, r_k=2)\, P(r_k=2) \end{aligned} \tag{2.29}$$

Because n_{2k} is a zero-mean Gaussian random variable, the above conditional probabilities all turn out to be equal and we may write

$$\begin{aligned} Pe &= 3/2\; P(\rho_{2k} \geq d \,|\, r_k=0) \\ &= 3/2\; P(n_{2k} \geq d) \end{aligned}$$

In duobinary systems, there are 3 system models which must be considered in calculating the probability of error:

(i) duobinary pulse shaping is equally split between the transmitter and receiver

(ii) duobinary pulse shaping is entirely performed at the transmitter

(iii) duobinary pulse shaping is entirely performed at the receiver

We shall neglect the third model since the intent of duobinary encoding is to restrict the required channel bandwidth and hence only the first and second models are of interest.

(i) Model 1 : shared pulse shaping

The transmitter filter in this case has transfer function

$$H_T(\omega) = H^{1/2}(\omega) = \begin{cases} (4T\cos\omega T)^{1/2} & |\omega| \leq \pi/2T \\ 0 & \text{elsewhere} \end{cases}$$

and the receiving filter has transfer function

$$H_R(\omega) = H^{1/2}(\omega) = \begin{cases} (4T\cos\omega T)^{1/2} & |\omega| \leq \pi/2T \\ 0 & \text{elsewhere} \end{cases}$$

The baseband system may be modelled as shown in Fig 2a.

For binary input data with values $\pm d$, we may calculate the average symbol power as

$P_S = d^2/2T$ where $1/2T$ is the data rate

The transmitted signal power may then be written as

$$P_T = (d^2/2T) \int_{-\pi/2T}^{\pi/2T} [(4T\cos\omega T)^{1/2}]^2 \frac{d\omega}{2\pi} \qquad (2.30)$$

$$= \frac{4}{\pi}\frac{d^2}{2T} = \frac{4}{\pi} P_S$$

At point A in Fig 2a, the noise power in the Nyquist band is

$$P_N = N_0/2T \tag{2.31}$$

and thus the SNR at this point is

$$\frac{P_T}{P_N} = \frac{4}{\pi}(2TP_S/N_0) = \frac{4}{\pi}\frac{P_S}{P_N} \tag{2.32}$$

At the output of the receiver filter, the noise power is given by

$$P_N' = N_0 \int_{\pi/2T}^{\pi/2T} [(4T\cos\omega T)^{1/2}]^2 \frac{d\omega}{2\pi}$$
$$= \frac{4 N_o}{\pi} \tag{2.33}$$

and we note that P_n' is the variance of the decision variable.

The probability of error at the detector (rectifier/threshold detector) is

$$Pe = \frac{3}{2} P(n_{2k} \; d) = \frac{3}{2\sqrt{2\pi}} \int_d^\infty \exp(-x^2/2\sigma^2) dx$$
$$= \frac{3}{2} Q(d/\sigma) \tag{2.34}$$

where σ^2 is the noise variance at the output of the receiver filter.

For the model in Fig 2a, $\sigma^2 = P_N'$, this yields

$$Pe = \frac{3}{2} Q(\frac{d}{\sqrt{4N_0/\pi}}) = \frac{3}{2} Q(\sqrt{\pi/4N_o}\; d) \tag{2.35}$$

The decision distance d can be expressed in terms of the transmitted signal power P_T as

$$d = (\pi TP_T/2)^{1/2} \tag{2.36}$$

and this allows us to write

$$Pe = \frac{3}{2} Q(\frac{\pi}{4}\sqrt{2TP_T/N_0}) \tag{2.37}$$

but $N_0/2T = P_N$ is the noise power in the Nyquist band at the input to the receiver filter and therefore

$$Pe = \frac{3}{2} Q\left(\frac{\pi}{4}\sqrt{P_T/P_N} \right) \qquad (2.38)$$

The effective SNR is therefore $\frac{\pi^2 P_T}{16 P_N}$, whereas with ideal binary signalling it would be $\frac{P_T}{P_N}$. There is therefore a degradation of 2.1 dB over ideal binary signalling neglecting the multiplying factor of 3/2. The actual receiver SNR is found as

$$\mu = \frac{P_T}{P_N} = \frac{16}{\pi^2} \left[Q^{-1}(2Pe/3) \right]^2 \qquad (2.39)$$

(ii) Model 2: transmitter pulse shaping

The transmitting filter in this case has transfer function

$$H_T(\omega) = H(\omega) = \begin{cases} 4T\cos\omega T & |\omega| \leq \pi/2T \\ 0 & \text{elsewhere} \end{cases}$$

and the receiving filter is ideally

$$H_R(\omega) = \begin{cases} 1 & |\omega| \leq \pi/2T \\ 0 & \text{elsewhere} \end{cases}$$

The received noise power at the decoder input is

$$\sigma^2 = P_N = N_0/2T = \frac{\pi}{2T} \cdot \frac{1}{4} \cdot (4N_0/\pi) = \pi P_N'/8T \qquad (2.40)$$

The transmitted signal power in this case is

$$P_T' = \frac{d^2}{2T} \int_{-\pi/2T}^{\pi/2T} 16T^2 \cos^2 \omega T \frac{d\omega}{2\pi}$$

$$= \frac{4d^2T}{\pi} \int_{-\pi/2T}^{\pi/2T} (1/2 + (1/2)\cos 2\omega T)\, d\omega$$

$$= 2d^2$$

$$= (\pi T)\, P_T \qquad (2.41)$$

The probability of error is now given as

$$Pe = \frac{3}{2} Q(d/\sigma) = \frac{3}{2} Q(\sqrt{2T/N_0}\, d)$$

$$= \frac{3}{2} Q(d/ \sqrt{P_N})$$

Since $d^2 = P_T'/2$, thus

$$\frac{d}{\sigma} = \frac{1}{\sqrt{2}} \cdot \sqrt{P_T'/P_N}$$

whence

$$Pe = \frac{3}{2} Q(\frac{1}{\sqrt{2}} \cdot \sqrt{P_T'/P_N}) \qquad (2.42)$$

The effective SNR is $P_T'/2P_N$ where P_T' is the transmitted signal power and P_N is the noise power in the Nyquist band. Therefore in this case there is a degradation of 3.01 dB from ideal binary signalling neglecting the factor of 3/2. The actual SNR is found as

$$\mu = P_T'/P_N = 2 \; [\; Q^{-1}(2Pe/3) \;]^2$$

The required SNR for ideal binary signalling is readily found to be

$$\mu = Q^{-1}(Pe) \qquad (2.43)$$

Consider an error rate of 10^{-4}, then

$Q^{-1}(Pe) \implies 8.4$ dB

$Q^{-1}(2Pe/3) \implies 8.7$dB

Table 2

Model	μ	Degradation
PAM(ideal binary)	8.4 dB	0 dB
Model 1	10.79 dB	2.39 dB
Model 2	11.71 dB	3.31 dB

At Pe = 10^{-5}, then

$$Q^{-1}(\text{Pe}) \Rightarrow 9.5 \text{ dB}$$

$$Q^{-1}(2\text{Pe}/3) \Rightarrow 9.7 \text{ dB}$$

Table 3

Model	μ	Degradation
PAM(ideal binary)	9.5 dB	0 dB
Model 1	11.79 dB	2.29 dB
Model 2	12.71 dB	3.21 dB

2.3.2 Effect of phase error on demodulation and error rate

As in the previous analysis let us consider the transmitted signal to be

$$x_2(t) = \sum_n c_n\, h(t-2nT)\, \cos\omega_c t - \sum_n d_n\, h(t-(2n+1)T)\, \sin\omega_c t \qquad (2.44)$$

where $\{c_n\}$ and $\{d_n\}$ are the differentially encoded binary data and h(t) is the duobinary pulse shape

$$h(t) = \frac{4}{\pi} \frac{\cos(\pi t/2T)}{1 - t^2/T^2}$$

for a rate of 1/2T baud with

$$H(\omega) = \begin{cases} 4T\cos\omega T & |\omega| \leq \pi/2T \\ 0 & \text{elsewhere} \end{cases}$$

In the previous analysis we considered system performance for the case of perfectly coherent demodulation with the only disturbance being the additive Gaussian noise.

In this analysis, we consider that a random phase shift is

introduced by the channel, so that demodulation is not perfectly coherent, but contains distortion due to phase error. We will, however, continue to assume that symbol timing is maintained.

Now the signal at the front end of the receiver can be written as

$$y'(t) = \sqrt{2}\,[\sum_n c_n\, h(t-2nT) + n_1(t)\,]\cos(\omega_c t + \theta(t)) - \sqrt{2}\,[\sum_n d_n\, h(t-(2n+1)T) + n_2(t)\,]\sin(\omega_c t + \theta(t)) \tag{2.45}$$

where $\theta(t)$ is the random phase shift and $n_1(t)$ and $n_2(t)$ are the in-phase and quadrature phase noise components respectively. This signal is demodulated by the quadrature carriers $\sqrt{2}\cos(\omega_c t+\hat{\theta})$ and $-\sqrt{2}\sin(\omega_c t+\hat{\theta})$, where $\hat{\theta}$ is a local estimate of the carrier phase θ, to produce the quadrature baseband components

$$r_I(t) = \sum_n c_n\, h(t-2nT)\cos\phi(t) - \sum_n d_n\, h(t-(2n+1)T)\sin\phi(t) + n_1(t)\cos\phi(t) - n_2(t)\sin\phi(t) \tag{2.46a}$$

and

$$r_Q(t) = \sum_n d_n\, h(t-(2n+1)T)\cos\phi(t) + \sum_n c_n\, h(t-2nT)\sin\phi(t) + n_1(t)\sin\phi(t) + n_2(t)\cos\phi(t) \tag{2.46b}$$

where $\phi(t)$ is the phase error defined as the difference between $\theta(t)$ and its local estimate $\hat{\theta}(t)$. We note that the effect of the phase error $\phi(t)$ is to introduce quadrature distortion terms ($\alpha\sin\phi$) into $r_I(t)$ and $r_Q(t)$ and this must inevitably degrade the performance of the system.

The signal $r_I(t)$ is sampled for detection purposes at the times $t=(2k-1)T$ (k integer). Consider the pulse $h(t-2nT)$ at this sampling time

$$h((2k-1)T-2nT) = h(2(k-n)T-T)$$

$$= \frac{4}{\pi} \frac{\cos \frac{\pi}{2} (2(k-n)-1)}{1 - (2(k-n)-1)^2}$$

$$= \begin{cases} 1 & n=k,k-1 \\ 0 & n\neq k,k-1 \end{cases} \qquad (2.47)$$

Similarly consider the pulse shape $h(t-(2n+1)T)$ in the quadrature distortion term at $t=(2k-1)T$ (k integer)

$$h((2k-1)T-(2n+1)T) = h(2(k-n-1)T)$$

$$= \frac{4}{\pi} \frac{\cos \frac{\pi}{2T} [2(k-n-1)T]}{1 - [2(k-n-1)T]^2/T^2}$$

$$= \frac{4}{\pi} \frac{\cos\pi(k-n-1)}{1 - 4(k-n-1)^2}$$

$$= \frac{4}{\pi} \frac{(-1)^{k-n-1}}{1 - 4(k-n-1)^2} \qquad (2.48)$$

In a similar manner, the signal $r_Q(t)$ is sampled for detection purposes at the times $t=2kT$ (k integer).

Consider the pulse shape in the in-phase component $h(t-(2n+1)T)$ which may be written as

$$h(2kT-(2n+1)T) = h(2(k-n)T-T)$$

$$= \begin{cases} 1 & n=k,k-1 \\ 0 & n\neq k,k-1 \end{cases} \qquad (2.49)$$

Next consider the pulse shape $h(t-2nT)$ in the quadrature distortion term

$$h(2kT-2nT) = h(2(k-n)T)$$

$$= \frac{4}{\pi} \frac{\cos [\ 2\ T(k-n)/2T\ ]}{1 - [2(k-n)T]^2/T^2}$$

$$= \frac{4}{\pi} \frac{\cos (k-n)}{1 - 4(k-n)^2}$$

$$= \frac{4}{\pi} \frac{(-1)^{k-n}}{1 - 4(k-n)^2} \qquad (2.50)$$

Using these results we may now write the sampled received sequences as

$$r_I(2k-1) = c_k \cos\phi(t) + c_{k-1} \cos\phi(t) - \frac{4}{\pi} \sum_n d_n \frac{(-1)^{k-n-1}}{1 - 4(k-n-1)^2} \sin\phi(t) + n_I(2k-1)$$

and

$$r_Q(2k) = d_k \cos\phi(t) + d_{k-1} \cos\phi(t) + \frac{4}{\pi} \sum_n c_n \frac{(-1)^{k-n}}{1 - 4(k-n)^2} \sin\phi(t) + n_Q(2k) \qquad (2.51)$$

The effect of a demodulation phase error ϕ is thus to

(i) degrade the amplitude of the desired signal component by an amount proportional to $\cos\phi$

(ii) cause quadrature distortion terms to appear.

By defining

$$A = \frac{4}{\pi} \sum_n d_n \frac{(-1)^{k-n-1}}{1 - 4(k-n-1)^2}$$

and

$$B = \frac{4}{\pi} \sum_n c_n \frac{(-1)^{k-n}}{1 - 4(k-n)^2} \qquad (2.52)$$

We may write

$$r_I(2k-1) = (c_k + c_{k-1}) \cos\phi(t) - A \sin\phi(t) + n_I(2k-1)$$

and

$$r_Q(2k) = (d_k + d_{k-1}) \cos\phi(t) + B \sin\phi(t) + n_Q(2k) \qquad (2.53)$$

and we note that these 2 sample sequences have the same form. In addition, if we for convenience set the detection or decision distance

d=1, we can then define the following error events

Table 4

Event	$c_k(d_k)$	$c_{k-1}(d_{k-1})$	$c_k+c_{k-1}(d_k+d_{k-1})$	Error region for r
1	+1	-1	0	r>1 or r<-1
2	-1	+1	0	r>1 or r<-1
3	+1	+1	+2	r<1
4	-1	-1	-2	r>-1

and each possible event has probability 1/4.

To find the average probability of error conditioned on both the phase error ϕ and the quadrature distortion symbols, we have to find the probability due to each error event and then sum the resulting probabilities. Because of the similarity in form the analysis for r_Q and r_I will be identical.

Event type 1 : In this case $c_k=1$, $c_{k-1}=-1$, $c_k+c_{k-1}=0$ and $r_I=-A\sin\phi+n_I$ and the corresponding error probability is

$$Pe_1 = 1/4[\ Pr(r_1>1) + Pr(r_1<-1)\ ]$$

where we implicitly assume through out this analysis conditioning on $A\sin\phi$, the quadrature distortion. Now $n_I=r_I+A\sin\phi$ is a Gaussian random variable with conditional mean = $A\sin\phi$ and variance σ^2 (dependent on the receiver filter). Therefore

$$Pe_1 = \frac{1}{4}\{\frac{1}{\sqrt{2\pi}\sigma}\int_1^{\infty} \exp[-(x+A\sin\phi)^2/2\sigma^2]dx$$

$$+ \frac{1}{\sqrt{2\pi}\sigma}\int_{-\infty}^{-1} \exp[-(x+A\sin\phi)^2/2\sigma^2]dx\ \}$$

and hence

$$Pe_1 = \frac{1}{4}\left[Q\left(\frac{1+A\sin\phi}{\sigma}\right) + 1 - Q\left(\frac{-1+A\sin\phi}{\sigma}\right) \right]$$

$$= \frac{1}{4} + \frac{1}{4}\left[Q\left(\frac{1+A\sin\phi}{\sigma}\right) - Q\left(\frac{-1+A\sin\phi}{\sigma}\right) \right] \qquad (2.54)$$

where

$$Q(x) = \frac{1}{\sqrt{2\pi}} \int_x^\infty \exp(-y^2/2)\,dy$$

Event type 2: Here, $c_k=-1$, $c_{k-1}=1$, $c_k+c_{k-1}=0$ and $r_I=-A\sin\phi + n_I$.

This event type produces identical results to event type 1 and thus

$$Pe_2 = Pe_1 = \frac{1}{4} + \frac{1}{4}\left[Q\left(\frac{1+A\sin\phi}{\sigma}\right) - Q\left(\frac{-1+A\sin\phi}{\sigma}\right) \right] \qquad (2.55)$$

Event type 3: In this case $c_k=1$, $c_{k-1}=1$, $c_k+c_{k-1}=2$ and $r_I=2\cos\phi-A\sin\phi+n_I$.

The probability of error in this case is

$$Pe_3 = \frac{1}{4} P(r_1<1) = \frac{1}{4} - \frac{1}{4} P(r_1>1)$$

$$= \frac{1}{4}\left\{ 1 - \frac{1}{\sqrt{2\pi}\sigma} \int_1^\infty \exp\left[- \frac{(x-2\cos\phi+A\sin\phi)^2}{2\sigma^2}\right] dx \right\} \qquad (2.56)$$

where as before σ^2 is the noise variance at the output of the receiver filter. Therefore

$$Pe_3 = \frac{1}{4}\left[1 - Q\left(\frac{1-2\cos\phi+A\sin\phi}{\sigma}\right) \right] \qquad (2.57)$$

Event type 4: Here, $c_k=-1$, $c_{k-1}=-1$, $c_k+c_{k-1}=-2$, and $r_I=-2\cos\phi-A\sin\phi+n_I$.

The error probability in this case is then

$$Pe_4 = \frac{1}{4} P(r_1>-1)$$

$$= \frac{1}{4\sqrt{2\pi}\sigma} \int_{-1}^\infty \exp\left[- \frac{(x+2\cos\phi+A\sin\phi)^2}{2\sigma^2} \right] dx$$

$$= \frac{1}{4} Q\left(\frac{-1+2\cos\phi+A\sin\phi}{\sigma}\right) \qquad (2.58)$$

The total probability of error is then easily found as

$$Pe = Pe_1 + Pe_2 + Pe_3 + Pe_4$$

$$= \frac{3}{4} + \frac{1}{2}\left[Q\left(\frac{1+A\sin\phi}{\sigma}\right) - Q\left(\frac{-1+A\sin\phi}{\sigma}\right)\right]$$

$$+ \frac{1}{4}\left[Q\left(\frac{-1+2\cos\phi+A\sin\phi}{\sigma}\right) - Q\left(\frac{1-2\cos\phi+A\sin\phi}{\sigma}\right)\right] \tag{2.59}$$

As a check let us consider the value of Pe when the phase error $\phi=0$. Then

$$Pe = \frac{3}{4} + \frac{1}{2}\left[Q(1/\sigma) - Q(-1/\sigma)\right] + \frac{1}{4}\left[Q(1/\sigma) - Q(-1/\sigma)\right]$$

$$= \frac{3}{2} Q(1/\sigma)$$

which is the same as our previously derived results. The property that $Q(1/\sigma)= 1 - Q(-1/\sigma)$ is proven in Appendix 2A.

Similar results are readily found for the quadrature channel samples as

$$Pe = \frac{3}{4} + \frac{1}{2}\left[Q\left(\frac{1+B\sin\phi}{\sigma}\right) - Q\left(\frac{-1+B\sin\phi}{\sigma}\right)\right.$$

$$\left. + \frac{1}{4}\left[Q\left(\frac{-1+2\cos\phi+B\sin\phi}{\sigma}\right) - Q\left(\frac{1-2\cos\phi+B\sin\phi}{\sigma}\right)\right]\right. \tag{2.60}$$

So far the error rate we have obtained is conditioned on both the phase error ϕ and the quadrature distortion terms (A or B). To obtain the average symbol error probability conditioned on the phase error only, we have to take the average over the quadrature distortion symbols in A(or B) as

$$Pe(\phi) = \sum_{A} Pe(\phi,A)P(A) \tag{2.61}$$

But in general A contains an infinite number of symbols, and equation (2.61) is thus very difficult to evaluate. This leads us to search for

some form of upper bound on the error rate $Pe(\phi)$. In order to do this, we can evaluate, for a fixed phase error ϕ, the largest possible distortion due to the quadrature distortion term A in (2.61). As shown in the previous section, the quadrature distortion term A is expressed as

$$A = \sum_n \frac{4}{\pi} \frac{d_n (-1)^{k-n-1}}{1 - 4(k-n-1)^2} \tag{2.62}$$

The worst case of this series can be written as

$$A = \frac{4}{\pi} + \frac{4}{\pi} \cdot \sum_{n \neq k-1} \frac{1}{4(k-n-1)^2 - 1} \tag{2.63}$$

Therefore

$$A = \frac{4}{\pi} + 2\left(\frac{4}{\pi}\right)\left(\sum_{m=1} \frac{1}{4m^2-1}\right) \qquad \text{where } m=k-n-1$$

$$= \frac{4}{\pi} + \frac{4}{\pi}\left(2 * 1/2\right) = \frac{8}{\pi} \tag{2.64}$$

Thus the upper bound of average probability of error conditioned on the phase error is readily found as

$$Pe(\phi) \leq 0.5 + 0.5\left[Q\left(\frac{1+\frac{8}{\pi}\sin\phi}{\sigma}\right) + Q\left(\frac{1-\frac{8}{\pi}\sin\phi}{\sigma}\right)\right]$$

$$-0.25\left[Q\left(\frac{1-2\cos\phi+\frac{8}{\pi}\sin\phi}{\sigma}\right) + Q\left(\frac{1-2\cos\phi-\frac{8}{\pi}\sin\phi}{\sigma}\right)\right] \tag{2.65}$$

For the case of system model 2 where the transmitter filter determines the shape of the frequency response, we have plotted in Fig 9 the error rate upper bound conditioned on the phase error against the signal to noise ratio as given in equation (2.65). The curves show that even a small phase error can degrade the system performance quite seriously, and as phase error increases, the degradation increases rapidly. For example there is a degradation of approximate 2.5 dB for a 6 degree phase error

Fig 9 Conditional error probability vs Δ^2 (d^2/σ^2)

UPPER SOUND CASE

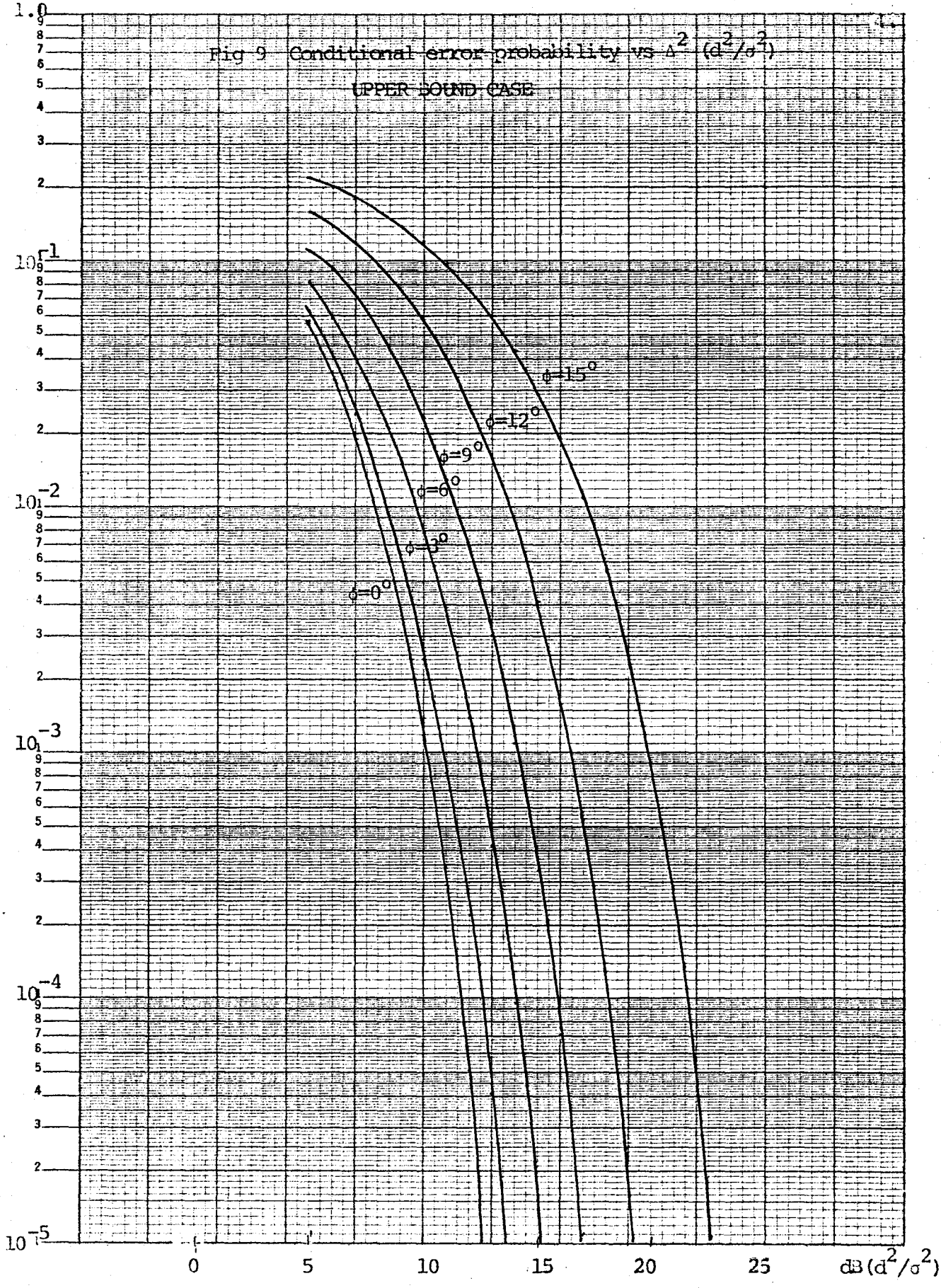

while there is a degradation of approximate 6.5 dB for 12 degree phase error at $Pe(\phi)$ equal 10^{-5}.

Another way to evaluate $Pe(\phi)$, at least approximately, is to approximate the quadrature term A using a finite number of symbols. For example, consider the case where only three symbols are used to evaluate (2.61). The quadrature distortion term A is now expressed as

$$A = \frac{4}{\pi}[\, d_k + \frac{1}{3} d_{k-1} + \frac{1}{3} d_{k+1} \,]$$

where $d_k = d_{k-1} = d_{k+1} = \pm 1$.

There are eight possible combinations for A and each combination has probability 1/8. We can construct a table to show these combinations as follows:

Table 5

i	d_k	d_{k+1}	d_{k-1}	A_i	Prob.
1	+1	+1	+1	$20/3\pi$	1/8
2	+1	+1	-1	$4/\pi$	1/8
3	+1	-1	+1	$-4/3\pi$	1/8
4	+1	-1	-1	$-4/\pi$	1/8
5	-1	+1	+1	$4/\pi$	1/8
6	-1	+1	-1	$4/3\pi$	1/8
7	-1	-1	+1	$-4/\pi$	1/8
8	-1	-1	-1	$-20/3\pi$	1/8

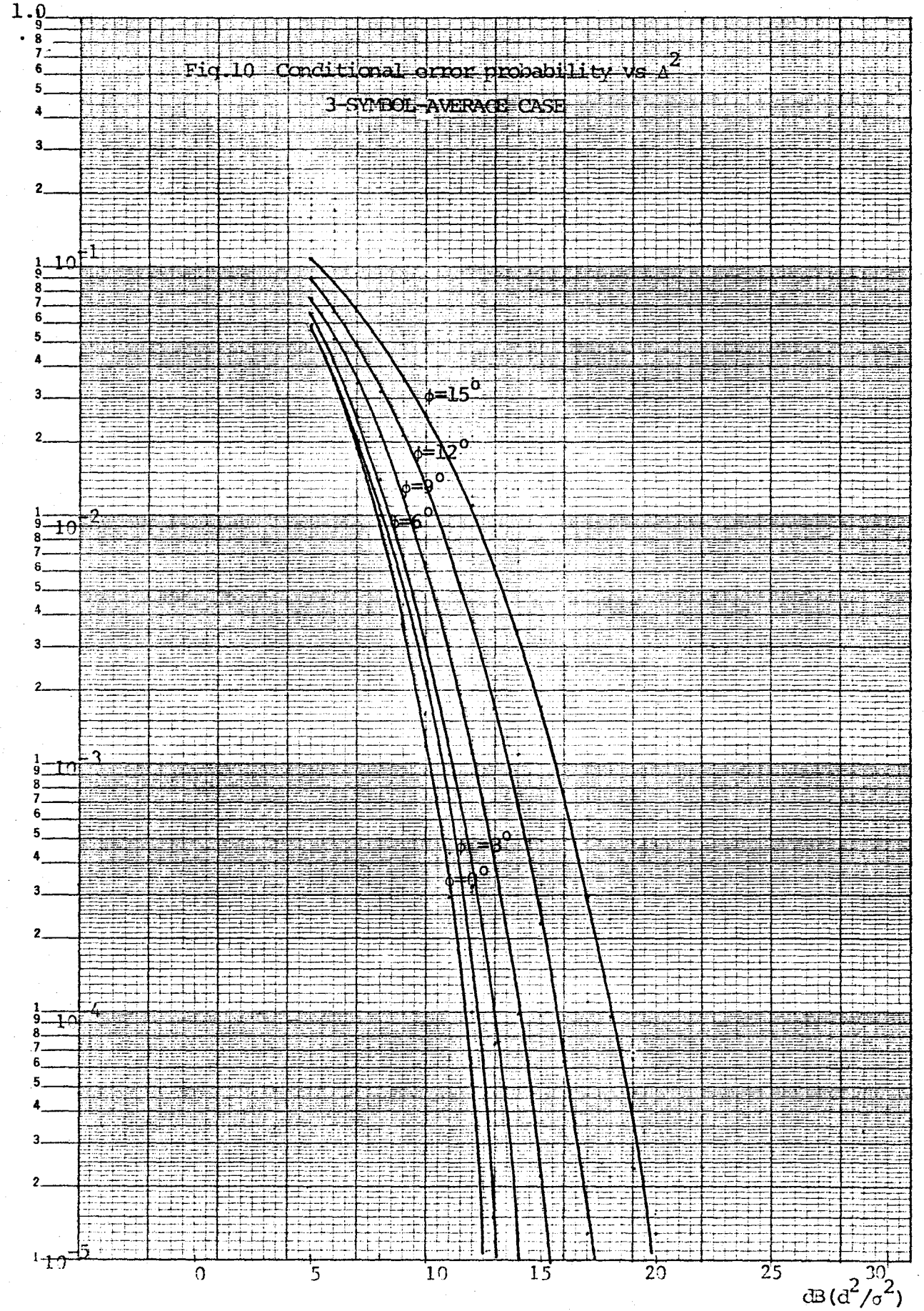
Fig.10 Conditional error probability vs Δ^2
3-SYMBOL-AVERAGE CASE
1.0
10^{-1}
10^{-2}
10^{-3}
10^{-4}
10^{-5}
$\phi=15^o$
$\phi=12^o$
$\phi=9^o$
$\phi=6^o$
$\phi=3^o$
$\phi=0^o$
0
5
10
15
20
25
30
$dB(d^2/\sigma^2)$

Thus we can write

$$Pe(\phi) = \frac{1}{8}\sum_{i=1}^{8} Pe(\phi, A_i)$$

$$= \frac{1}{8}\sum_{i=1}^{8}\{\, 0.5+0.5[\, Q(\frac{1+A_i\sin\phi}{\sigma}) + Q(\frac{1-A_i\sin\phi}{\sigma})\,]$$

$$-0.25[\, Q(\frac{1-2\cos\phi-A_i\sin\phi}{\sigma}) + Q(\frac{1-2\cos\phi+A_i\sin\phi}{\sigma})\,]\} \qquad (2.66)$$

The approximate error rate conditioned on the phase error ϕ as given by (2.66) is plotted against the signal to noise ratio in Fig 10, and plotted against the phase error ϕ withΔ, where $\Delta \triangleq d/\sigma$, as a parameter in Fig 11.

2.4 Simulation of the system performance in the presence of a steady-state phase error and additive Gaussian noise

In this section, we shall evaluate the system performance in the presence of a steady state phase error and additive noise via simulations on the CDC 1700 digital computer. The simulation procedure will be briefly described and the results are discussed, and compared with the foregoing theory.

2.4.1 Description of the simulation

A block diagram of the simulation program is illustrated in Fig 12. The simulation procedure is more or less the same as in [31], where in the noise-free signal is simulated and effects of noise are computed. A pseudorandom binary sequence of 127 signal symbols was processed in the simulation. The signal are Fast Fourier transformed into the frequency domain, and multiplied with the transmit filter transfer function, which

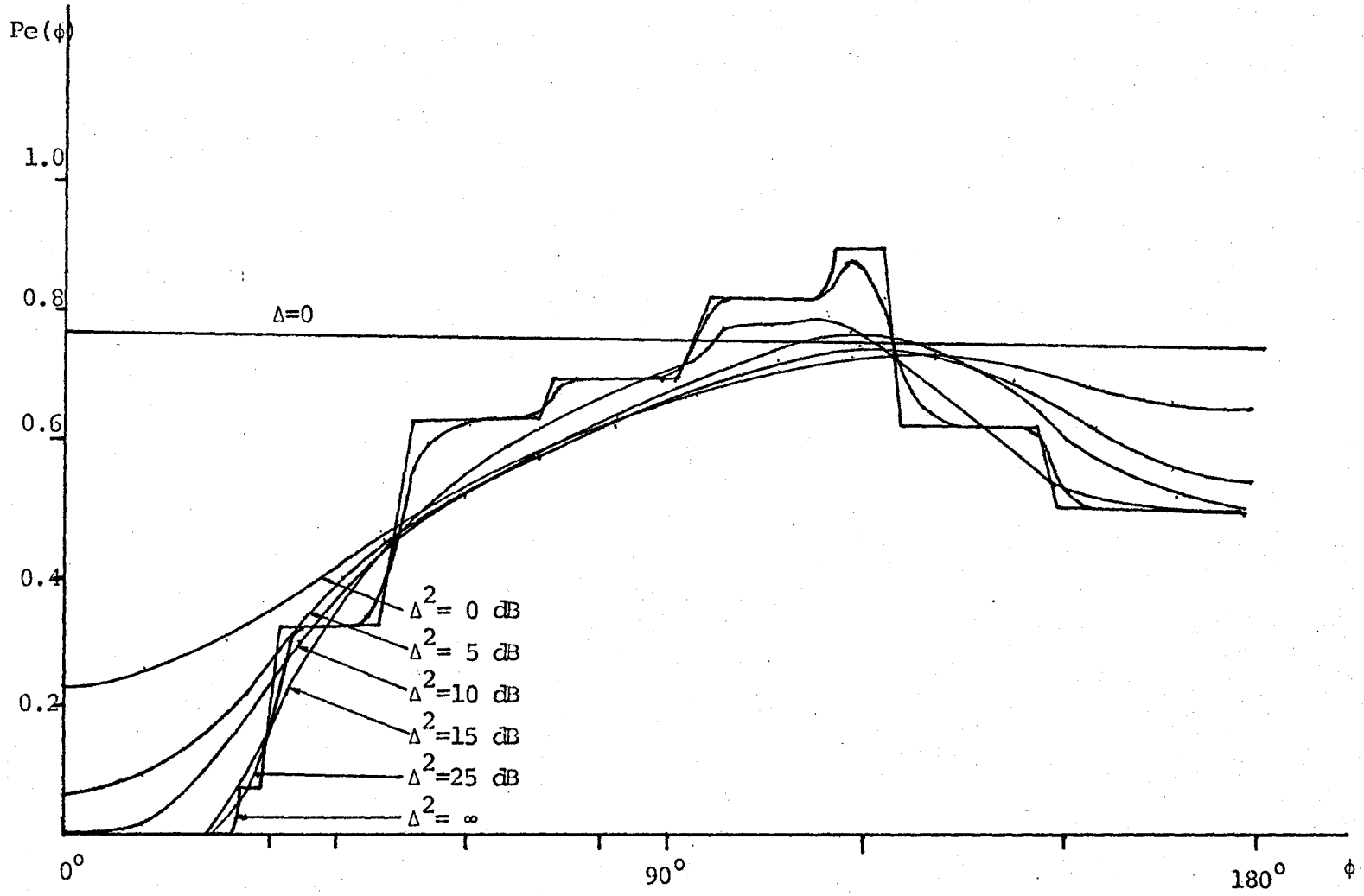

Fig. 11 Conditional error probability for offset QPSK duobinary system

is defined by

$$H_T(\omega) = \begin{cases} 4T\cos\omega T & |\omega| \leq \pi/2T \\ 0 & \text{elsewhere} \end{cases}$$

The result is then inverse Fast Fourier transformed to obtain the time-domain filter output. The continuous signal stream is constructed and passed to the simulated receiver. At the same time, the eye diagram for the duobinary signals was generated on the Tetronix computex 4 display unit. Fig 13 shows the resulting three level eye pattern of the signal.

After the decision making process, the number of incorrectly received bits was counted and a conditional probability of error of each received bit is computed. A computed noise approach [31] was used, where the noise is moved to the output of the receiver filter. In this system, the receiver filter has a transfer function

$$H_R(\omega) = \begin{cases} 1 & |\omega| \leq \pi/2T \\ 0 & \text{elsewhere} \end{cases}$$

The equivalent noise power at the output of this filter is computed according to theory. The signal is simulated in the absence of noise. The purpose of using this computed noise approach is to reduce computing time. The probabilities of error computed for individual bits at each value of SNR are summed and then divided by the total number of bits processed to obtain an average probability of error for each Δ^2 where $\Delta^2 \triangleq d^2/\sigma^2$ with d the level separation and σ^2 the noise variance at the output of the receiver filter.

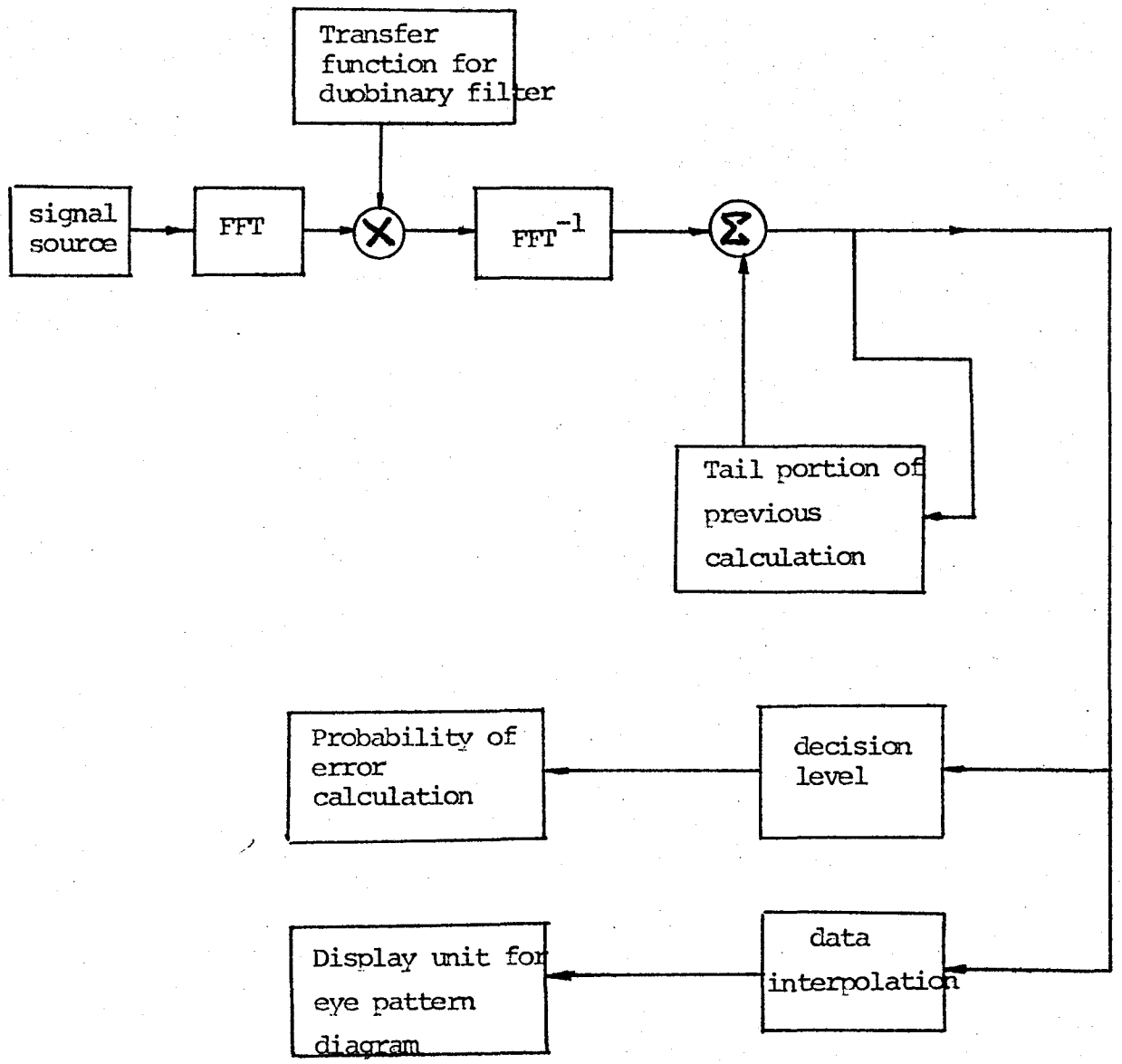

Fig. 12 Simulation Block Diagram

2.4.2 Results and conclusions

The average probability of error is plotted against Δ^2 in Fig 14 where the degradation in performance for fixed probability of error as the steady state phase error increases is shown. Again we can see that as phase error increases, the degradation increases rapidly.

In the simulation, rectangular pulses are used as input to the duobinary pulse-shaping filter instead of impulses. The pulse response of this filter introduces some small additional intersymbol interference (ISI) and causes a small performance degradation of the simulation from the theoretical results. When we compare the simulation curves with the curves obtained theoretically (upper bound and 3-symbol-average cases) for 0° phase error, the curve obtained by simulation shows worse performance than the theoretical curve. We can see that the simulated curves are approximately 1 dB worse than the theoretical curves. This 1 dB difference is, as mentioned previously , mainly due to the spreading of the pulse response we used in simulation. Some other possibilities which may cause this difference are the limited number of samples per pulse used in the simulation, the truncation and window errors of the FFT, etc. In chapter 2, we have designed a filter $D(\omega)$ which can produce the duobinary pulse shape when a pulse is used as its input. When this filter $D(\omega)$ is used in the simulation, the 1 dB degradation from theoretical should be eliminated. However, this has not as yet been done.

Assuming that the 1 dB difference is removed, and we compare the simulated curve for 9° phase error case with the 3-symbol-average and upper bound theoretical curves as shown in Fig 15e, they essentially

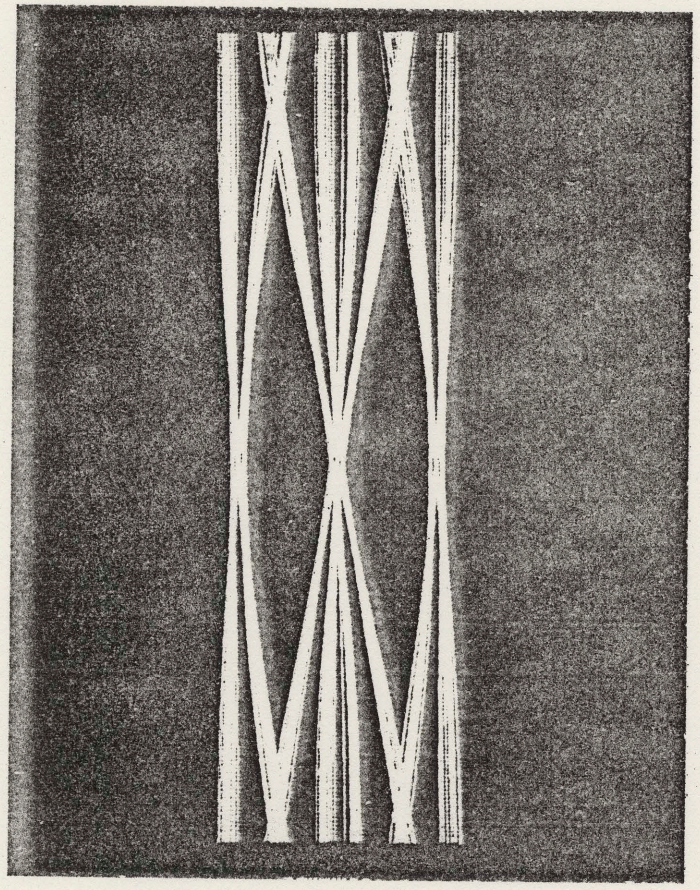

Fig. 13 Eye diagram for duobinary signal

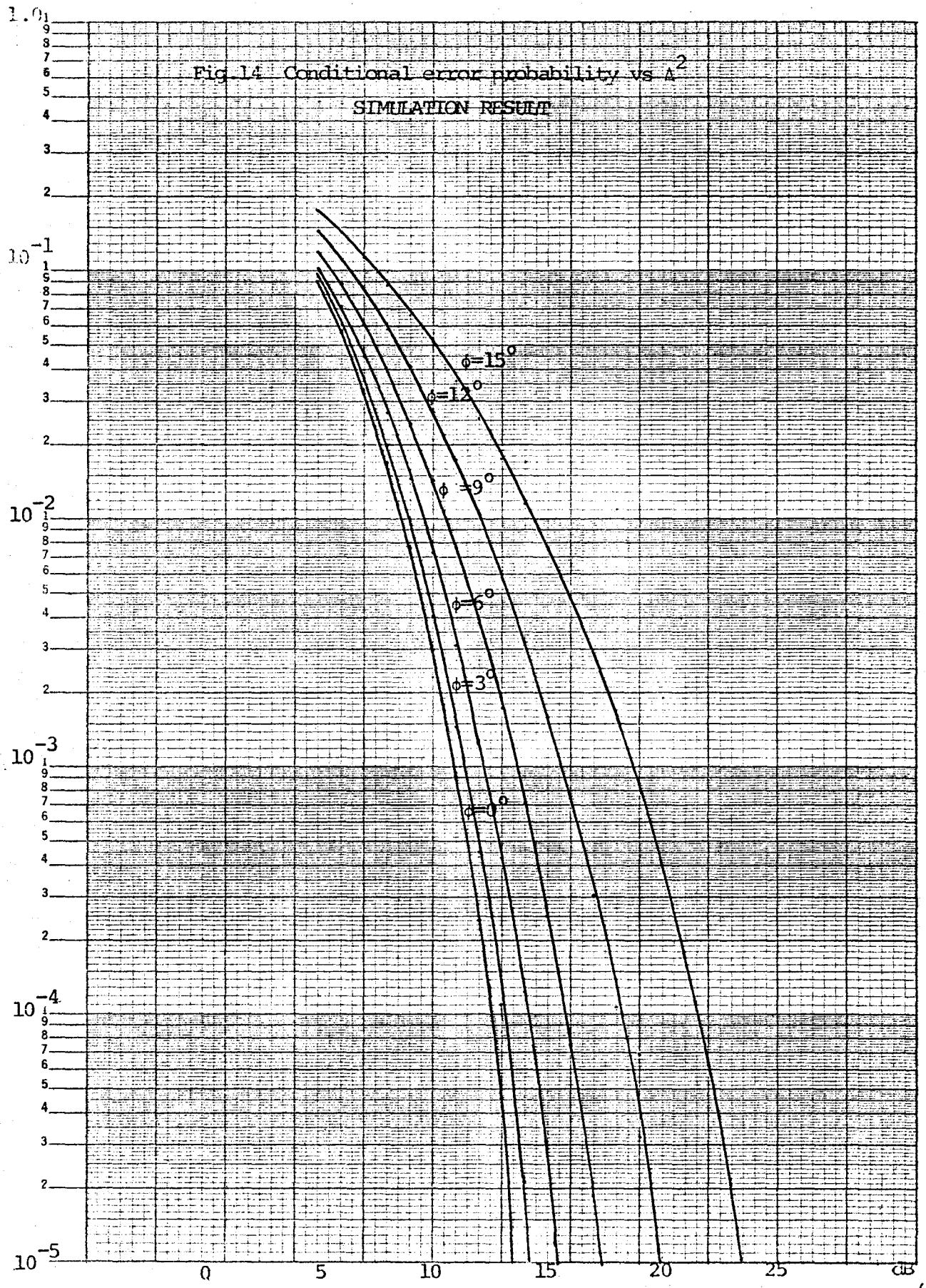
Fig.14 Conditional error probability vs A^2
SIMULATION RESULT
ϕ=15°
ϕ=12°
ϕ=9°
ϕ=6°
ϕ=3°
ϕ=0°
1.0
10^{-1}
10^{-2}
10^{-3}
10^{-4}
10^{-5}
0
5
10
15
20
25
dB
(d^2/σ^2)

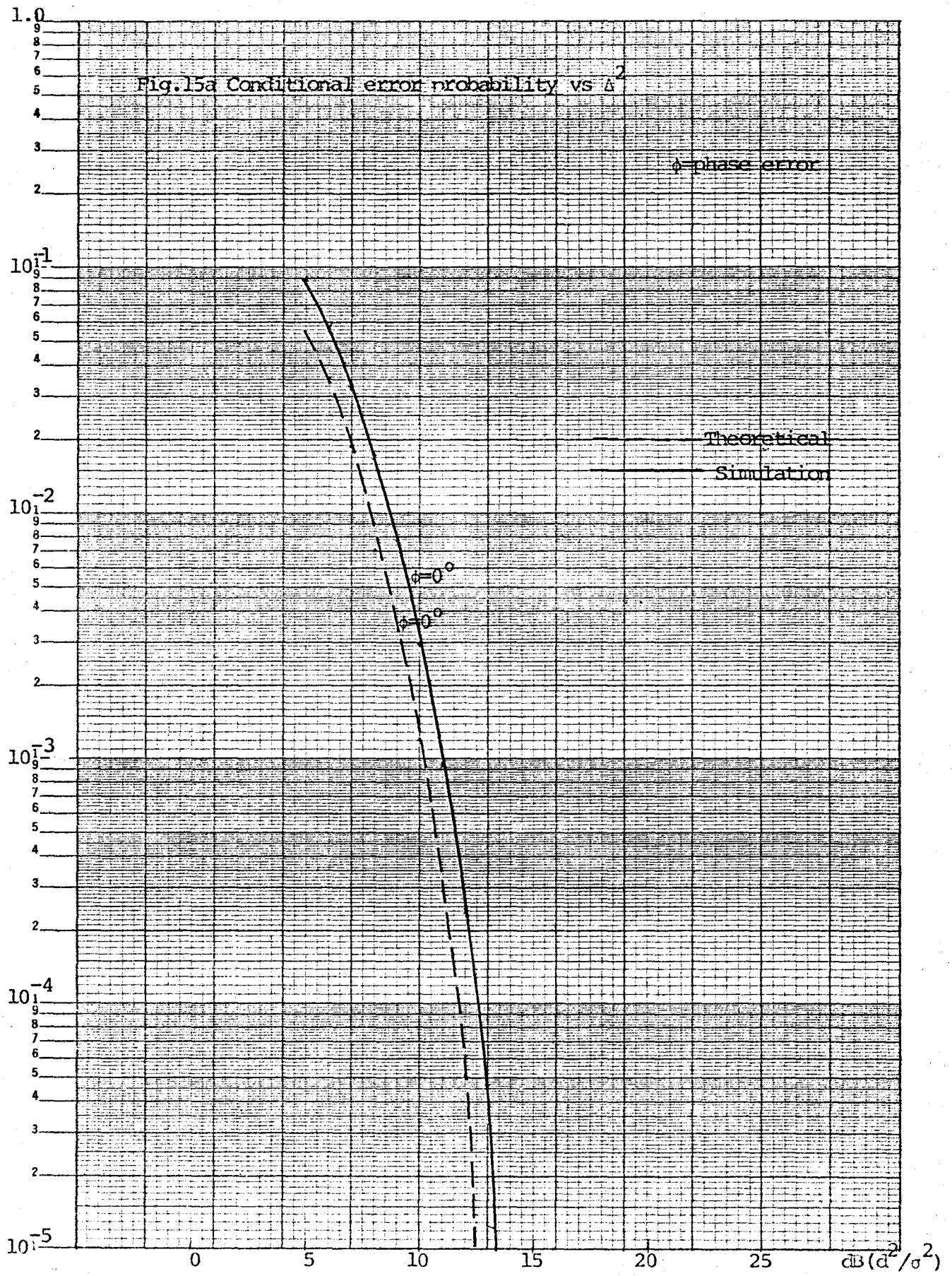
Fig.15a Conditional error probability vs Δ^2
ϕ=phase error
Theoretical
Simulation
ϕ=0°
ϕ=0°
1.0
10^{-1}
10^{-2}
10^{-3}
10^{-4}
10^{-5}
0
5
10
15
20
25
dB(d^2/σ^2)

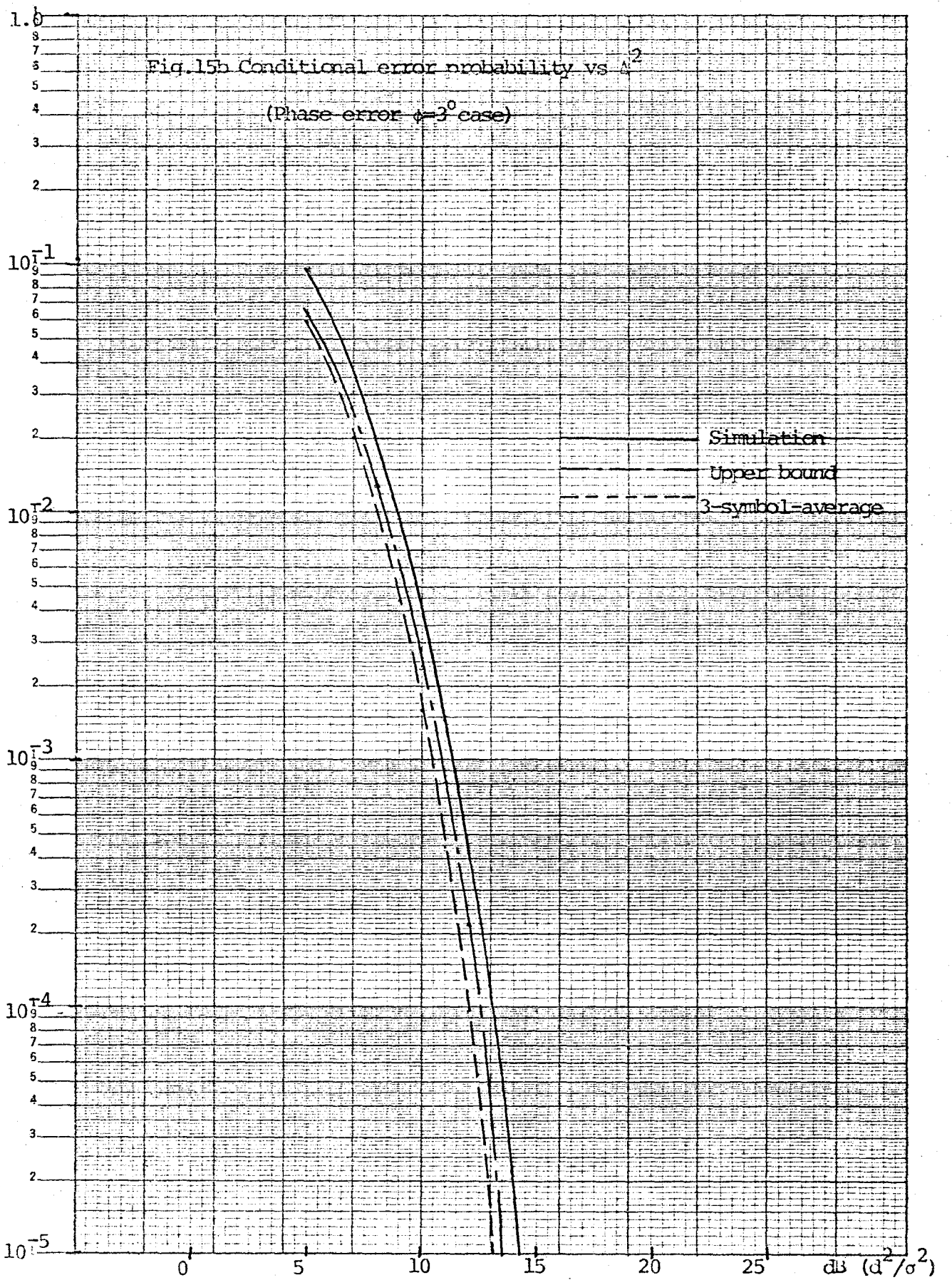
Fig.15b Conditional error probability vs Δ^2
(Phase error ϕ=3° case)
Simulation
Upper bound
3-symbol-average
1.0
10^{-1}
10^{-2}
10^{-3}
10^{-4}
10^{-5}
0
5
10
15
20
25
dB (d^2/σ^2)

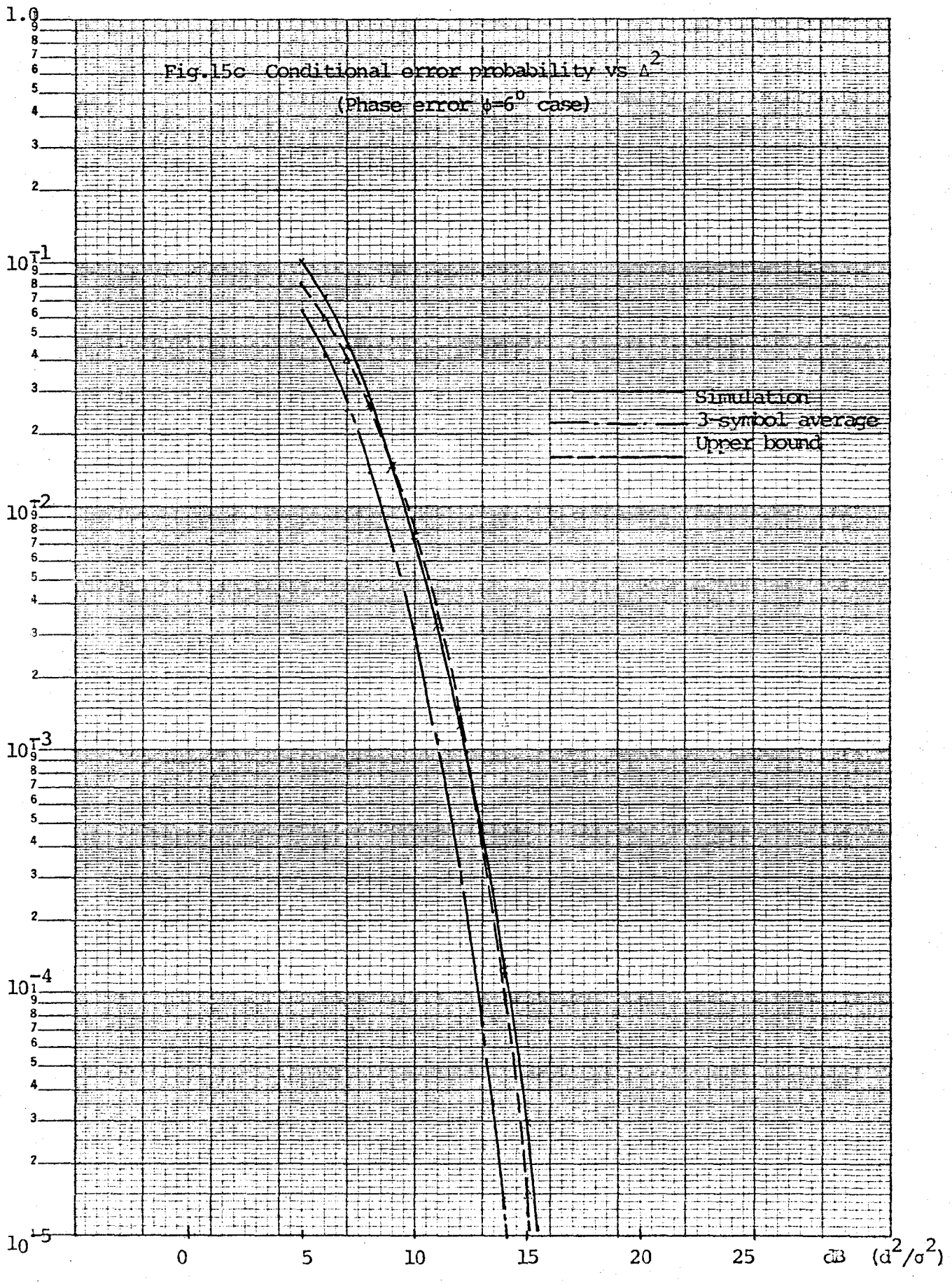

Fig.15c Conditional error probability vs Δ^2
(Phase error $\phi=6^0$ case)

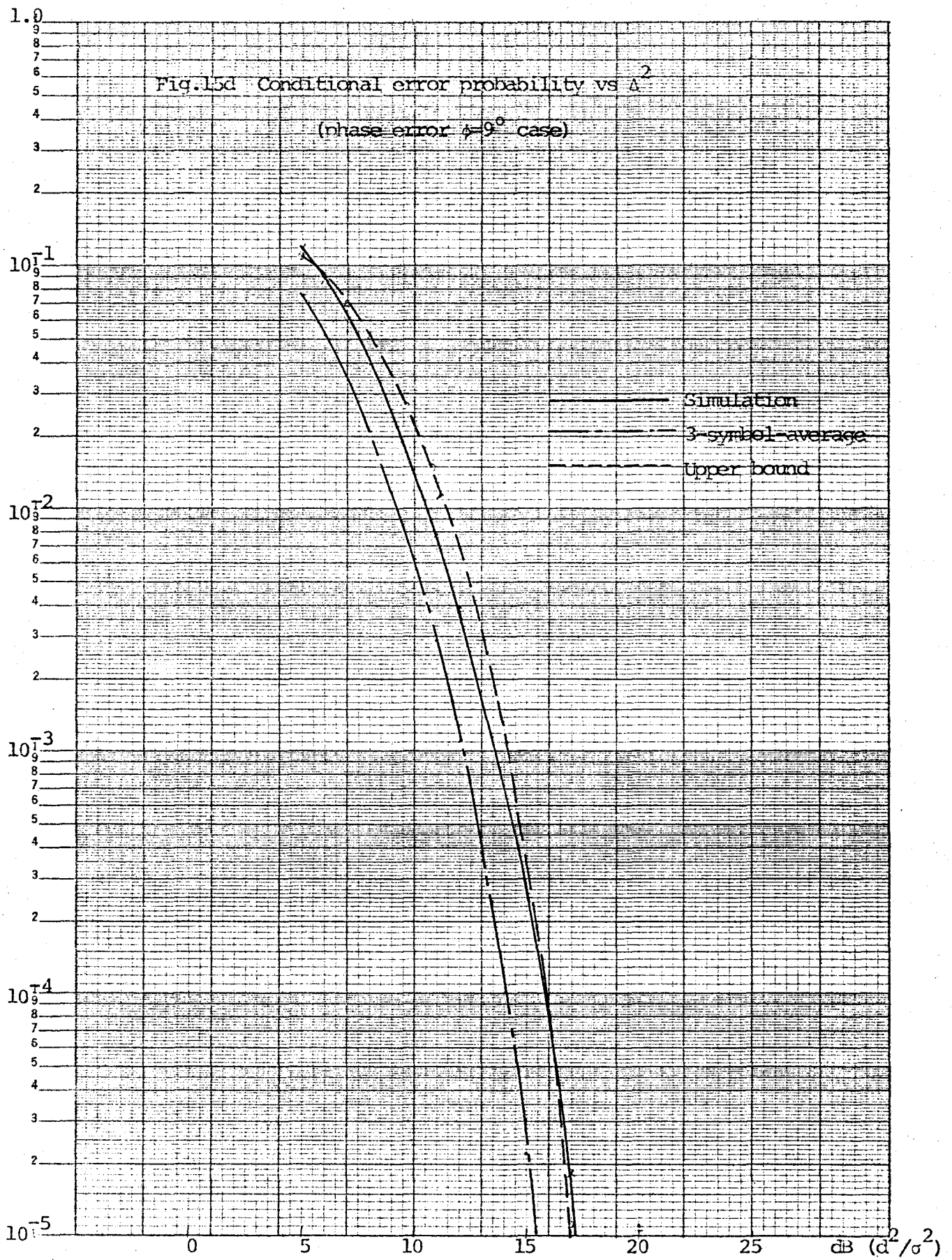
Fig.15d Conditional error probability vs Δ^2
(phase error ϕ=9° case)
Simulation
3-symbol-average
Upper bound
1.0
10^{-1}
10^{-2}
10^{-3}
10^{-4}
10^{-5}
0
5
10
15
20
25
dB (d^2/σ^2)

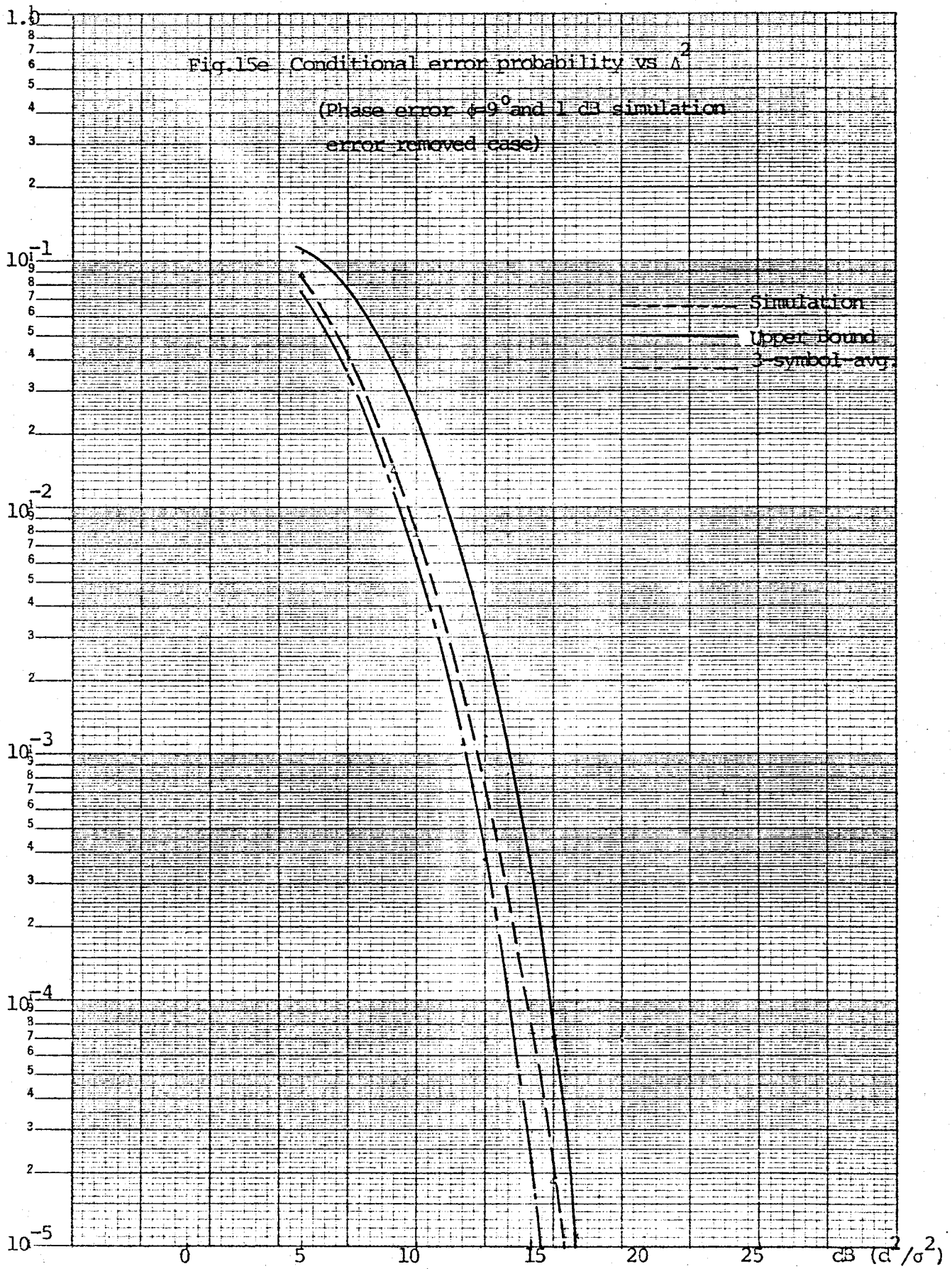

Fig.15e Conditional error probability vs Δ^2

(Phase error ϕ=9° and 1 dB simulation error removed case)

agree with each other. Also, we can see that the simulated curve is approximately the same as the 3-symbol-average curve when the 1 dB difference is removed. Thus we can conclude that the 3-symbol-average curve may be the better one for using to calculate the average symbol error probability.

CHAPTER 3

ESTIMATE-AIDED CARRIER TRACKING LOOP

3.1 Introduction

In the previous chapter, the effect of imperfect carrier synchronization on coherent detection of offset QPSK duobinary signals was studied and was seen to cause a significant loss of performance. To reduce the phase error and thus to achieve more coherent demodulation, various carrier synchronizers [25] and suppressed carrier tracking loops [19-21] have been suggested for use with M-ary PSK signals. The offset duobinary-coded QPSK signal is a suppressed carrier signal, and a successful carrier recovery and phase tracking system must generate highly coherent quadrature reference carrier signals with ideally no penalty in signal to noise ratio and without the need for transmission of a pilot carrier. Furthermore, the reference signal coherence must be independent of the data modulating the carrier. There are several potential candidate techniques for reconstructing the carrier signals. The one proposed in this chapter is an estimate-aided suppressed carrier recovery loop which is illustrated in block diagram form in Fig 16.

In this structure the in-phase channel (I-channel) and quadrature channel (Q-channel) baseband signals $r_I(t)$ and $r_Q(t)$ (cf. Fig.16) are sampled at the times $t=2kT$ and $t=(2k+1)T$ (k integer) respectively and, without being passed to a threshold detector, are directly fed back as shown to cross-multiply the baseband analog signal in the quadrature channel. The purpose of the estimates being fed to the carrier recovery circuit in this way is to create a spectral line at the carrier frequency which may be extracted

by conventional phase-locked loop methods. In the absence of these feedback signals the upper loop output $Z_I(t)$ and the lower loop output $Z_Q(t)$ are small. This is due to the fact that the modulation bandwidth greatly exceeds that of the carrier phase variations and as this latter bandwidth determines the lower and upper loop bandwidth, the filter F(p) would average the modulation to a negligible value. The concept of feeding the estimates back, without being passed to the threshold detector, is suggested in [5]. If we use the detector outputs in the I-channel and Q-channel (i.e. decisions have been made) for feedback purposes, it would complicate the derivation of the loop equation as the nonlinear operation of quantization makes finding the statistics of the detector outputs difficult. But the statistics of the unquantized estimate are easily obtained by using this technique.

The principal theorectical result obtained in this chapter is the solution of the Fokker-Planck equation for the steady-state probability density function of the tracking loop phase error. The study is based on the use of a first order loop in order to obtain a tractable analysis.

3.2 Loop analysis

The loop we propose here is illustrated in Fig 16. The received signal is as in (2.45):

$$y'(t)=\sqrt{2}\{\sum_n c_n h(t-2nT)\cos(\omega_c t+\theta)-\sum_n d_n h(t-(2n+1)T)\sin(\omega_c t+\theta) + n_1(t)\cos(\omega_c t+\theta) - n_2(t)\sin(\omega_c t+\theta)\} \qquad (3.1)$$

where $\{c_n\}$ and $\{d_n\}$ are the differentially encoded binary data bits, with values ± 1; $h(t)$ is the duobinary pulse shape defined in (2.10) and ω_c is the carrier frequency. The carrier phase θ is considered to be a slowly vary-

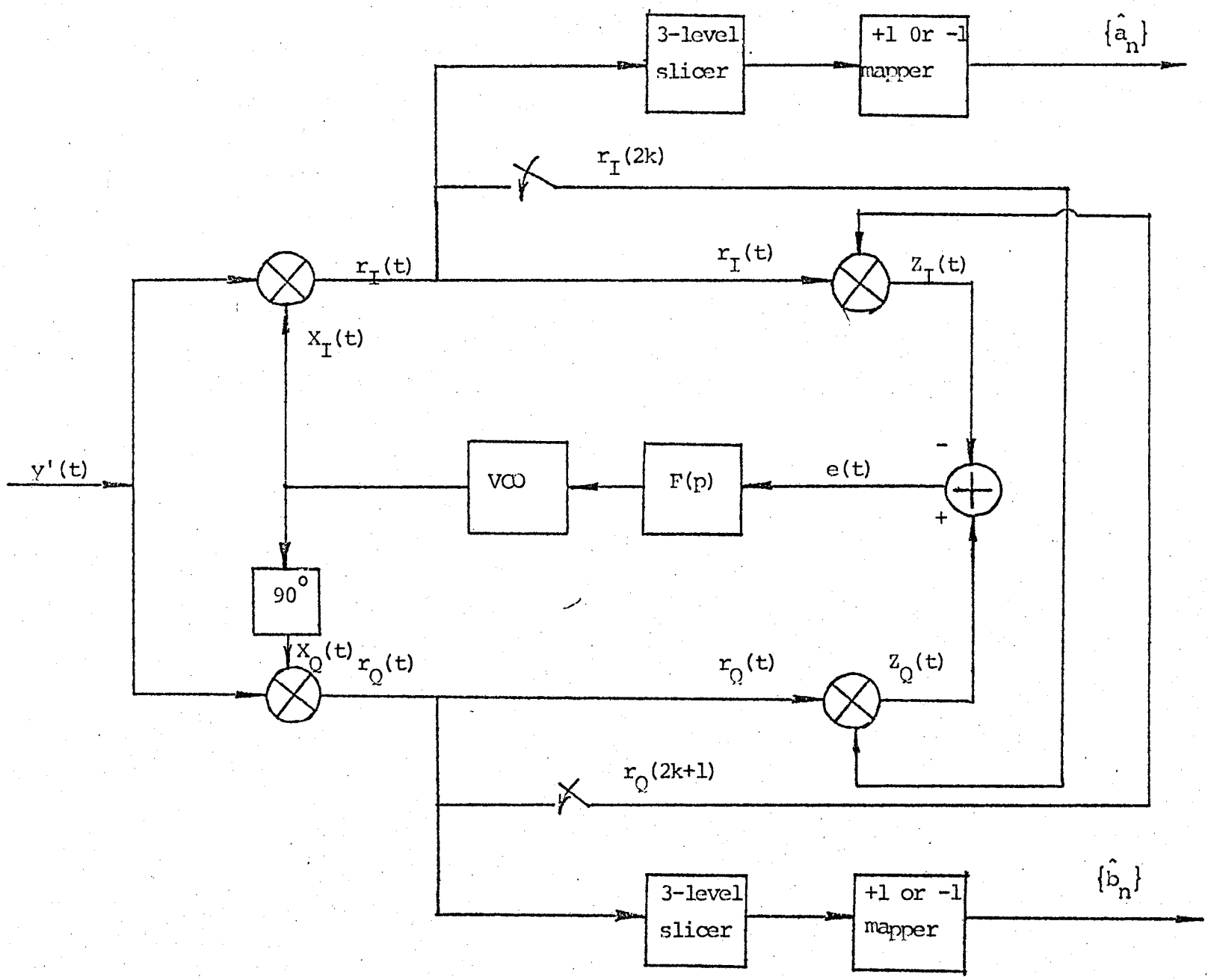

Fig 16. Estimate-aided carrier tracking loop

ing random variable and is taken to be uniformly distributed on $[-\pi,\pi]$. This random phase shift $\theta(t)$ is defined equal to $\theta_o + \Omega_o t$ with θ_o a uniformly distributed random phase and Ω_o the Doppler shift in the input frequency from its nominal value of ω_c. $n_1(t)$ and $n_2(t)$ are the in-phase and quadrature-phase noise components respectively. Here we assume that the noise is characterized as a narrowband Gaussian process, so that $n_1(t)$ and $n_2(t)$ are identically distributed baseband Gaussian processes.

The signal $y'(t)$ is multiplied by the two locally generated quadrature reference signals

$$X_I(t) = \sqrt{2}\, K_1 \cos(\omega_c t + \hat{\theta}(t))$$

$$X_Q(t) = \sqrt{2}\, K_1 \sin(\omega_c t + \hat{\theta}(t))$$

where K_1 is the voltage-controlled oscillator (VCO) rms amplitude, and $\hat{\theta}(t)$ is the local estimate of $\theta(t)$. The two products of the multiplication (neglecting double frequency terms) are

$$r_I(t) = K_m y'(t) X_I(t)$$

$$= K_1 K_m \{ \sum_n c_n h(t-2nT) \cos \phi(t) - \sum_n d_n h(t-(2n+1)T) \sin\phi(t) + N_I(t,\phi) \}$$

and (3.2a)

$$r_Q(t) = K_m y'(t) X_Q(t)$$

$$= K_1 K_m \{ \sum_n d_n h(t-(2n+1)T) \cos\phi(t) + \sum_n c_n h(t-2nT) \sin\phi(t) + N_Q(t,\phi) \}$$

(3.2b)

where K_m is the phase detector gain and $\phi(t)$ is defined as the loop phase error and is equal $\theta(t)-\hat{\theta}(t)$. Also the noise terms $N_I(t,\theta)$ and $N_Q(t,\theta)$ are given by

$$N_I(t,\phi) = n_1(t)\cos\phi(t) - n_2(t)\sin\phi(t) \tag{3.3a}$$

$$N_Q(t,\phi) = n_1(t)\sin\phi(t) + n_2(t)\cos\phi(t) \tag{3.3b}$$

In each signal the second term is known as the quadrature distortion term and is proportional to $\sin\phi$. The baseband signals $r_I(t)$ and $r_Q(t)$ are then sampled at the times $t=2kT$ and $t=(2k+1)T$ (k integer) respectively for feedback purposes.

Now consider the pulse $h(t-2nT)$ at the sampling times $t=2kT$. It may be written as

$$\begin{aligned} h(t-2nT) &= h(2kT-2nT) \\ &= \frac{4}{\pi} \cdot \frac{\cos\left[\frac{\pi}{2T}(2k-2n)T\right]}{1 - \frac{(2k-2n)^2T^2}{T^2}} \\ &= \frac{4}{\pi}\frac{(-1)^{k-n}}{1-4(k-n)^2} \end{aligned} \tag{3.4a}$$

Similarly, the pulse shape $h(t-(2n+1)T)$ in the quadrature distortion term at the same time $t=2kT$ is given by

$$\begin{aligned} h(t-(2n+1)T) &= h(2kT-2nT-T) \\ &= \frac{4}{\pi}\frac{\cos\left[\frac{\pi}{2T}(2k-2n-1)T\right]}{1-\frac{(2k-2n-1)^2T^2}{T^2}} \\ &= \frac{4}{\pi}\frac{\cos\left[(k-n-1/2)\pi\right]}{1-(2k-2n-1)^2} \\ &= \begin{cases} 1 & n=k,k-1 \\ 0 & n\neq k,k-1 \end{cases} \end{aligned} \tag{3.4b}$$

In the same manner, the signal $r_Q(t)$ is sampled at the times $t=(2k+1)T$. The pulse $h(t-(2n+1)T)$ at these sampling instants is

$$h(t-(2n+1)T) = h(\ (2k+1)T - (2n+1)T\ )$$

$$= h(\ (2k-2n)T\ )$$

$$= \frac{4}{\pi}\ \frac{(-1)^{k-n}}{1-4(k-n)^2} \qquad (3.5a)$$

Similarly, the pulse shape in the quadrature distortion term at $t=(2k+1)T$ is given by

$$h(t-2nT) = h(\ (2k+1)T - 2nT\ )$$

$$= \frac{4}{\pi}\ \frac{\cos\ [\ (k-n+1/2)\pi\ ]}{1\ -\ (2k-2n+1)^2}$$

$$= \begin{cases} 1 & n=k,k+1 \\ 0 & n\neq k,k+1 \end{cases} \qquad (3.5b)$$

Using these results we may write the sampled sequences $r_I(2k)$ and $r_Q(2k+1)$ as

$$r_I(2k) = K_1K_m\ \{\ \frac{4}{\pi}\ \sum_n\ c_n\ \frac{(-1)^{k-n}}{1-4(k-n)^2}\cos\phi(t)\ -\ (d_k+d_{k-1})\sin\phi(t)\ +\ N_I(2k)\ \} \qquad (3.6a)$$

$$r_Q(2k+1) = K_1K_m\ \{\ \frac{4}{\pi}\ \sum_n\ d_n\ \frac{(-1)^{k-n}}{1-4(k-n)^2}\cos\phi(t)+(c_k+c_{k+1})\sin\phi(t)\ +\ N_Q(2k+1)\ \} \qquad (3.6b)$$

where $N_I(2k)$ and $N_Q(2k+1)$ are Gaussian random variables.

The sampled signal $r_I(2k)$ is then cross-multiplied with the continuous low pass signal $r_Q(t)$ as shown in Fig 16 and produces the signal $Z_Q(t)$. Similarly, the sampled signal $r_Q(2k+1)$ is cross-multiplied with the signal $r_I(t)$ and produces the signal $Z_I(t)$. These two signals are then subtracted and their difference forms an error signal at the input to the loop filter $F(p)$. This error signal, denoted by $e(t)$, is given by

$$e(t) = Z_I(t) - Z_Q(t)$$

$$= r_I(t)r_Q(2k+1) - r_Q(t)r_I(2k)$$

Therefore e(t) can be written as

$$e(t) = K_1K_m \{ [\sum_n r_Q(2k+1)c_n h(t-2nT)\cos\phi(t) - \sum_n r_Q(2k+1)d_n h(t-(2n+1)T\sin\phi(t) + r_Q(2k+1)N_I(t,\phi)] - [\sum_n r_I(2k)d_n h(t-(2n+1)T)\cos\phi(t) + \sum_n r_I(2k)c_n h(t-2nT)\sin\phi(t) + r_I(2k)N_Q(t,\phi)] \} \quad (3.7)$$

The instantaneous frequency of the VCO output is proportional to the filtered error signal via the relation

$$\dot{\hat{\theta}}(t) = K_V F(p)e(t)$$

where K_V is the VCO gain in rad/V/sec and the dot denotes differentiation w.r.t. time. Recalling that $\hat{\theta}(t)=\theta(t)-\phi(t)$, we can write

$$\dot{\phi}(t) = \dot{\theta}(t) - \dot{\hat{\theta}}(t)$$

$$= \dot{\theta}(t) - K_V F(p)e(t) \quad (3.8)$$

which is a stochastic integro-differential equation. Since $\theta(t) \triangleq \theta_o + \Omega_o t$ where θ_o is a uniformly distributed random phase and Ω_o is the Doppler shift in the input frequency from its norminal value of ω_c we obtain

$$\dot{\theta}(t) = \Omega_o$$

Thus equation (3.8) can be rewritten as

$$\dot{\phi}(t) = \Omega_o - K_V F(p)e(t) \quad (3.9)$$

The analysis of the loop to find the phase detector characteristic including the effect of noise rests on the assumption [20] that

$$W_L << \frac{1}{2T} \quad (3.10)$$

where W_L is the two-sided loop bandwidth. This assumption indicates that the phase process varies much more slowly than the signal (modulation) process. Since we assumed previously that the noise is characterized as a

narrowband process, its correlation time [19] is much less than the length 2T of the signaling interval, and thus the signal sees the noise as essentially white. Also the assumption in (3.10) implies that we can take the statistical average of the stochastic differential equation in (3.9) over the data. Thus we can evaluate statistical averages as follow:

$$E\,[\,r_Q(2k+1)c_n\,]$$
$$= E\{K_1K_m[\,\frac{4}{\pi}\sum_n c_n d_n\,\frac{(-1)^{k-n}}{1-4(k-n)^2}\cos\phi(t) + c_n(c_k+c_{k+1})\sin\phi(t) + c_n N_Q(2k+1)\,]\}$$
$$= \begin{cases} K_1K_m\sin\phi(t) & n=k,k+1 \\ 0 & n\neq k,k+1 \end{cases}$$

and

$$E\,[r_Q(2k+1)d_n]$$
$$= E\,\{K_1K_m[\,\frac{4}{\pi}\sum_n d_n d_n\,\frac{(-1)^{k-n}}{1-4(k-n)^2}\cos\phi(t) + d_n(c_k+c_{k+1})\sin\phi(t) + d_n N_Q(2k+1)\,]\}$$
$$= K_1K_m\frac{4}{\pi}\,\frac{(-1)^{k-n}}{1-4(k-n)^2}\cos\phi(t)$$

Similarly, we obtain

$$E\,[\,r_I(2k)d_n\,]$$
$$= \begin{cases} -K_1K_m\sin\phi(t) & n=k,k-1 \\ 0 & n\neq k,k-1 \end{cases}$$

and

$$E\,[\,r_I(2k)c_n\,]$$
$$= K_1K_m\,\frac{4}{\pi}\,\frac{(-1)^{k-n}}{1-4(k-n)^2}\cos\phi(t)$$

Hence we can write under the above assumptions the stochastic integrodifferential equation of the loop as

$$\dot{\phi}(t) = \Omega_o - K_v\{(K_1K_m)^2[\sum_k^{k+1}\sin\phi(t)\,(\frac{1}{2T}\int_{2kT}^{(2k+2)T} h(t-2nT)\,dt)\cos\phi(t)$$

$$- \sum_n \left(\frac{4}{\pi} \frac{(-1)^{k-n}}{1 - 4(k-n)^2} \cos\phi(t) \right) \left(\frac{1}{2T} \int_{2kT}^{(2k+2)T} h(t-(2n+1)T)\,dt \right) \sin\phi(t)$$

$$+ \frac{1}{K_1 K_m} E\left(N_I(t,\phi) r_Q(2k+1) \right) - \frac{1}{K_1 K_m} E\left(N_Q(t,\phi) r_I(2k) \right)$$

$$- \sum_n \left(\frac{4}{\pi} \frac{(-1)^{k-n}}{1 - 4(k-n)^2} \cos\phi(t) \right) \left(\frac{1}{2T} \int_{(2k-1)T}^{(2k+1)T} h(t-2nT)\,dt \right) \sin\phi(t)$$

$$- \sum_n (-\sin\phi(t)) \left(\frac{1}{2T} \int_{(2k-1)T}^{(2k+1)T} h(t-(2n+1)T)\,dt \right) \cos\phi(t) \Big] \Big\} \qquad (3.11)$$

where we have assumed, for the sake of simplicity, a first order loop ($F(p)=1$ in (3.9)). Also, we have taken a time average of the stochastic differential equation in (3.9) over the signal as implied in the assumption in (3.10). In the appendix (3A), these corresponding numerical time average values are evaluated where we can see that the values from the term

$$\frac{2}{35} \left(\frac{1}{2T} \int_{2kT}^{(2k+2)T} h(t-(2k+7)T)\,dt \right)$$

are so small that they can be neglected, and only 3 terms needed to be included in subsequent work. Substituting these values into equation (3.11), we obtain

$$\dot{\phi}(t) = \Omega_o - K_v (K_1 K_m)^2 [\, K \sin 2\phi(t) + n'(t) \,] \qquad (3.12)$$

where $K \simeq 2 * 1.95 - \frac{4}{\pi} [\, 1.174 + \frac{2}{3}(0.45) + \frac{2}{15}(0.055) \,]$

$= 1.9$ (a finite constant term)

The noise term $n'(t)$ is essentially Gaussian white noise with spectral height

$$N = 2N_o \Big[\sum_n \left(\frac{4}{\pi} \frac{(-1)^{k-n}}{1 - 4(k-n)^2} \right)^2 \cos^2\phi(t) + 2 \sin^2\phi(t) + \sigma^2 \Big]$$

where σ^2 is the variance of $N_I(2k)$ and $N_Q(2k+1)$, and both are zero mean Gaussian random variables defined in (3.2). The form of $n'(t)$ arises because $N_I(t,\phi)$ and $N_Q(t,\phi)$ in the last term of (3.11) is approximated as Gaussian white noise term as discussed above. The assumption of $n'(t)$ Gaussian is necessary because the problem cannot be solved by Fokker-Planck techniques otherwise.

Let $\sigma_m^2 = \sum_n \left(\frac{4}{\pi} \frac{(-1)^{k-n}}{1 - 4(k-n)^2} \right)^2$. This series converges to a constant value of 2 (Appendix 3B). Thus

$$N = 2N_o(2\cos^2\phi + 2\sin^2\phi + \sigma^2) = N_o(4 + 2\sigma^2)$$

Equation (3.12) can then be rewritten as

$$\begin{aligned}\dot{\phi}(t) &= \Omega_o - K_v(K_1K_m)^2 K\sin 2\phi(t) - K_v(K_1K_m)^2 n'(t) \\ &= \Omega_o - K_o K\sin 2\phi(t) - K_o n'(t) \\ &= \Omega_o - K_o K\sin 2\phi(t) - n''(t) \end{aligned} \qquad (3.13)$$

Where $K_o \triangleq K_v K_1^2 K_m^2$ is the open loop gain and $n''(t)$ is a white noise process with spectral density

$$S(w) = K_o N_o(4 + 2\sigma^2) = \frac{N_o}{2}[2K (4+2\sigma^2)] \qquad (3.14)$$

3.3 Nonlinear analysis of the first order data-aided loop

For the zero detuning situation (i.e. $\Omega_o=0$), the loop equation may be written as

$$\dot{\phi}(t) = -KK_o \sin 2\phi(t) - n''(t) \qquad (3.15)$$

The pdf of ϕ may be obtained by invoking the Fokker-Planck equation [22,p86]. For the stochastic differential equation

$$\dot{\phi}(t) = P(\phi) + \sqrt{G(\phi)}\ \underline{n}(t) \qquad (3.16)$$

where $\underline{n}(t)$ is Gaussian white noise, the Fokker-Planck equation is

$$\frac{\partial}{\partial t} p(\phi,t) = -\frac{\partial}{\partial \phi} P(\phi)p(\phi) + \frac{N_o}{4} \frac{\partial^2 G(\phi)p(\phi)}{\partial \phi^2} \qquad (3.17)$$

where $p(\cdot)$ is the probability density function of ϕ and $N_o/2$ is the two-sided spectral height of $\underline{n}(t)$. The steady state modulo 2π solution is of principle interest (i.e. $\frac{\partial p}{\partial t} = 0$) since it characterizes steady state system behavior. Therefore equation (3.17) becomes

$$\frac{d}{d\phi} G(\phi)p(\phi) - \frac{4}{N_o} P(\phi)p(\phi) = C \qquad \text{(C-constant)} \qquad (3.18)$$

Comparing equations (3.15) and (3.16), we can see that

$$P(\phi) = -KK_o \sin 2\phi$$

$$G(\phi) = K_o(4+2\sigma^2)$$

Using these results in equation (3.18), integrating and invoking the boundary condition $p(\pi) = p(-\pi)$, yields the probability density function (pdf) of the loop phase error as

$$p(\phi) = N_c \exp[U(\phi)] \qquad (3.19)$$

where N_c is a normalization constant and the potential function $U(\phi)$ is given by

$$U(\phi) = \alpha \cos 2\phi$$

where $\alpha \triangleq \frac{K}{N_o(2+\sigma^2)}$

An explanation of the pdf derivation is given in Appendix 3C and $p(\phi)$ is plotted against ϕ in Fig 18.

3.4 Results and Conclusions

The loop phase detector characteristic (S-curve)-$G(\phi)$ is a sinusoidal function. In equation (3.12), it is seen that $G(\phi)=\sin 2\phi$ and this is plotted in Fig 17. This S-curve is independent of the signal to noise ratio. Also, the loop integral-differential equation in (3.12) shows that this estimate-aided loop structure is similar to the conventional Costas loop [30]. We note that the loop exhibits the desired stable lock points at $\phi=0^{\circ}$ and $\phi=180^{\circ}$. This shows that only two phase ambiguities exist for offset QPSK system which is true since the bit transitions for one binary channel occur at the middle of the bit intervals for the other channel. Thus a 180° phase ambiguity cannot exist. A detailed discussion of the phase ambiguity in an offset QPSK system is given in [3][4] and [7].

In chapter 2, we established expressions for the average probability of symbol error conditioned on a given loop phase error. From these expressions and the pdf $p(\phi)$ of the carrier phase error in (3.19) associated with the carrier tracking loop, we can, assuming that a "genie" correctly resolves the quadrant phase ambiguity, compute the average symbol error probability as

$$P_E = 2 \int_{-\pi/2}^{\pi/2} P_e(\phi) p(\phi) d\phi \qquad (3.20)$$

where $p(\phi)$ is given by (3.19) and $P_e(\phi)$ is given by (2.65) or (2.66).

This estimate-aided loop requires exact multiplication of the analog signals $r_I(t)$ and $r_Q(2k+1)$, and, $r_Q(t)$ and $r_I(2k)$. In practice,

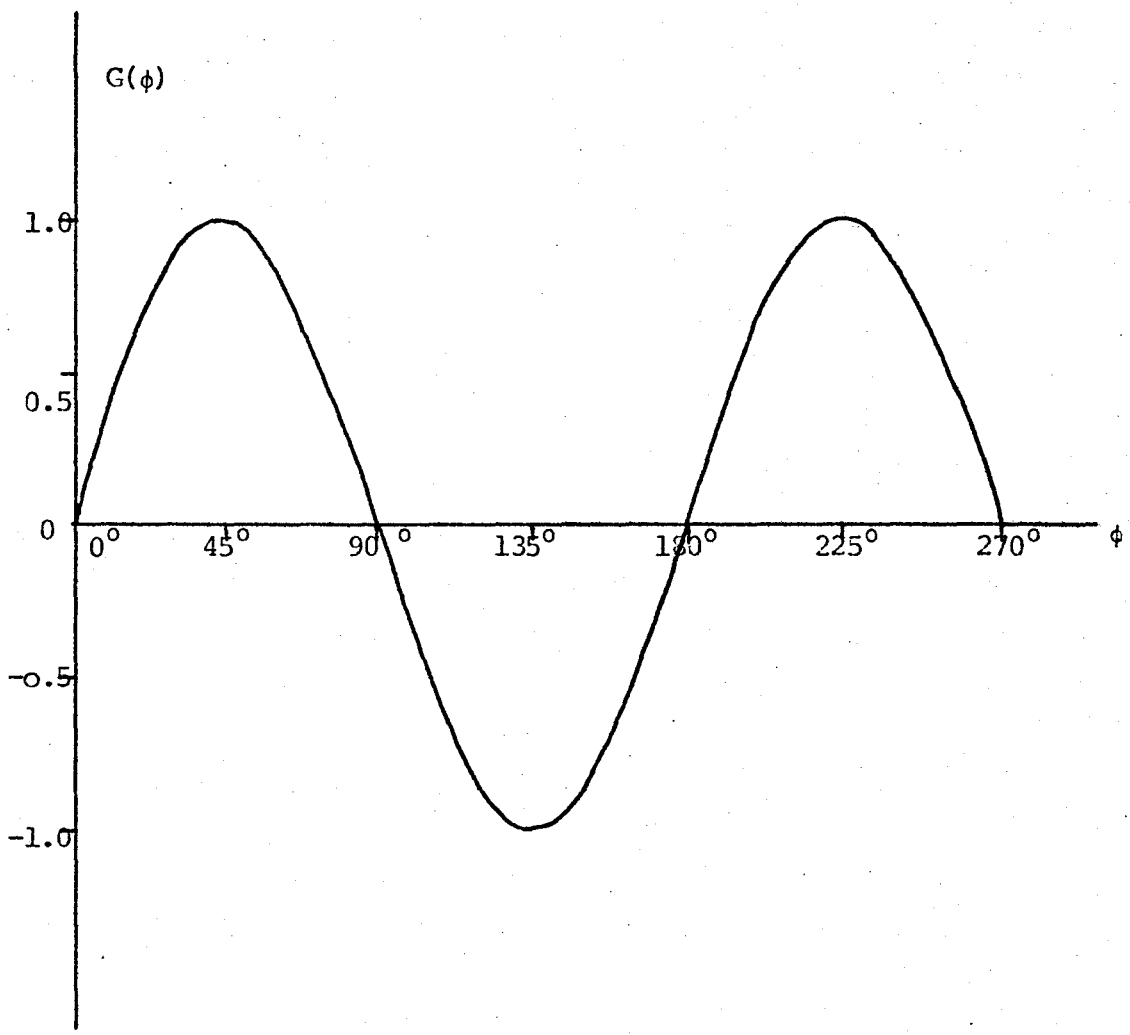

Fig.17 The phase detector characteristic (S-curve) for estimate-aided carrier tracking loop.

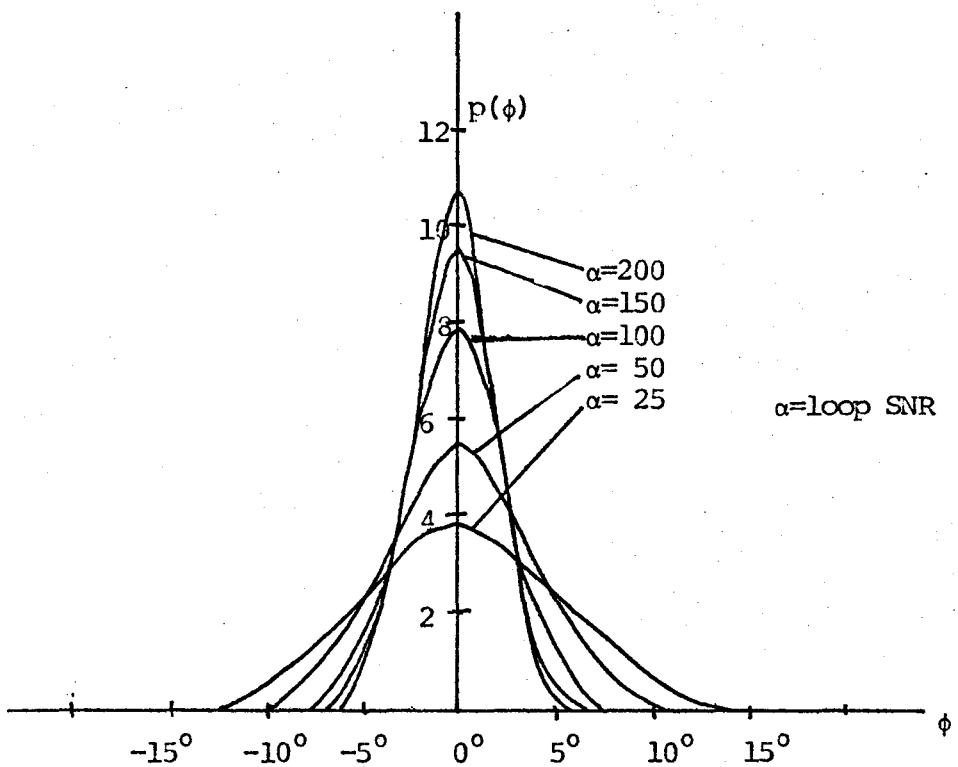

Fig.18 Probability density function of the phase error for estimate-aided carrier tracking loop

precise analog wideband multiplier are both difficult to implement and expensive. Thus the loop described in this chapter may be difficult to implement. Also the time delays required may be a problem for this loop structure since no decision has been made before any feedback operation, and analog delay lines must be used. In the next chapter, we will investigate decision-directed feedback carrier tracking loop structures which tend to avoid the problems mentioned above. Decision feedback has the advantage that the quantities being fed back are clean decisions which even though they may be in error are noise free.

CHAPTER 4

DECISION DIRECTED FEEDBACK LOOP

4.1 Introduction

Due to the implementation and time delay problems for the estimate data-aided loop, a suppressed carrier quadriphase decision feedback loop which has been modified to accomodate the offset QPSK duobinary signal is investigated in this chapter. Simon and Smith also modified a similar decision feedback loop structure to accomodate QASK signals [6] and offset QASK signals [7]. In our system, the modification of the basic structure is the inclusion of sample and hold circuit elements in the in-phase and quadrature arms, and some delay elements. The three-level decoder output is then fed back for tracking purposes.

4.2 Development of the Stochastic Integro-differential Equation of Operation for a decision-feedback Loop.

The loop structure is illustrated in Fig 19. The received signal $y'(t)$ is demodulated to obtain baseband signals, $r_I(t)$ and $r_Q(t)$, in the I-channel and Q-channel respectively. Similar to the development in chapter 2, the sampled sequences of $r_I(t)$ and $r_Q(t)$ at the times $t=(2k-1)T$ and $t=2kT$ (k integer) are given as

$$r_I(2k-1) = K_1K_m\left[c_k\cos\phi + c_{k-1}\cos\phi - \frac{4}{\pi}\sum_n d_n \frac{(-1)^{k-n-1}}{1-4(k-n-1)^2}\sin\phi + N_I(2k-1)\right] \tag{4.1a}$$

and

$$r_Q(2k) = K_1K_m\left[d_k\cos\phi + d_{k-1}\cos\phi + \frac{4}{\pi}\sum_n c_n \frac{(-1)^{k-n}}{1-4(k-n)^2}\sin\phi + N_Q(2k)\right] \tag{4.1b}$$

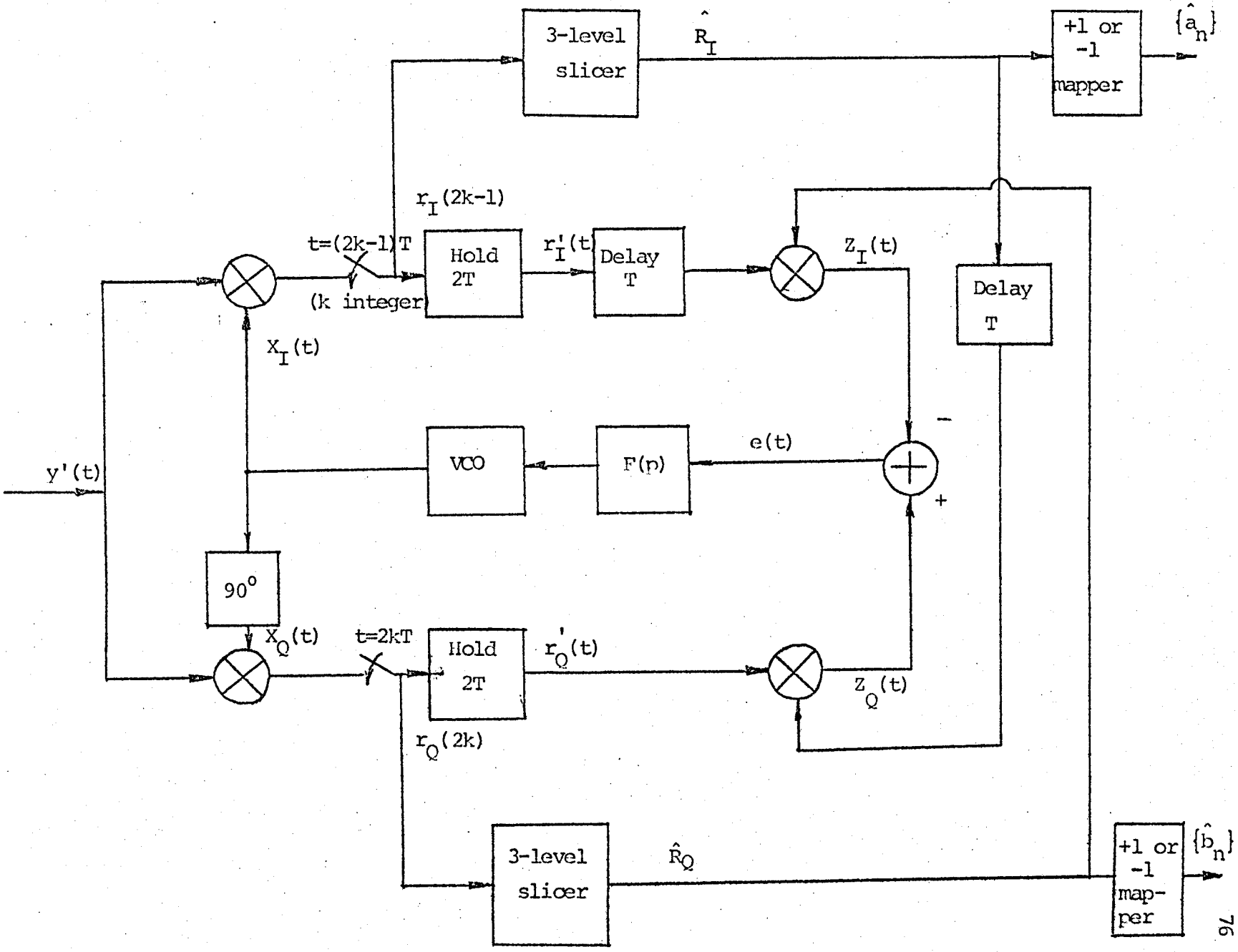

Fig 19. Decision directed feedback loop

where K_1 is the voltage-controlled oscillator (VCO) rms amplitude, K_m is the phase detector gain and $\phi(t)$ is the loop phase error as defined previously.

The sampled sequences are then passed through the threshold detector to obtain the outputs $\hat{R}_I$ and $\hat{R}_Q$ having the three values ±2 or 0. At the same time the signals $r_I(2k-1)$ and $r_Q(2k)$ are passed through the hold circuits having a hold time of 2T sec. Thus the outputs of the hold circuits for the I- and Q-channels can be written as

$$r_I'(t) = \sum_i r_I(2k-1)g(t-iT) \qquad i=2k-1 \tag{4.2a}$$

and

$$r_Q'(t) = \sum_j r_Q(2k)g(t-jT) \qquad j=2k \tag{4.2b}$$

assuming that $g(t)$ is a rectangular pulse shape ($g(t)=1$ for $0 \le t < 2T$), $r_I'(t)$ and $r_Q'(t)$ can be rewritten as

$$r_I'(t) = K_1K_m[\, R_I\cos\phi - D_Q\sin\phi + N_I'] \qquad iT \le t < (i+2)T \tag{4.3a}$$

and

$$r_Q'(t) = K_1K_m[\, R_Q\cos\phi + D_I\sin\phi + N_Q' \,] \qquad jT \le t < (j+2)T \tag{4.3b}$$

where

$$R_I \triangleq c_k + c_{k-1}$$

$$R_Q \triangleq d_k + d_{k-1}$$

$$D_Q \triangleq \frac{4}{\pi}\sum_n d_n \frac{(-1)^{k-n-1}}{1 - 4(k-n-1)^2}$$

$$D_I \triangleq \frac{4}{\pi}\sum_n c_n \frac{(-1)^{k-n}}{1 - 4(k-n)^2} \tag{4.4}$$

The low pass signal $r_I'(t)$ is then delayed by T sec and cross-multiplied by the current data decision $\hat{R}_Q$. At the same time, the current data decision $\hat{R}_I$ is delayed by T sec and cross-multiplied by the signal $r_Q'(t)$. The difference is then fed as an error signal to the loop filter F(p). This error signal,denoted by e(t),is given by

$$e(t) = [\exp(-pT)\hat{R}_I][r_Q'(t)] - [\exp(-pT)r_I'(t)][\hat{R}_Q] \qquad (4.5)$$

$$iT \leq t < (i+1)T$$

Now, as previously the instantaneous frequency of the VCO output is proportional to the filtered error signal via the relation

$$\dot{\hat{\theta}}(t) = K_V F(p)e(t) \qquad (4.6)$$

where K_V is the VCO gain in rad/V/sec and the dot denotes differentiation w.r.t. time. Recalling that $\hat{\theta}(t)=\theta(t)-\phi(t)$, we can write

$$\dot{\phi}(t) = \dot{\theta}(t) - \dot{\hat{\theta}}(t)$$

$$= \dot{\theta}(t) - K_V F(p)e(t) \qquad (4.7)$$

Substituting (4.5) into (4.7), we obtain

$$\dot{\phi}(t) = \dot{\theta}(t) - K_V K_m K_1 [\exp(-pT)F(p)][\hat{R}_I(R_Q\cos\phi+D_I\sin\phi+N_Q') - \hat{R}_Q(R_I\cos\phi-D_Q\sin\phi+N_I')] \qquad (4.8)$$

Therefore,

$$\dot{\phi}(t) = \dot{\theta}(t) - K_0 F(p)\exp(-pT)[(\hat{R}_I R_Q-\hat{R}_Q R_I)\cos\phi+(\hat{R}_I D_I+\hat{R}_Q D_Q)\sin\phi + \hat{R}_I N_Q' - \hat{R}_Q N_I'] \qquad (4.9)$$

where $K_0 = K_1 K_m K_V$ (4.10)

Under the same assumptions as made in chapter 3, we can take the statistical average of the stochastic equation over the data.

Thus let

$$G(\phi) \triangleq E[(\hat{R}_I D_I + \hat{R}_Q D_Q)|\phi(t)]\sin\phi + E[(\hat{R}_I R_Q - \hat{R}_Q R_I)|\phi(t)]\cos\phi$$

and

$$H(\phi) \triangleq E[\hat{R}_I^2|\phi(t)] + E[\hat{R}_Q^2|\phi(t)] \qquad (4.11)$$

Assuming that the loop is first order (i.e. $F(p)=1$), then the stochastic integro-differential equation describing loop operation can be rewritten as

$$\dot{\phi}(t) = \dot{\theta}(t) - K_0[G(\phi) + H^{1/2}(\phi)N_e(t)] \qquad (4.12)$$

Since we assumed $W_L << 1/2T$ as in(3.10), $\exp(-j\omega T)$ is approximately unity for all ω within the loop bandwidth, and from a steady state performance standpoint, it can be neglected. However, the delay elements are important in assuring that the $r_I'(t)$ and $r_Q'(t)$ signal components are multiplied by the $\hat{R}_I$ and $\hat{R}_Q$ decisions corresponding to the same symbol interval.

4.3 Evaluation of the loop phase detector characteristic (S-curve)--$G(\phi)$.

The loop S-curve $G(\phi)$ of equation (4.11) can be written as

$$G(\phi) = G_1(\phi)\sin\phi + G_2(\phi)\cos\phi \qquad (4.13)$$

where

$$G_1(\phi) = E[(\hat{R}_I D_I + \hat{R}_Q D_Q)|\phi(t)]\sin\phi \qquad (4.14)$$

$$G_2(\phi) = E[(\hat{R}_I R_Q - \hat{R}_Q R_I)|\phi(t)]\cos\phi \qquad (4.15)$$

Determination of the S-curve $G(\phi)$ requires evaluation of $E(\hat{R}_I D_I|\phi)$ and $E(\hat{R}_I R_Q|\phi)$ only, since $E(\hat{R}_Q D_Q|\phi)=E(\hat{R}_I D_I|\phi)$ and $E(\hat{R}_Q R_I|\phi)=-E(\hat{R}_I R_Q|\phi)$ (Appendix 4A).

Before evaluating $G(\phi)$, we make the approximation in order to permit straight forward evaluation that

$$D_Q = \frac{4}{\pi}\left[d_{k-1} + \frac{1}{3} d_k + \frac{1}{3} d_{k-2} \right]$$
$$D_I = \frac{4}{\pi}\left[c_k + \frac{1}{3} c_{k+1} + \frac{1}{3} c_{k-1} \right] \qquad (4.16)$$

The worst case for taking only three symbols can be evaluated as

$$D_Q = \frac{4}{\pi}\left[1 + \frac{1}{3} + \frac{1}{3} \right] = \frac{20}{3\pi}$$

where we have assumed d_k, d_{k-1} and d_{k-2} equal 1.

The corresponding situation for taking an infinite number of symbols into account for D_Q and D_I is equal $8/\pi$ as in equation (2.64).

The percentage error in this case is

$$\frac{\frac{4}{\pi}(2-5/3)}{\frac{4}{\pi}(2)} \cdot 100\ \% = 16.67\ \% \qquad (4.17)$$

Bearing this in mind, we can evaluate $G(\phi)$. Now we note that

$$\hat{R}_I = 2,\ 0 \text{ or } -2$$
$$\hat{R}_Q = 2,\ 0 \text{ or } -2$$
$$D_Q = \frac{4}{\pi}\left[d_{k-1} + \frac{1}{3} d_k + \frac{1}{3} d_{k-2} \right]$$
$$D_I = \frac{4}{\pi}\left[c_k + \frac{1}{3} c_{k-1} + \frac{1}{3} c_{k+1} \right]$$
$$R_I = c_k + c_{k-1}$$
$$R_Q = d_k + d_{k-1}$$

and define the sets

$$\bar{D} = \{ d_{k-1}, d_k, d_{k-2} \}$$
$$C = \{ c_k, c_{k-1}, c_{k+1} \} \qquad (4.18)$$

We can now evaluate $E[\hat{R}_I R_Q|\phi]$ as

$$E[\hat{R}_I R_Q|\phi]$$
$$=E[E(\hat{R}_I R_Q|C,D,\phi)]$$
$$=E[2R_Q|\hat{R}_I=2]Pr[\hat{R}_I=2|\phi,C,D] + E[-2R_Q|\hat{R}_I=-2]Pr[\hat{R}_I=-2|\phi,C,D]$$
$$= \sum_C \sum_D 2R_Q[Pr(\hat{R}_I=2|\phi,C,D) - Pr(\hat{R}_I=-2|\phi,C,D)]Pr(D)Pr(C)$$
$$= 2\sum_D R_Q \{ \sum_C [Pr(\hat{R}_I=2|\phi,C,D) - Pr(\hat{R}_Q=-2|\phi,C,D)]Pr(C) \} Pr(D) \quad (4.19)$$

Similarly

$$E[\hat{R}_Q R_I|\phi]$$
$$=2\sum_C R_I \{ \sum_D [Pr(\hat{R}_Q=2|\phi,C,D) - Pr(\hat{R}_Q=-2|\phi,C,D)]Pr(D) \} Pr(C) \quad (4.20)$$

$$E[\hat{R}_I D_I|\phi]$$
$$= 2\sum_C D_I \{ \sum_D [Pr(\hat{R}_I=2|\phi,C,D) - Pr(\hat{R}_I=-2|\phi,C,D)]Pr(D) \} Pr(C) \quad (4.21)$$

$$E[\hat{R}_Q D_Q|\phi]$$
$$= 2\sum_D D_Q \{ \sum_C [Pr(\hat{R}_Q=2|\phi,C,D) - Pr(\hat{R}_Q=-2|\phi,C,D)]Pr(C) \} Pr(D) \quad (4.22)$$

From equation (4.3), it can be shown that

$$N_I' = r_I(2k-1) - R_I\cos\phi + D_Q\sin\phi \quad (4.23)$$

$$N_Q' = r_Q(2k) - R_Q\cos\phi - D_I\sin\phi \quad (4.24)$$

Conditioned on the phase error ϕ, and the symbols $c_k, c_{k-1}, d_k, d_{k-1}$ and d_{k-2}, N_I' is Gaussian distributed and thus the conditional probability density function (pdf) for $r_I(2k-1)$ is

$$p(r_I(2k-1)|R_I\cos\phi - D_Q\sin\phi)$$
$$= \frac{1}{\sqrt{2\pi}\sigma} \exp[-(r_Q(2k) - R_Q\cos\phi - D_I\sin\phi)^2/2\sigma^2] \quad (4.25)$$

Similarly, the conditional pdf for $r_Q(2k)$ is

$$p[\, r_Q(2k) \,|\, R_Q\cos\phi + D_I\sin\phi \,]$$

$$= \frac{1}{\sqrt{2\pi}\sigma} \exp[\, -(r_Q(2k) - R_Q\cos\phi - D_I\sin\phi)^2/2\sigma^2] \qquad (4.26)$$

Hence

$$\Pr(\hat{R}_I = 2 \,|\, \phi, C, D)$$

$$= \int_1^{\infty} \frac{1}{\sqrt{2\pi}\sigma} \exp[\, -(r_I(2k-1) - R_I\cos\phi + D_Q\sin\phi)^2/2\sigma^2]\, dr_I(2k-1)$$

$$= Q\left(\frac{1 - R_I\cos\phi + D_Q\sin\phi}{\sigma}\right) \qquad (4.27)$$

where $Q(x) \triangleq \frac{1}{\sqrt{2\pi}} \int_x^{\infty} \exp(-y^2/2)\, dy$

Similarly,

$$\Pr(\hat{R}_I = -2 \,|\, \phi, C, D)$$

$$= \int_{-\infty}^{-1} \frac{1}{\sqrt{2\pi}\sigma} \exp[\, -(r_I(2k-1) - R_I\cos\phi + D_Q\sin\phi)^2/2\sigma^2]\, dr_I(2k-1)$$

$$= Q\left(\frac{1 + R_I\cos\phi - D_Q\sin\phi}{\sigma}\right) \qquad (4.28)$$

Therefore

$$\Pr(\hat{R}_I = 2 \,|\, \phi, C, D) - \Pr(\hat{R}_I = -2 \,|\, \phi, C, D)$$

$$= Q\left(\frac{1 - R_I\cos\phi + D_Q\sin\phi}{\sigma}\right) - Q\left(\frac{1 + R_I\cos\phi - D_Q\sin\phi}{\sigma}\right) \qquad (4.29)$$

In a similar manner, we obtain

$$\Pr(\hat{R}_Q = 2 \,|\, \phi, C, D) - \Pr(\hat{R}_Q = -2 \,|\, \phi, C, D)$$

$$= Q\left(\frac{1 - R_Q\cos\phi - D_I\sin\phi}{\sigma}\right) - Q\left(\frac{1 + R_Q\cos\phi + D_I\sin\phi}{\sigma}\right) \qquad (4.30)$$

The detailed evaluation of the loop phase detector characteristic $G(\phi)$ is shown in Appendix 4B where $G(\phi)$ is given by equation (4B.6).

The function $G(\phi)$ we obtained for this loop structure is plotted versus ϕ in Fig 20 over the interval $(-\pi/2, \pi/2)$ for different values of Δ where Δ is defined as d/σ. We note that when Δ is small, besides the desired stable lock point at $\phi=0^{\circ}$, $G(\phi)$ exhibits another stable but undesirable lock point at $\phi=90^{\circ}$. As Δ increases, the number of undesirable lock points increases. The loop exhibits as many as 10 undesirable lock points wihtin this interval. These undesirable lock points cannot be resolved by differential coding of any of the data bits in the transmitted symbols and must be resolved by an appropriate prefix sequence. This creates a major problem in operation of this loop, particularly during initial acquisition.

We note that the fundamental period of these S-curves is from $-\pi/2$ to $\pi/2$. This shows that to obtain carrier synchronization using the decision-directed feedback loop for the offset QPSK duobinary signal, only a two-fold phase ambiguity needs to be resolved. Various methods to resolve the phase ambiguity problem have been suggested and discussed in [20][21]. This problem is not discussed further here.

4.4 Evaluation of the noise function $H(\phi)$

From equation (4.11) the noise function $H(\phi)$ is given by

$$H(\phi) = E[\, \hat{R}_I^2 \,|\, \phi(t) \,] + E[\, \tilde{R}_Q^2 \,|\, \phi(t) \,]$$

Following the same procedure as shown in the previous section, $H(\phi)$ is evaluated and shown in Appendix 4C. The noise function in equation (4C.5)

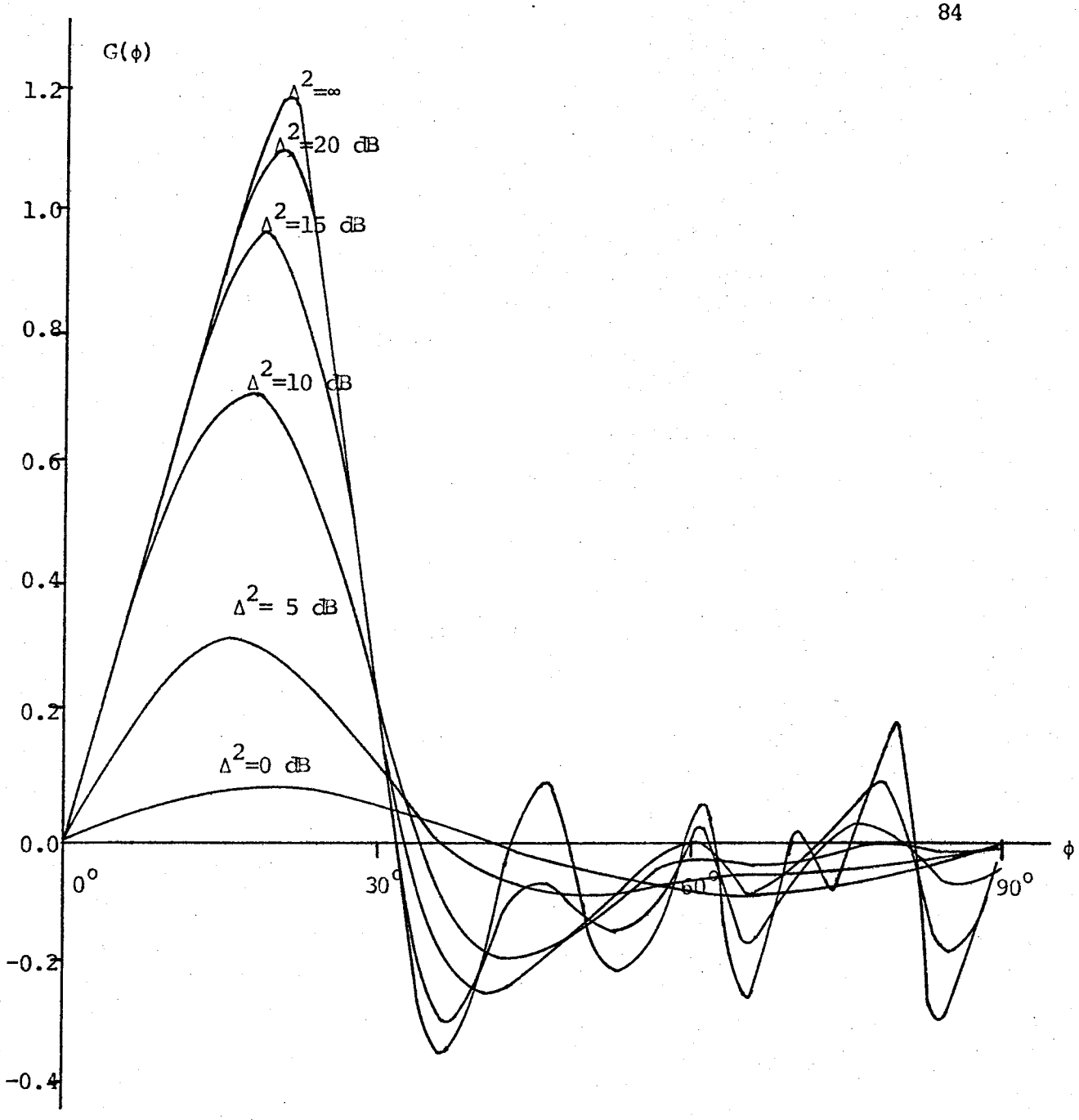

Fig.20.Phase detector characteristic (S-curve) for decision directed feedback carrier tracking loop

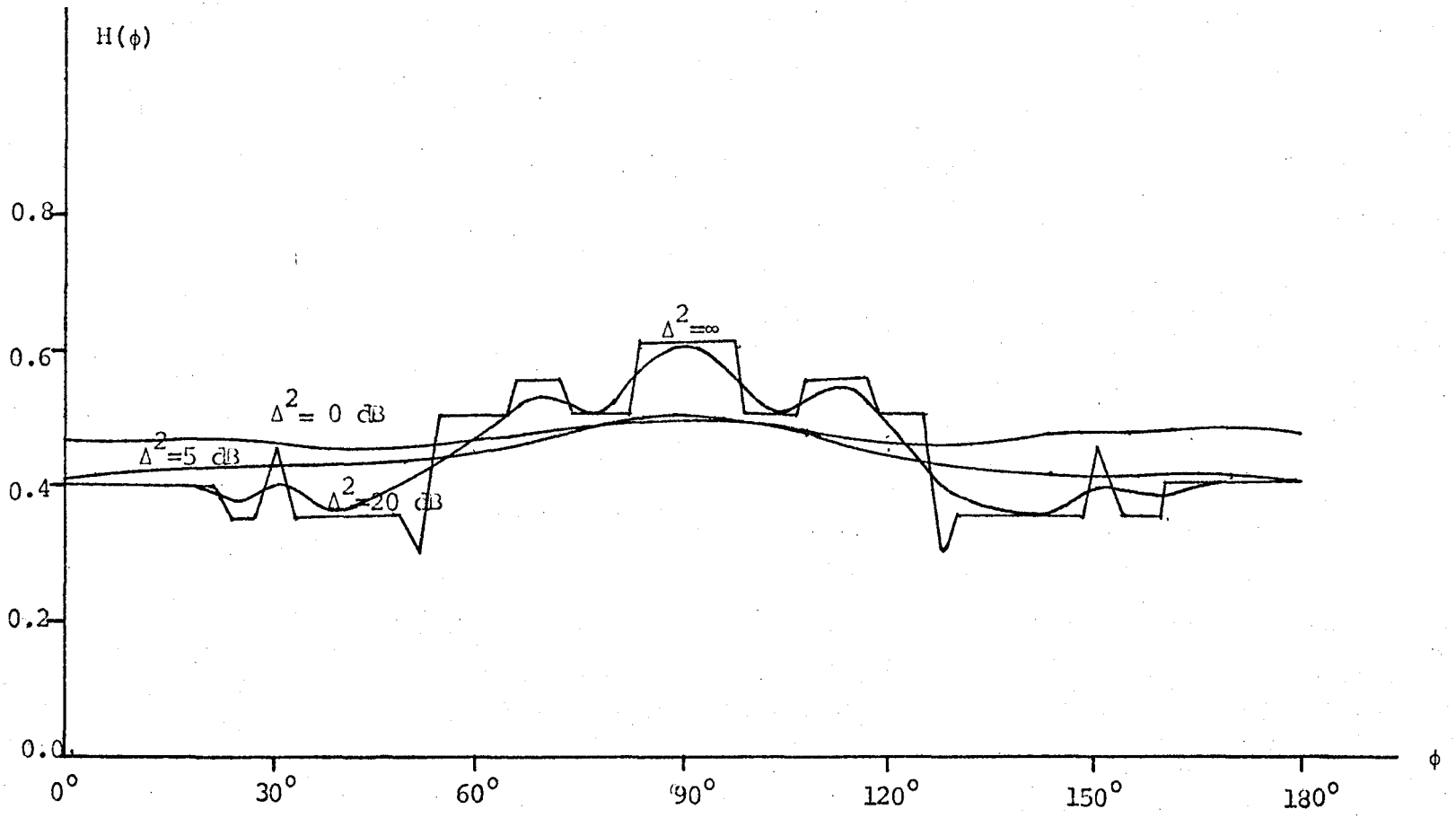

Fig.21 Noise function for 3-level decision feedback (decision directed feedback and half-shifted decision directed feedback) carrier tracking loop structure.

is plotted versus ϕ for various values of Δ in Fig 21.

4.5 The probability density function of the phase error process

The Fokker-Planck technique can be applied to obtain the steady state probability density function $p(\phi)$ of the modulo-2π reduced phase error.

The stochastic integro-differential equation of equation (4.12) is written as

$$\dot{\phi}(t) = \dot{\theta}(t) - K_0[G(\phi) + H^{1/2}(\phi)Ne(t)]$$
$$= \Omega_0 - K_0G(\phi) - K_0H^{1/2}(\phi)Ne(t) \qquad (4.29)$$

where Ω_0 is the Doppler shift in the input frequency from its nominal value of ω_0 and K_0 is the open loop gain defined as $K_1K_mK_v$. We assume as previously that the loop is a first order loop with zero detuning (i.e. $\Omega_0 = 0$). Therefore $p(\phi)$ satisfies the equation

$$\frac{d}{d\phi}[\,A_0(\phi)p(\phi)\,] = \frac{1}{2}\frac{d^2}{d\phi^2}[\,B_0(\phi)p(\phi)\,] \qquad (4.30)$$

where

$$A_0(\phi) = -K_0G(\phi)$$
$$B_0(\phi) = N_0K_0^2H(\phi)/2 \qquad (4.31)$$

The solution to (4.30) is well known [19] and is given by

$$p(\phi) = C_1 \exp\left[\int_0^{\phi} \frac{2A_0(x)-B_0'(x)}{B_0(x)}dx\right] \qquad (4.32)$$

Substituting equation (4.31) into (4.32) gives

$$p(\phi) = C_1 \exp\left[-\int_0^{\phi} \frac{\alpha G(x)+H'(x)}{H(x)}dx\right] \qquad (4.33)$$

where

$\alpha = 4/N_oK_0$ is the loop signal-to-noise ratio and $K_0=K_1K_mK_v$

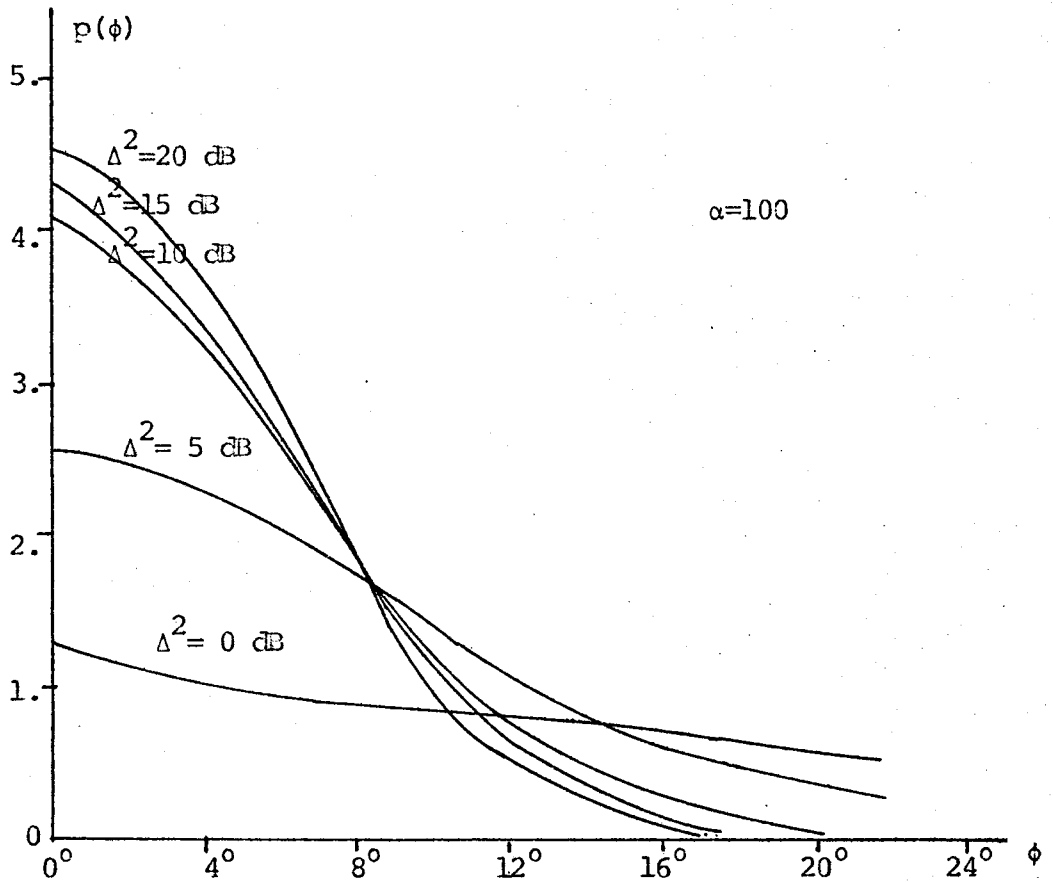

Fig.22 Probability density function of the phase error for the decision directed feedback carrier tracking loop

The pdf of the phase error as given by equation (4.33) is evaluated numerically and plotted versus ϕ for various values of Δ in Fig 22.

4.6 Discussions

In this chapter, we have evaluated a suppressed-carrier dicision feedback carrier synchronization loop for offset QPSK duobinary signal and analyzed its tracking ability. Unfortunately, there are numerous false lock points present in the S-curve and these will cause a major acquisition problem. It thus appears that the loop structure proposed in this chapter could not be used without the use of special prefix data sequences both during initial acquisition and during recovery of lock after some form of loss such as a power failure or a deep fade.

To avoid this problem, we will in the next chapter investigate modified decision directed loop structures.

CHAPTER 5

SHIFTED AND HALF-SHIFTED DECISION-DIRECTED FEEDBACK CARRIER TRACKING LOOP STRUCTURES.

5.1 Shifted decision-directed feedback loop

5.1.1 Introduction

In the preceding chapter, a loop structure was developed in which the baseband signals in I-channel and Q-channel were sampled at the times $t=(2k-1)T$ and $t=2kT$ respectively. These two sampled signal sequences were then passed into a quantizer where decisions were made as 2,0 or -2. Before decoding into binary values +1 or -1, these three level decisions were used for feedback purposes in the carrier recovery system. In this section, we propose another loop structure which is a modification of the one described in chapter 4. In this loop design, the three-level estimated data is used mainly to recover the original data sequences. For feedback purposes, the I-channel and Q-channel baseband analog signal are sampled at the times $t=2kT$ and $t=(2k+1)T$ respectively. This shifted sampling instant design makes the sampling instant at the peak of the symbol pulse we wish to detect. These sampled sequences are then passed to a quantizer where the decision is made to 1 when the sampled value is greater than zero and the decision is made to -1 when the sampled value is less than zero. These binary decisions are then used for feedback purposes. The operation of this loop is quite similar to the previous loop and we shall be brief in the presentation of the development of its equation of operation.

5.1.2 Loop analysis

The loop structure is illustrated in Fig 23. Since the demodulated baseband signals $r_I(t)$ and $r_Q(t)$ are, respectively, sampled at the times $t=2kT$ and $t=(2k+1)T$, we can write down the sampled sequences $r_I(2k)$ and $r_Q(t)$ as in (3.6)

$$r_I(2k) = K_1K_m \left\{ \frac{4}{\pi} \sum_n c_n \frac{(-1)^{k-n}}{1-4(k-n)^2} \cos\phi - (d_k+d_{k-1})\sin\phi + N_I(2k) \right\} \tag{5.1a}$$

and

$$r_Q(2k+1) = K_1K_m \left\{ \frac{4}{\pi} \sum_n d_n \frac{(-1)^{k-n}}{1-4(k-n)^2} \cos\phi + (c_k+c_{k+1})\sin\phi + N_Q(2k+1) \right\} \tag{5.1b}$$

where K_1 is the VCO rms amplitude, K_m is the phase detector gain and $N_I(2k)$ and $N_Q(2k+1)$ are Gaussian random variable. The samples are then passed through quantizers where the decision +1 is made when $r_I(2k)$ or $r_Q(2k+1)$ is greater than zero and the decision -1 is made when $r_I(2k)$ or $r_Q(2k+1)$ is less than zero. We note that, from equation (5.1), these decisions are affected by infinite number of intersymbol interference terms (ISI) due to the adjacent pulses. Also, the reduced signal amplitude, the quadrature distortion term and additive Gaussian noise affect the correctness of this decision making. But this time only two symbols are in the quadrature term instead of an infinite number of symbols. These sampled sequences $r_I(2k)$ and $r_Q(2k+1)$ are then passed to the hold circuits which hold the signal for a 2T sec time interval. Thus the outputs $r'_I(t)$ and $r'_Q(t)$ of the hold circuit in I-channel and Q-channel, respectively, can be expressed by

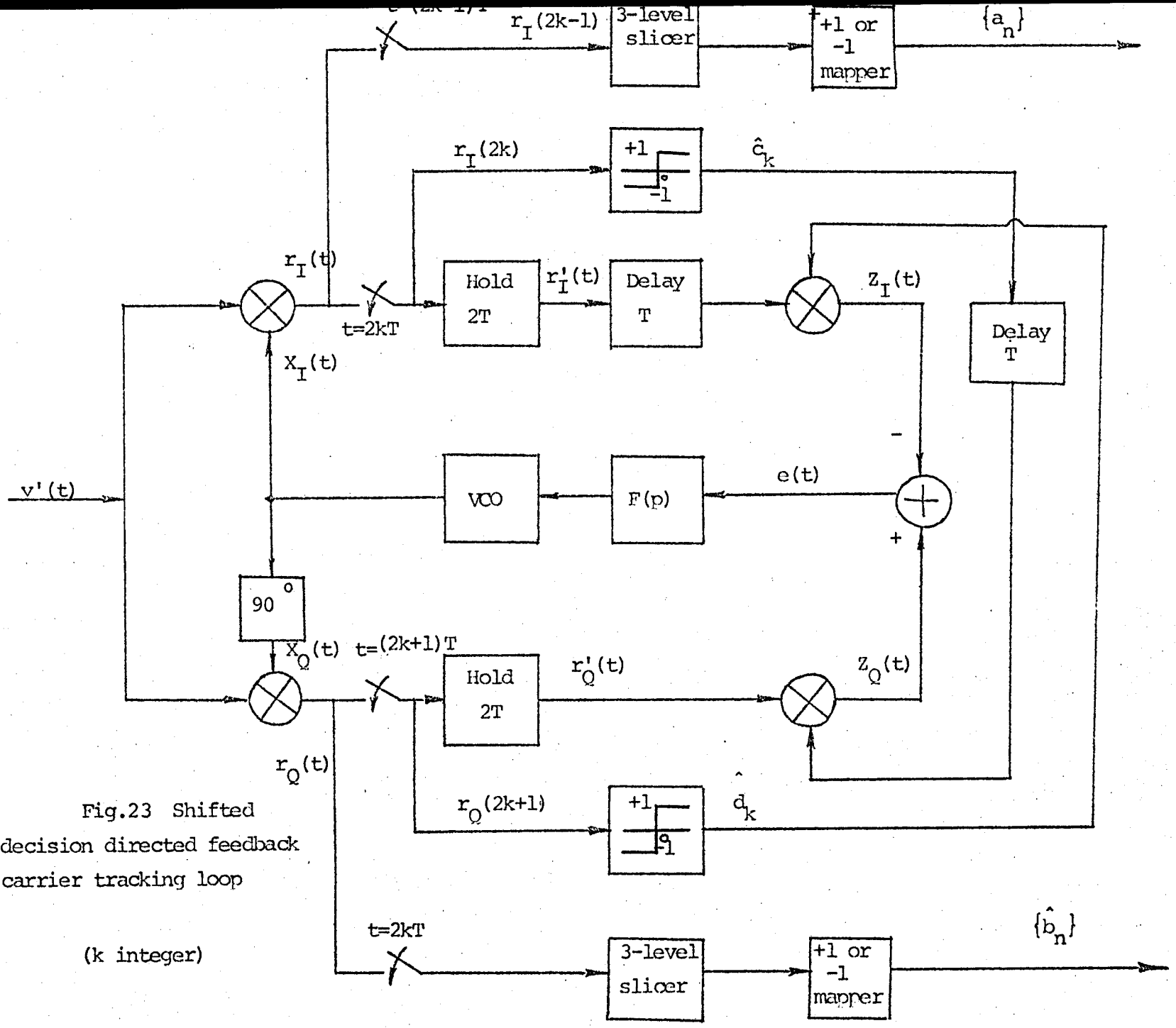

Fig.23 Shifted decision directed feedback carrier tracking loop

(k integer)

$$r_I'(t) = \sum_k r_I(2k)\,g(t-2kT) \qquad (5.2a)$$

$$r_Q'(t) = \sum_k r_Q(2k+1)\,g(t-(2k+1)T) \qquad (5.2b)$$

Again, we assume that g(t) is a rectangular pulse which is equal 1 for $0 \le t < 2T$. Thus we can write

$$r_I'(t) = K_1K_m\left\{ \frac{4}{\pi} \sum_n c_n \frac{(-1)^{k-n}}{1-4(k-n)^2} \cos\phi - (d_k+d_{k-1})\sin\phi + N_I(2k) \right\}$$

$$2kT \le t < (2k+2)T$$

and

$$r_Q'(t) = K_1K_m\left\{ \frac{4}{\pi} \sum_n d_n \frac{(-1)^{k-n}}{1-4(k-n)^2} \cos\phi + (c_k+c_{k+1})\sin\phi + N_Q(2k+1) \right\}$$

$$(2k+1) \le t < (2k+3)T \qquad (5.3)$$

$r_I'(t)$ is then delayed by T sec and cross-multiplied by the current data estimate $\hat{d}_k$ which is the output of the Q-channel quantizer. Similarly $r_Q'(t)$ is cross-multiplied by the current data estimate $\hat{c}_k$ (delayed by T sec). The difference is then fed as an error signal to the loop filter F(p). Thus the error signal e(t) is given by

$$e(t) = [\exp(-pT)\hat{c}_k][r_Q'(t)] - \hat{d}_k[\exp(-pT)r_I'(t)] \qquad (5.4)$$

Therefore, corresponding to the k^{th} transmission symbol, the error signal e(t) can be rewritten as

$$e(t) = K_1K_m\exp(-pT)\left[\frac{4}{\pi} \sum \hat{c}_k d_n \frac{(-1)^{k-n}}{1-4(k-n)^2} \cos\phi + \hat{c}_k(c_k+c_{k+1})\sin\phi \right.$$
$$+ N_Q(2k+1)\hat{c}_k - \frac{4}{\pi} \sum_n \hat{d}_k c_n \frac{(-1)^{k-n}}{1-4(k-n)^2} \cos\phi + \hat{d}_k(d_k+d_{k-1})\sin\phi$$
$$\left. - N_I(2k)\hat{d}_k \right]$$

$$2kT \quad t \quad (2k+1)T \qquad (5.5)$$

Recalling that $\dot{\theta}(t)=K_VF(p)e(t)$ and $\hat{\theta}(t)=\theta(t)-\phi(t)$, we obtain

$$\dot{\phi}(t) = \dot{\theta}(t) - K_v F(p)e(t)$$

$$= \dot{\theta}(t) - K_0 F(p)\exp(-pT)\{ [\hat{c}_k(c_k+c_{k+1})+\hat{d}_k(d_k+d_{k-1})]\sin\phi$$

$$+ [\frac{4}{\pi}\sum_n \hat{c}_k d_n \frac{(-1)^{k-n}}{1-4(k-n)^2} - \frac{4}{\pi}\sum_n \hat{d}_k c_n \frac{(-1)^{k-n}}{1-4(k-n)^2}]\cos\phi$$

$$+ N_Q(2k+1)\hat{c}_k - N_I(2k)\hat{d}_k \} \qquad (5.6)$$

where $K_0=K_1K_mK_v$ is the open loop gain.

Again making the same assumptions as in the previous analyses where the loop bandwidth is assumed to be very much small with respect to the data rate, we can take the statistical average of the stochastic integro-differential equation in (5.6) over the data to obtain

$$\dot{\phi}(t) = \dot{\theta}(t) - K_0 F(p)\exp(-pT)\{E[(\hat{c}_k(c_k+c_{k+1})+\hat{d}_k(d_k+d_{k-1})|\phi]\sin\phi$$

$$+ E[(\frac{4}{\pi}\sum_n \hat{c}_k d_n \frac{(-1)^{k-n}}{1-4(k-n)^2} - \frac{4}{\pi}\sum_n \hat{d}_k c_n \frac{(-1)^{k-n}}{1-4(k-n)^2})|\phi]\cos\phi$$

$$+ [E(\hat{c}_k^2|\phi(t))+E(\hat{d}_k^2|\phi(t))]^{1/2}Ne(t)\} \qquad (5.7)$$

where $Ne(t)$ is approximately white Gaussian noise of single-sided spectral density N_0 Watt/Hz .

Now let $G(\phi) = E[(\hat{c}_k(c_k+c_{k+1})+\hat{d}_k(d_k+d_{k-1})|\phi]\sin\phi$

$$+ E[(\frac{4}{\pi}\sum_n \hat{c}_k d_n \frac{(-1)^{k-n}}{1-4(k-n)^2} - \frac{4}{\pi}\sum_n \hat{d}_k c_n \frac{(-1)^{k-n}}{1-4(k-n)^2})]\cos\phi$$

and

$$H(\phi) = E(\hat{c}_k^2|\phi) + E(\hat{d}_k^2|\phi) \qquad (5.8)$$

Since the statistical average over $\hat{c}_k^2$ and $\hat{d}_k^2$ conditioned on ϕ are equal 1, we find that $H(\phi)$ is equal 2.

Assuming the loop is a first order loop and exponential factor $\exp(-pT) \approx 1$ as before, equation (5.7) can be written as

$$\dot{\phi}(t) = \dot{\theta}(t) - K_0[G(\phi) + 2Ne(t)]$$
$$= \dot{\theta}(t) - 2K_0[G(\phi)/2 + Ne(t)] \qquad (5.9)$$

5.1.3 Evaluation of the loop phase detector characteristic(S-curve)—$G(\phi)$

The S curve $G(\phi)$ can be written as

$$G(\phi) = G_1(\phi)\sin\phi + G_2(\phi)\cos\phi \qquad (5.10)$$

where

$$G_1(\phi) = E[(\hat{c}_k(c_k+c_{k+1})+\hat{d}_k(d_k+d_{k-1}))|\phi]$$

$$G_2(\phi) = E\{[\frac{4}{\pi}\sum_n \hat{c}_k d_n \frac{(-1)^{k-n}}{1-4(k-n)^2} - \frac{4}{\pi}\sum_n \hat{d}_k c_n \frac{(-1)^{k-n}}{1-4(k-n)^2}]|\phi\} \qquad (5.11)$$

Determination of the S-curve requires evaluation of $E[\hat{c}_k(c_k+c_{k+1})|\phi]$ and $E\{[\frac{4}{\pi}\sum_n \hat{c}_k d_n \frac{(-1)^{k-n}}{1-4(k-n)^2}]|\phi\}$ only since $E[\hat{c}_k(c_k+c_{k+1})|\phi] = E[\hat{d}_k(d_k+d_{k-1})|\phi]$ and $E\{[\frac{4}{\pi}\sum_n \hat{c}_k d_n \frac{(-1)^{k-n}}{1-4(k-n)^2}]|\phi\} = -E\{[\frac{4}{\pi}\sum_n \hat{d}_k c_n \frac{(-1)^{k-n}}{1-4(k-n)^2}]|\phi\}$ (Appendix 5B).

Again, we make the approximation that only the adjacent two symbols affect the detection of c_k in I-channel. Thus $E[\hat{c}_k c_k|\phi]$ and $E[\hat{c}_k c_{k+1}|\phi]$ can be written as

$$E[\hat{c}_k c_k|\phi] = E[E(\hat{c}_k c_k|\phi,C,D)|\phi]$$

and

$$E[\hat{c}_k c_{k+1}|\phi] = E[E(\hat{c}_k c_{k+1}|\phi,C,D)|\phi]$$

where we define the sets

$$C = \{c_k,\ c_{k+1},\ c_{k-1}\}$$

$$D = \{d_k,\ d_{k-1}\}$$

Similarly to equation (4.19), we can show that

$$E[\hat{c}_k c_k|\phi]$$

$$=\sum_C c_k \{\sum_D [Pr(\hat{c}_k=1|\phi,C,D) - Pr(\hat{c}_k=-1|\phi,C,D)]Pr(D)\}Pr(C) \tag{5.12}$$

From equation (5.1), we can write

$$N_I(2k) = r_I(2k) - \frac{4}{\pi}(c_k + \frac{1}{3}c_{k+1} + \frac{1}{3}c_{k-1})\cos\phi + (d_k + d_{k-1})\sin\phi$$

$$N_Q(2k+1) = r_Q(2k+1) - \frac{4}{\pi}(d_k + \frac{1}{3}d_{k+1} + \frac{1}{3}d_{k-1})\cos\phi - (c_k + c_{k+1})\sin\phi$$

Conditioned on the phase error ϕ and the symbols c_k, c_{k+1}, c_{k-1}, d_k and d_{k-1}, $N_I(2k)$ is Gaussian distributed, and the conditioned pdf of $r_I(2k)$ is

$$p[r_I(2k)\,|\,\frac{4}{\pi}(c_k + \frac{1}{3}c_{k+1} + \frac{1}{3}c_{k-1})\cos\phi - (d_k + d_{k-1})\sin\phi]$$

$$= \frac{1}{\sqrt{2\pi}\sigma}\exp\{-\frac{[r_I(2k) - 4(c_k + \frac{1}{3}c_{k+1} + \frac{1}{3}c_{k-1})\cos\phi/\pi + (d_k + d_{k-1})\sin\phi]^2}{2\sigma^2}\} \tag{5.13}$$

Similarly, the conditioned pdf of $r_Q(2k+1)$ is

$$p[\,r_Q(2k+1)\,|\,\frac{4}{\pi}(\,d_k + \frac{1}{3}d_{k+1} + \frac{1}{3}d_{k-1})\cos\phi + (\,c_k + c_{k+1})\sin\phi\,]$$

$$= \frac{1}{\sqrt{2\pi}\sigma}\exp\{-\frac{[r_Q(2k+1) - \frac{4}{\pi}(\,d_k + \frac{1}{3}d_{k+1} + \frac{1}{3}d_{k-1})\cos\phi - (c_k + c_{k+1})\sin\phi]^2}{2\sigma^2}\} \tag{5.14}$$

Hence

$$Pr(\hat{c}_k=1|\phi,C,D)$$

$$= \int_0^\infty p[r_I(2k)\,|\,\frac{4}{\pi}(c_k + \frac{1}{3}c_{k+1} + \frac{1}{3}c_{k-1})\cos\phi - (d_k + d_{k-1})\sin\phi]dr_I(2k)$$

$$= 1 - Q\left[\frac{\frac{4}{\pi}(c_k + \frac{1}{3}c_{k+1} + \frac{1}{3}c_{k-1})\cos\phi - (d_k + d_{k-1})\sin\phi}{\sigma}\right] \tag{5.15}$$

Similarly,

$$\Pr(\hat{c}_k=-1|\phi,C,D) = Q\left[\frac{\frac{4}{\pi}(c_k + \frac{1}{3}c_{k+1} + \frac{1}{3}c_{k-1})\cos\phi - (d_k + d_{k-1})\sin\phi}{\sigma}\right] \tag{5.16}$$

From equations (5.15) and (5.16),

$$\Pr(\hat{c}_k=1|\phi,C,D) - \Pr(\hat{c}_k=-1|\phi,C,D) = 1 - 2Q\left[\frac{\frac{4}{\pi}(c_k + \frac{1}{3}c_{k+1} + \frac{1}{3}c_{k-1})\cos\phi - (d_k + d_{k-1})\sin\phi}{\sigma}\right] \tag{5.17}$$

In the same manner, $E[\hat{d}_k d_k|\phi]$ and $E[\hat{d}_k d_{k-1}|\phi]$ can be expressed as

$$E[\hat{d}_k d_k|\phi] = \sum_{D'} d_k \left\{\sum_{C'} [\Pr(d_k=1|\phi,C',D') - \Pr(d_k=-1|\phi,C',D')]\Pr(C')\right\}\Pr(D') \tag{5.18}$$

and

$$E[\hat{d}_k d_{k-1}|\phi] = \sum_{D'} d_{k-1} \left\{\sum_{C'} [\Pr(d_k=1|\phi,C',D') - \Pr(d_k=-1|\phi,C',D')]\Pr(c')\right\}\Pr(D') \tag{5.19}$$

where we define the sets

$$C' = \{c_k, c_{k+1}\}$$

$$D' = \{d_k, d_{k+1}, d_{k-1}\}$$

Thus we can evalute

$$\Pr(\hat{d}_k=1|\phi,C',D') = \int_0^\infty p[r_Q(2k+1)|\ \tfrac{4}{\pi}(d_k + \tfrac{1}{3}d_{k+1} + \tfrac{1}{3}d_{k-1})\cos\phi + (c_k + c_{k+1})\sin\phi]\, dr_Q(2k+1)$$

$$= 1 - Q\left[\frac{\frac{4}{\pi}(d_k + \frac{1}{3}d_{k+1} + \frac{1}{3}d_{k-1})\cos\phi + (c_k + c_{k+1})\sin\phi}{\sigma}\right] \tag{5.20}$$

and

$$\Pr(\hat{d}_k=-1|\phi,C',D')$$
$$= \int_{-\infty}^{0} p[r_Q(2k+1) \mid \frac{4}{\pi}(d_k + \frac{1}{3}d_{k+1} + \frac{1}{3}d_{k-1})\cos\phi + (c_k + c_{k+1})\sin\phi]\, dr_Q(2k+1)$$
$$= Q\left[\frac{\frac{4}{\pi}(d_k + \frac{1}{3}d_{k+1} + \frac{1}{3}d_{k-1})\cos\phi + (c_k + c_{k+1})\sin\phi}{\sigma}\right] \tag{5.21}$$

Hence from equations (5.20) and (5.21) we can write that

$$\Pr(\hat{d}_k=1|\phi,C',D') - \Pr(\hat{d}_k=-1|\phi,C',D')$$
$$= 1 - 2Q\left[\frac{\frac{4}{\pi}(d_k + \frac{1}{3}d_{k+1} + \frac{1}{3}d_{k-1})\cos\phi + (c_k + c_{k+1})\sin\phi}{\sigma}\right] \tag{5.22}$$

$G_1(\phi)$ is evaluated in Appendix 5C.1 .

To evaluate $G_2(\phi)$, we simply need to evaluate the following conditional expectations:

$$\frac{4}{\pi}\left[E(\hat{c}_k d_k|\phi) + \frac{1}{3}E(\hat{c}_k d_{k-1}|\phi) - E(c_k \hat{d}_k|\phi) - \frac{1}{3}E(\hat{d}_k c_{k+1}|\phi) \right] \tag{5.23}$$

Because the decision $\hat{c}_k$ is dependant only on d_k and d_{k-1} (5.1a) in the Q-channel and the decision $\hat{d}_k$ is dependant only on c_k and c_{k+1} (5.1b) in the I-channel, other uncorrelated symbols will result in zero when taking the statistical average.

Similar to equation (4.19), the four conditional expectations in equation (5.23) can be written as follows:

$$E(\hat{c}_k d_k|\phi) = \sum_D d_k \left\{ \sum_C [\Pr(\hat{c}_k=1|\phi,C,D) - \Pr(\hat{c}_k=-1|\phi,C,D)]\Pr(C) \right\}\Pr(D) \tag{5.24}$$

$$E(\hat{c}_k d_{k-1}|\phi)$$

$$= \sum_D d_{k-1} \{\sum_C [Pr(\hat{c}_k=1|\phi,C,D) - Pr(\hat{c}_k=-1|\phi,C,D)]Pr(C)\}Pr(D) \tag{5.25}$$

$$E(c_k \hat{d}_k|\phi)$$

$$= \sum_{C'} c_k \{\sum_{D'} [Pr(\hat{d}_k=1|\phi,C',D') - Pr(\hat{d}_k=-1|\phi,C',D')]Pr(D')\}Pr(C') \tag{5.26}$$

$$E(\hat{d}_k c_{k+1}|\phi)$$

$$= \sum_{C'} c_{k+1} \{\sum_{D'} [Pr(\hat{d}_k=1|\phi,C',D') - Pr(\hat{d}_k=-1|\phi,C',D')]Pr(D')\}Pr(C') \tag{5.27}$$

where we define the sets $C=\{c_k, c_{k+1}, c_{k-1}\}$, $D=\{d_k, d_{k-1}\}$, $C'=\{c_k, c_{k+1}\}$ and $D'=\{d_k, d_{k+1}, d_{k-1}\}$.

In Appendix 5B, it can be shown that

$$E(\hat{c}_k d_k|\phi) = - E(c_k \hat{d}_k|\phi)$$

and

$$E(\hat{c}_k d_{k-1}|\phi) = - E(c_{k+1} \hat{d}_k|\phi)$$

$G_2(\phi)$ is evaluated in Appendix 5C.2 and $G(\phi)$ is evaluated in Appendix 5C.3 .

The function $G(\phi)$ is plotted versus ϕ for various values of Δ in Fig 24. We note that false lock points are still exhibited in the S-curve. For $\Delta=\infty$, four undesirable lock points exist in the fundamental period $(-\pi/2,\pi/2)$ of this $G(\phi)$ curve. As mentioned previously, we thus need a prefix sequence to lock at the desired point ($\phi=0^{\circ}$). Thus the performance of this loop structure is still not satisfactory in the same sense as the loop of chapter 4.

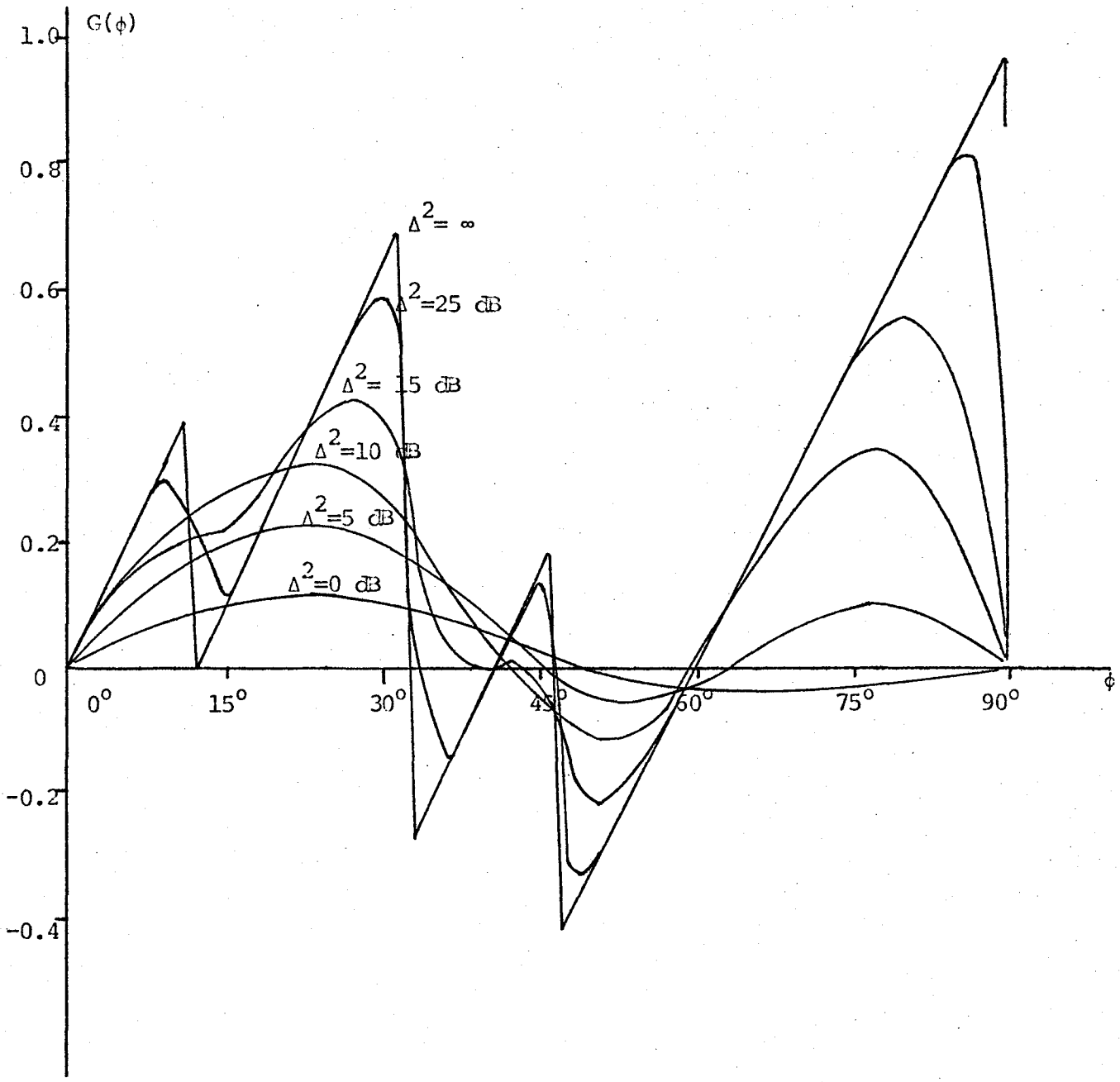

Fig.24 Phase detector characteristic (S-curve) for shifted decision directed feedback carrier tracking loop

5.1.4 The probability density function of the phase error process

Parallel to the development in section 4.5 we can obtain the steady state probability density function $p(\phi)$ of the modulo-2π reduced phase error by using the Fokker-Planck technique.

The stochastic integro-differential equation of the loop operation is given as in equation(5.9)

$$\dot{\phi}(t) = \Omega_0 - K_0 G(\phi) - 2K_0 Ne(t) \qquad (5.29)$$

where $K_0=K_1K_mK_v$ is the open loop gain.

Assuming $\Omega_0=0$ as before, we obtain the solution for the steady-state pdf $p(\phi)$ in the form

$$p(\phi) = C_2 \exp[- \int^{\phi} \alpha G(x)\,dx\,] \qquad (5.30)$$

where $\alpha=2/N_0K_0$ is the loop signal-to-noise ratio and C_2 is a normalization constant.

The pdf of the phase error as given by equation (5.30) is plotted versus ϕ for various values of Δ in Fig 25 a and for various values of α in Fig 25b.

5.1.5 Discussions

Although this loop performs the carrier synchronization function, the performance is not satisfactory due to the appearance of as many as four undesirable lock points in the $G(\phi)$ curve. Thus another loop structure is investigated in the search for better performance in the following sections.

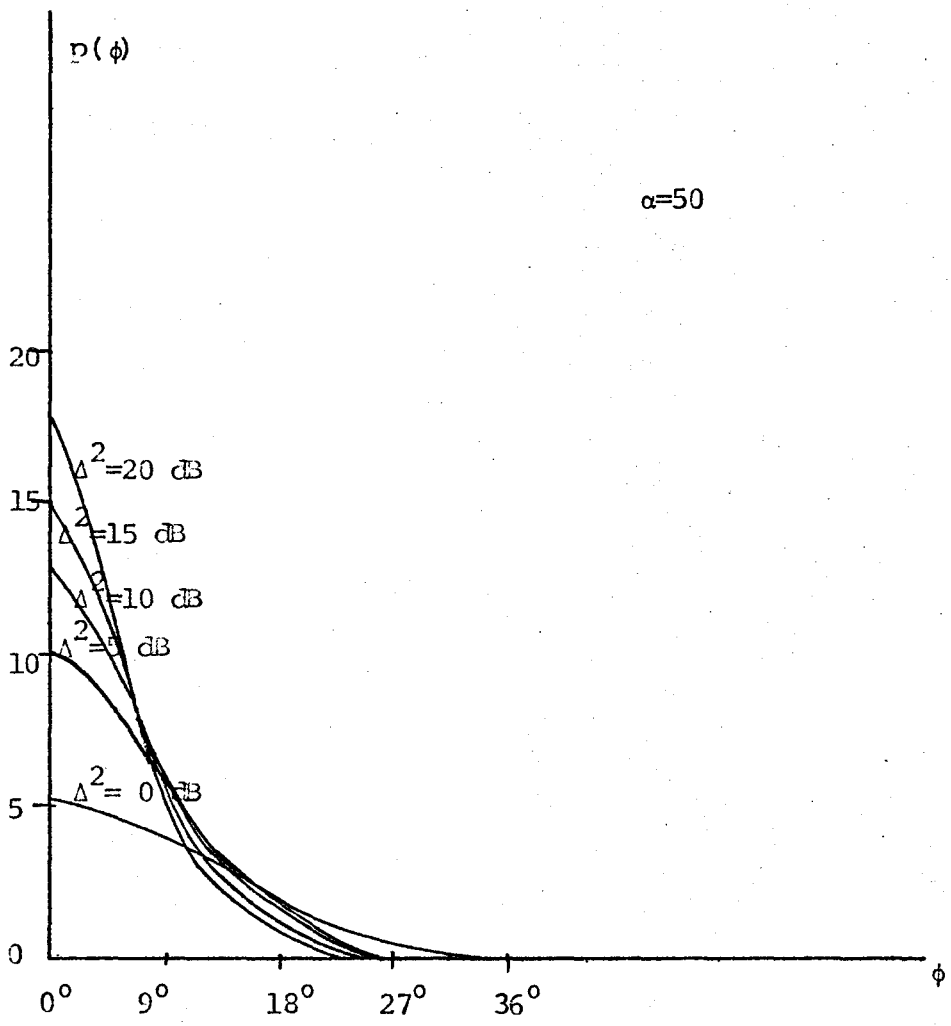

Fig.25a Probability density function of the phase error for the shifted decision directed feedback carrier tracking loop

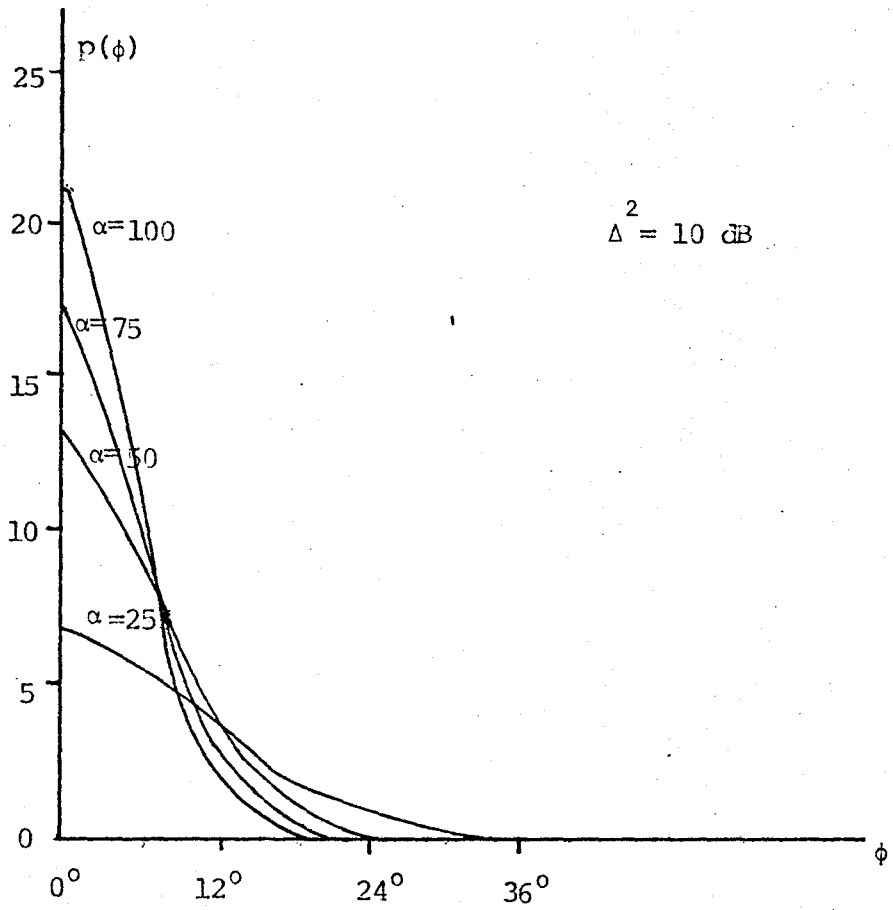

Fig 25b Probability density function of the phase error

for shifted decision directed feedback carrier tracking loop

5.2 Half-shifted decision directed feedback carrier tracking loop

5.2.1 Introduction

The loop we are going to investigate here is a modification of the previous loop structures. The only difference is that the demodulated baseband signals in the I-channel and Q-channels, before being passed to the hold circuits, are sampled at the times t=2kT and t=(2k+1)T (k integer) instead of t=(2k-1)T and t=2kT respectively. However, in the decision arms, the sampling time for I-channel and Q-channel are still, respectively, keeping sampling at t=(2k-1)T and t=2kT. In this structure, delay elements are not necessary, only two sample-and-hold circuits are required. Since the loop is similar to the previous loops, the analysis for this loop is presented rather concisely.

5.2.2 Loop analysis

The loop structure is illustrated in Fig 26. The demodulated baseband signals $r_I(t)$ and $r_Q(t)$ in the I-channel and Q-channel decision arms are sampled at the times t=(2k-1)T and t=2kT. The sampled sequence are defined in equations (4.3) and (4.4).

Similarly to the analysis in section 5.1, the outputs $r'_I(t)$ and $r'_Q(t)$ of the sample-and-hold circuits in I-channel and Q-channel can be represented by equations (5.3a) and (5.3b) respectively. Thus we can rewrite $r'_I(t)$ and $r'_Q(t)$ as

$$r'_I(t) = K_1K_m[D_I\cos\phi - R_Q\sin\phi + N_I(2k)\ ] \qquad 2kT < t < (2k+2)T$$

and

$$r'_Q(t) = K_1K_m[\ D_Q\cos\phi + R_I\sin\phi + N_Q(2k-1)\ ] \qquad (2k-1)T \leq t < (2k+1)T$$

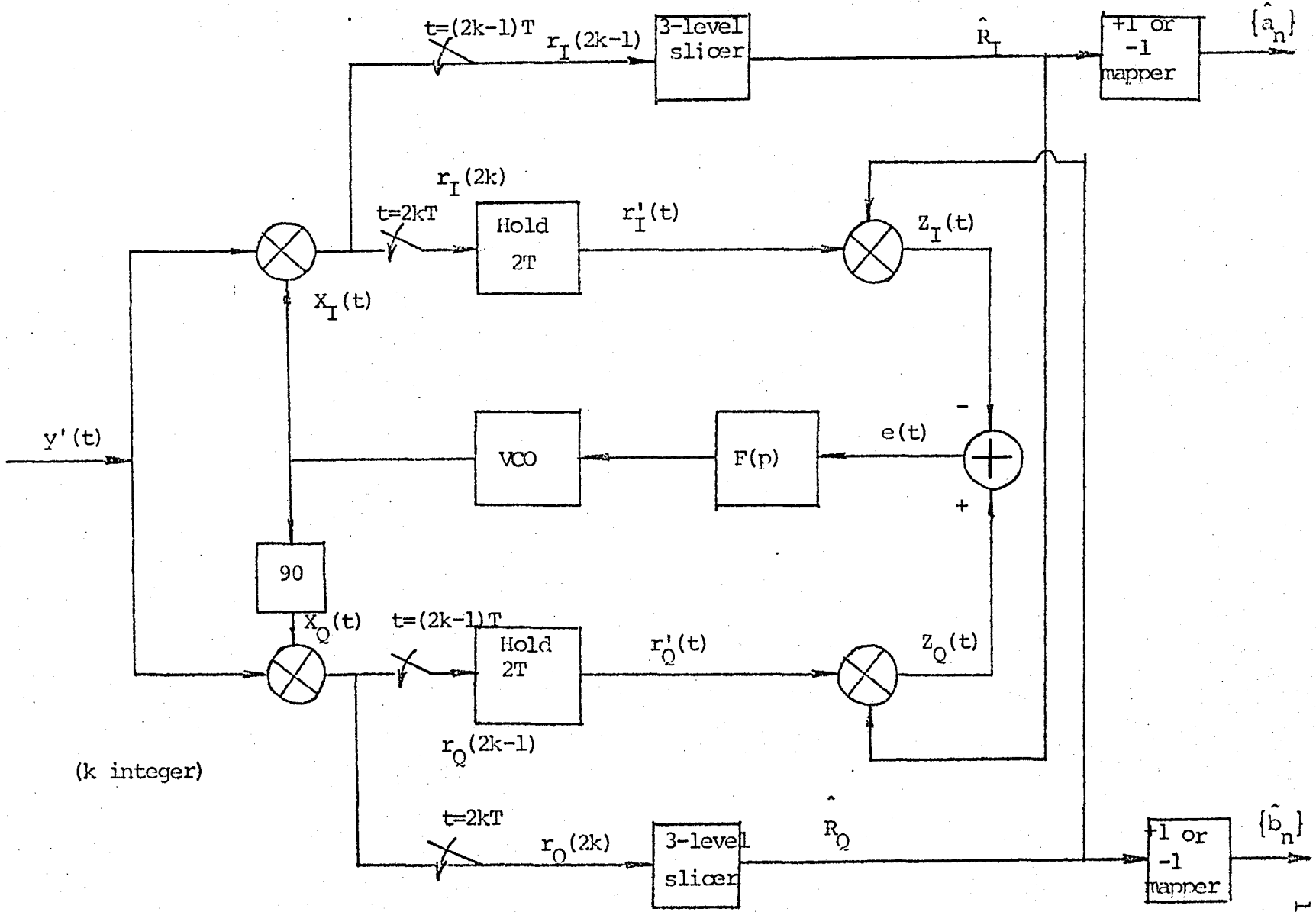

Fig.26 Half-shifted decision directed feedback carrier tracking loop

where R_I, R_Q, D_I, D_Q are defined in equation (4.4).

The lowpass signal $r'_I(t)$ is cross-multiplied by the current data decision $\hat{R}_Q$ and the low pass signal $r'_Q(t)$ is cross-multiplied by the current data decision $\hat{R}_I$. The difference is fed as an error signal to the loop filter F(p). This error signal, denoted by e(t), is thus given by

$$e(t) = [\, r_Q(t)R_I - r_I(t)R_Q \,] \tag{5.20}$$

Recall that $\dot{\hat{\theta}}(t) = K_v F(p)e(t)$ and $\hat{\theta}(t)=\theta(t)-\phi(t)$, we can write

$$\dot{\phi}(t)= \dot{\theta}(t) - K_v F(p)e(t) \tag{5.21}$$

Therefore substituting (5.20) into (5.21), we obtain

$$\dot{\phi}(t)=\dot{\theta}(t)-K_0F(p)\{\, \hat{R}_I[D_Q\cos\phi + R_I\sin\phi + N_Q(2k-1)] - \hat{R}_Q[\, D_I\cos\phi - R_Q\sin\phi + N_I(2k) \,] \tag{5.22}$$

where $K_0=K_1K_mK_v$ is the open loop gain.

The analysis which follows is based on the same assumption as made in chapter 3, that we can take the statistical average of the stochastic equation in (5.22) over the data to obtain

$$\dot{\phi}(t) = \dot{\theta}(t) - K_0F(p)[\, G(\phi) + H^{1/2}(\phi)Ne(t) \,] \tag{5.23}$$

where Ne(t) is approximately white Gaussian noise of single-sided spectral density N_0 Watt/Hz and

$$G(\phi) = E[(\hat{R}_IR_I + \hat{R}_QR_Q)\,|\,\phi]\sin\phi(t) + E[(\hat{R}_ID_Q - \hat{R}_QD_I)\,|\,\phi]\cos\phi(t)$$

and

$$H(\phi) = E[R_I^2\,|\,\phi] + E[R_Q^2\,|\,\phi] \tag{5.24}$$

In equation (5.24), the operation $E\{\cdot\}$ denotes the statistical average. The separation of the noise term into a white noise term multiplied by a phase-dependent term follows the previously stated assumptions in chapter 3.

5.2.3 Evaluation of the loop phase detector characteristic(S-curve)---$G(\phi)$

The loop S-curve of equation (5.23) can be written as

$$G(\phi) = G_1(\phi)\sin\phi + G_2(\phi)\cos\phi \tag{5.25}$$

where

$$G_1(\phi) = E[\ (\hat{R}_I R_I + \hat{R}_Q R_Q)\,|\,\phi(t)\ ] \tag{5.26}$$

$$G_2(\phi) = E[\ (\hat{R}_I D_Q - \hat{R}_Q D_I)\,|\,\phi(t)\ ] \tag{5.27}$$

Since $E(\hat{R}_Q R_Q|\phi) = E(\hat{R}_I R_I|\phi)$ and $E(\hat{R}_Q D_I|\phi) = -E(\hat{R}_I D_Q|\phi)$ (Appendix 5 D), determination of the S-curve $G(\phi)$ requires evaluation of $E(\hat{R}_I R_I|\phi)$ and $E(\hat{R}_I D_Q|\phi)$ only.

We make the same approximation as before where 3 symbols in the quadrature distortion terms are taken into account instead of an infinite number of symbols for taking statistical averages.

Referring to the definitions in equation (4.18) and, similar to the evaluation in (4.19), we obtain the conditional expectations as follows:

$$E(\hat{R}_I R_I|\phi)$$

$$= 2 \sum_C R_I \{ \sum_D [\ Pr(\hat{R}_I=2|\phi,C,D) - Pr(\hat{R}_I=-2|\phi,C,D)\ ]Pr(D)\}Pr(C) \tag{5.28}$$

$$E(\hat{R}_Q R_Q|\phi)$$

$$= 2 \sum_D R_Q \{\sum_C [Pr(\hat{R}_Q=2|\phi,C,D) - Pr(\hat{R}_Q=-2|\phi,C,D)]Pr(C)\}Pr(D) \tag{5.29}$$

$$E(\hat{R}_I D_Q|\phi)$$

$$= 2 \sum_D D_Q \{\sum_C [Pr(\hat{R}_I=2|\phi,C,D) - Pr(\hat{R}_I=-2|\phi,C,D)]Pr(C)\}Pr(D) \tag{5.30}$$

$$E(\hat{R}_Q D_I|\phi)$$

$$= 2 \sum_C D_I \{\sum_D [Pr(\hat{R}_Q=2|\phi,C,D) - Pr(\hat{R}_Q=-2|\phi,C,D)]Pr(D)\}Pr(C) \tag{5.31}$$

Similar to the analysis in section 4.3, $G_1(\phi)$ and $G_2(\phi)$ are evaluated in Appendix 5 E and 5 F respectively and the loop phase detector characteristic $G(\phi)$ is presented in Appendix 5G.

The function $G(\phi)$ is plotted versus ϕ for various values of Δ in Fig 27. We note that the fundamental period is from $-\pi/2$ to $\pi/2$. As stated previously, there is here only a two-fold phase ambiguity when we obtain carrier synchronization from this decision feedback loop for offset QPSK. This result is in agreement with Simon and Smith's paper in [7]. In our analysis, we implicitly assume that the resolution of phase ambiguities can be accomplished perfectly.

The S-curve $G(\phi)$ for this loop shows the improved performance. There are no undesirable lock points, besides the desirable lock point at $\phi=0^\circ$, for Δ^2 less than 50 dB (or $\Delta=7$). Another lock point at $\phi=90^\circ$ is presented when Δ^2 increases beyond this value and up to infinit

The noise function $h(\phi)$ is exactly the same as in section 4.4. As we can see the noise function is an even function about $\phi=90^\circ$.

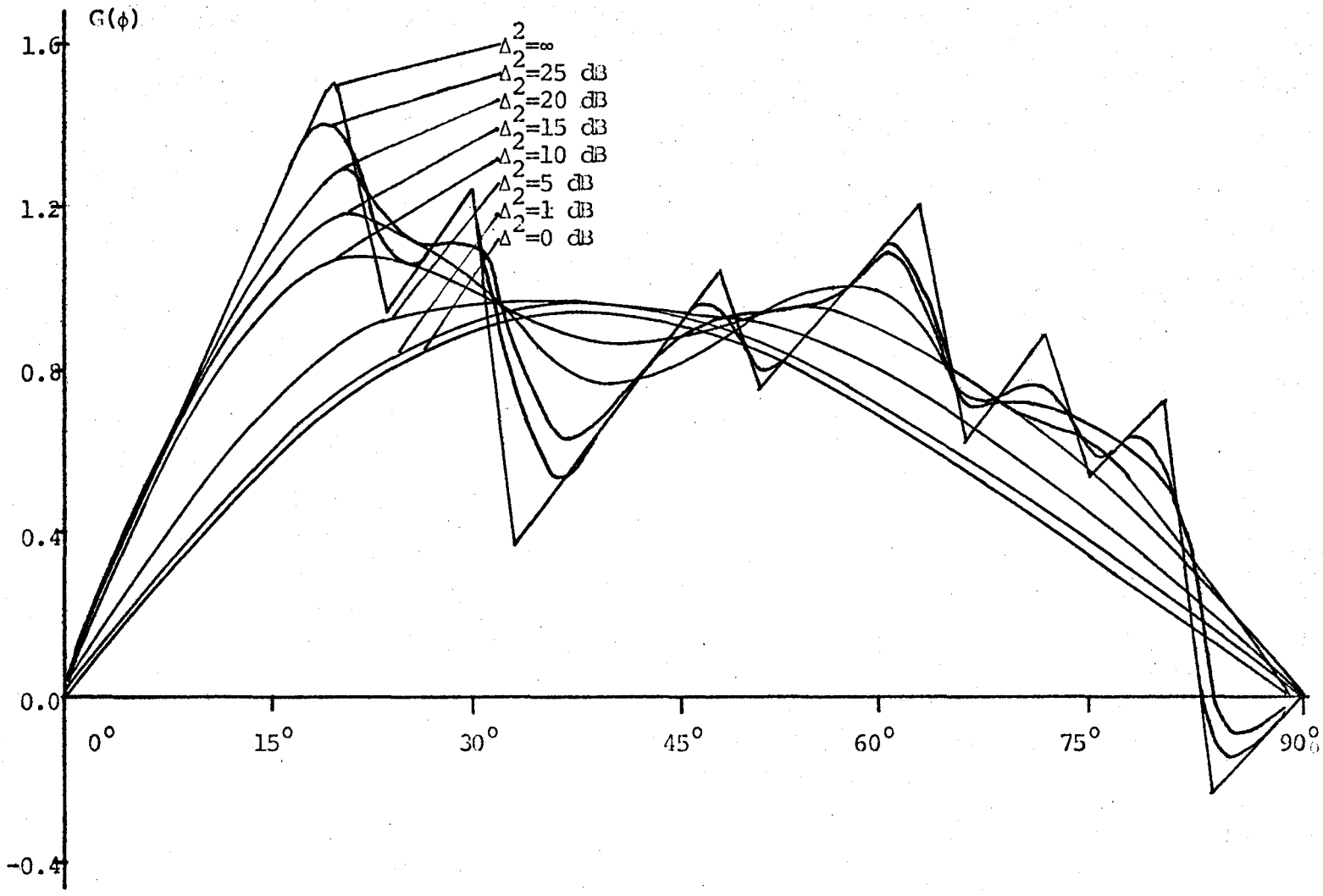

Fig.27 Phase detector characteristic (S-curve) for half-shifted decision directed feedback carrier tracking loop.

5.2.4 Probability density function of the phase error process

Following closely the evaluation as in section 4.5, $p(\phi)$ can be evaluated as

$$p(\phi) = C_3 \exp\left[- \int_0^{\phi} \frac{\alpha G(x)+H'(x)}{H(x)} dx \right] \qquad (5.32)$$

where $\alpha = 4/N_0K_0$ is the loop signal-to-noise ratio and C_3 is a normalization constant. The pdf of the phase error as given by equation (5.32) is plotted versus ϕ for various values of Δ in Fig 28 and plotted versus ϕ for various values of loop signal-to-noise ratio α in Fig 29.

5.2.5 Discussions and conclusions

The $G(\phi)$ curve we obtained for this loop structure shows better performance than the previous two loops suggested in chapter 4 and section 5.1. For Δ^2 approximately less than 50dB (or $\Delta \approx 7$), only one desirable lock point at 0° is exhibited in the loop phase detector characteristic curve. For Δ^2 greater than 50dB (approximately), two undesirable lock points at -90° and $+90^\circ$ within the interval $(-\pi/2, \pi/2)$ appeared. The greatest possible phase error range for the loop locking at -90° is from -97° to -83° and the greatest possible phase error range for the loop locking at 90° is from 83° to 97°.

If the intial phase error is known, or a prefix data sequence is used as mentioned previously, the above problem can be resolved and the loop will be locked at the desired lock point ($\phi=0^\circ$).

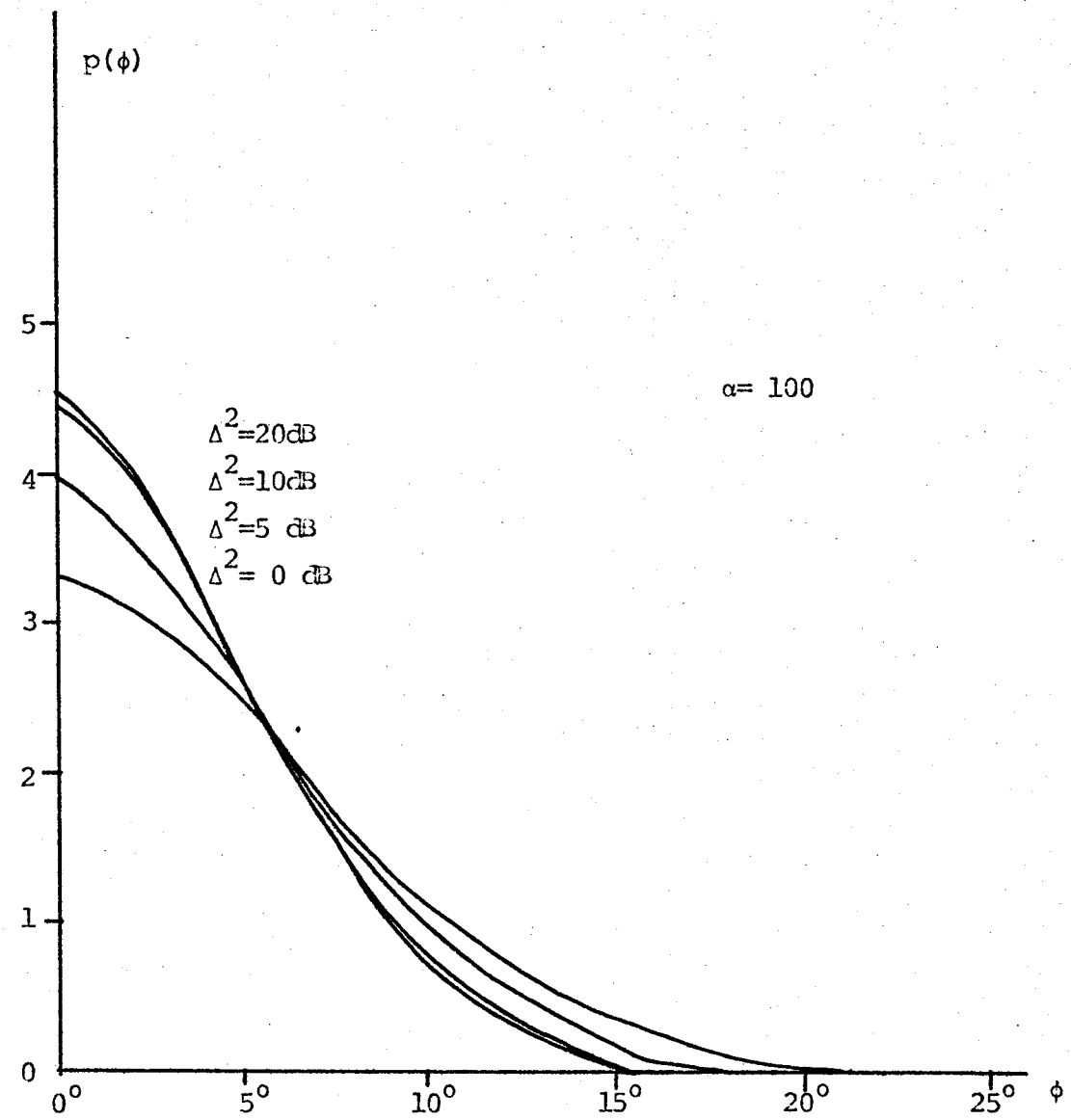

Fig.28 Probability density function of the phase error for half-shifted decision directed feedback carrier tracking loop

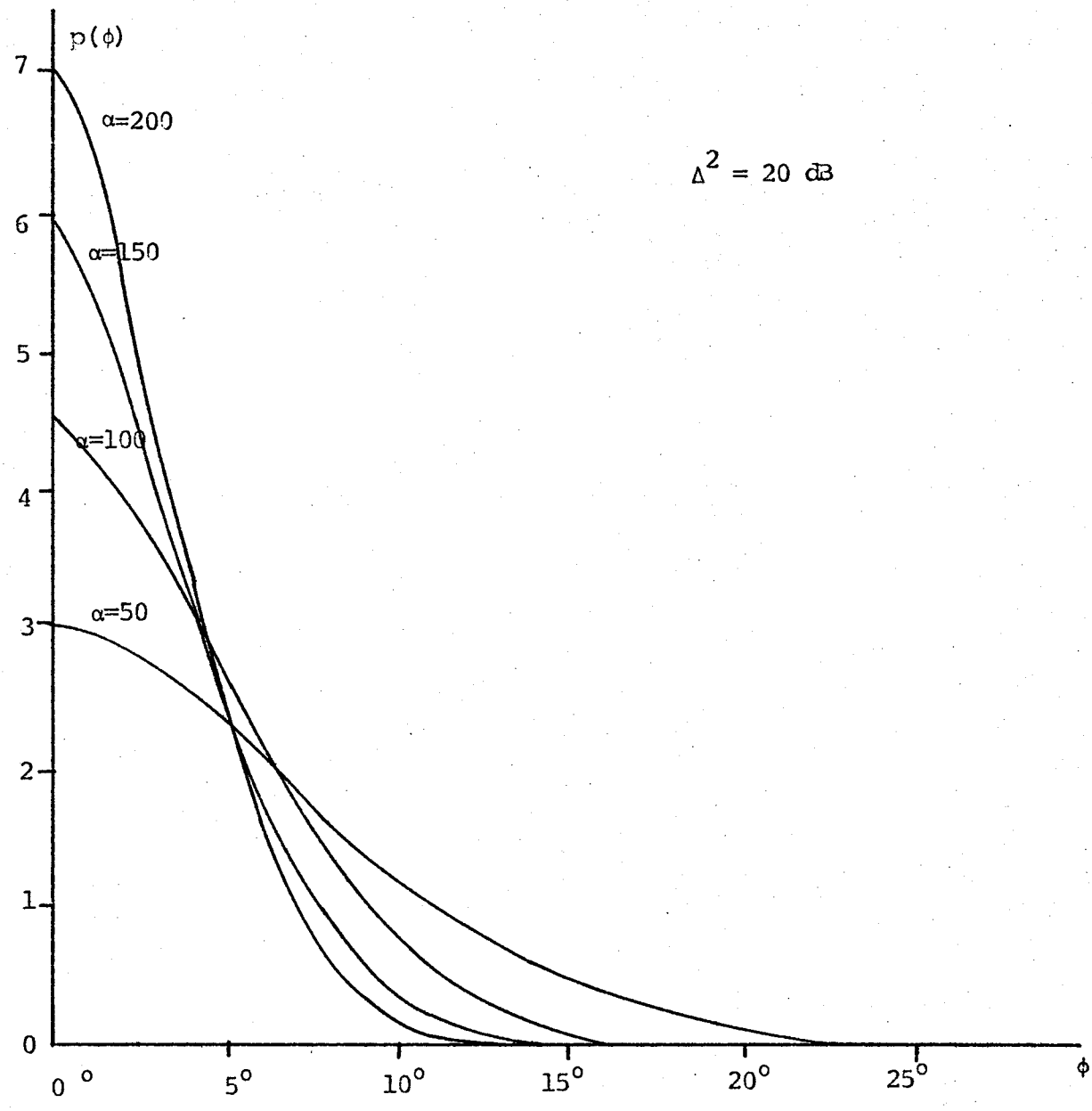

Fig. 29 Probability density function of the phase error for half-shifted decision directed feedback carrier tracking loop

CHAPTER 6

CONCLUSIONS AND FUTURE STUDIES

6.1 CONCLUSIONS

A highly efficient digital radio communication system, the so-called offset QPSK duobinary system has been investigated. The performance as a function of steady-state phase error has been investigated analytically and by simulation.

Carrier recovery and its effects on the performance of this system have also been investigated in detail in this thesis. We have investigated four possible carrier regeneration loops, all based on the remodulation principle, and analysed their steady-state operating behavior. For each loop, analytical expressions for the loop detector characteristic (S-curve) and the steady-state phase error probability density function (pdf) have been derived.

The performance of the communication system in the presence of phase jitter can be easily determined once the pdf of the steady-state phase error has been obtained.

The estimate-aided loop suggested in Chapter 3 requires highly accurate analog wideband multiplier and delay lines which are both difficult to implement and expensive. However, it exhibits excellent steady-state behavior very similar to that of a conventional Costas loop.

Three other loop structures have been proposed in chapters 4 and 5. They essentially employ data-aided carrier synchronization which

is well known in the literature [9]. These loop structures avoid the implementation problems of the estimate data aided loop. The loop suggested in section 5.2 shows better performance than the other two loops in Chapter 4 and in section 5.1. Therefore this loop structure is recommended for possible implementation of an actual carrier recovery circuit.

6.2 Future Studies

Since the estimates $(\hat{a},\hat{b})$ we obtained are not the maximum likelihood estimates, a further investigation for the implementation of the data detector to obtain maximum likelihood estimates is suggested. The best decision directed loop we obtained in our study still exhibits 2 undesirable lock points at $\pm$ 90° within the interval $(-\pi/2,\pi/2)$ for higher values of Δ^2 ($\Delta^2 \triangleq d^2/\sigma^2$). These undesirable lock points may be due to the 3-symbol-average approximation we made in the derivation of the loop detector characteristic (S-curve). To demonstrate the theoretical results reported in this thesis, the feasibility evaluation via simulations on a digital computer and the experimental verification of the results are suggested.

REFERENCES

[1] P.Kabal and S.Pasupathy,"Partial Response Singalling," IEEE Trans. Commun., vol. COM-23, pp 921-934, September 1975.

[2] R.K.Kwan, "The effects of filtering and limiting a double-binary PSK signal," IEEE Trans. Aerosp. Electron. Syst., vol. AES-5, pp.589-594, July 1969.

[3] S.A.Phodes, "Effects of hardlimiting on bandlimited transmissions with conventional and offset QPSK modulation," in 1 st IEEE Nat. Conf. Telecommun., Houston, Tex., Dec 1972.

[4] S.A.Rhodes, "Effects of Noisy phase reference on coherent detection of offset-QPSK signals," IEEE Trans. Commun., vol. COM-22, pp 1046-1055, August 1974.

[5] R.Matyas and P.J.Mclane, "Decision-aided tracking loops for channels with phase jitter and intersymbol interfere ce," IEEE Trans. Commun.,vol. COM-22,No.8, August 1974.

[6] M.K.Simon and J.G.Smith, "Carrier synchronization and detection of QASK signal sets," IEEE Trans. Commun., vol. COM-22,No.2, February 1974.

[7] M.K.Simon and J.G.Smith, "Offset quadrature communications with decision-feedback carrier synchronization," IEEE Trans. Commun., vol. COM-22,No.10, October 1974.

[8] C.J.Wolejsza,A.M.Walker, and A.M.Werth,"PSK modems for sattellite communications," in Proc. First Instelsat Int. Conf. on Digital Satellite Communications, London,England, Nov.1969, pp 127-143.

[9] W.C.Lindsey and M.K.Simon, "Data-aided carrier tracking loops," IEEE Trans Commun. Technol., vol. COM-19, pp 157-168,April 1971.

[10] W.C.Lindsey and M.K.Simon,"Carrier synchronization and detection of polyphase signals," IEEE Trans. Commun., vol. COM-20, pp 441-454, June 1972.

References Continued

[11] R.D.Gitlin and E.Y.Ho, "The performance of staggered quadrature amplitude modulation in the presence of phase jitter," IEEE Trans. Commun.,vol.COM-23, No.3, pp 348-352, March 1975.

[12] R.K.Kwan, "Advances in Digital Radio Systems," IEEE Trans. Commun., pp 147-151, February 1973.

[13] M.R,Liger,P.C.Magne and J.P.R.Poitevin,"Pharaon Urbain, a digital radio relay system for urban areas," IEEE Trans. Commun., vol. COM-22, No.9, pp 1226-1235, September 1974.

[14] J.F. GUNN and J.A.Lombardi, "Error detection for partial-response systems," IEEE Trans. Commun. Technology, vol. COM-17, No.6, pp 734-736, December 1969.

[15] I.Kalet and S.B.Weinstein, "In-band generation of synchronous linear data signals," IEEE Trans. Commun., vol. COM-21, No.10, pp 1116-1122, October 1973.

[16] M.R.Mathwich.,J.F.Balcewicz and M.Hecht,"The effect of tandem band and amplitude limiting on the Eb/N_0 performance of minimun (frequency) shift keying (MSK)," IEEE Trans. Commun.,vol. COM-22 pp 1525-1537, October 1974.

[17] W.R.Bennet and J.R.Davey, Data Transmission. New York: McGraw-Hill, 1965.

[18] R.W.Lucky,J.Salz,and E.J.Weldon, Principles of Data Communications. New York: McGraw-Hill, 1968.

[19] W.C.Lindsey, Synchronization Systems in Communications and Control. Englewood Cliffs, N.J.:Prentice-Hall, 1972.

[20] W.C.Lindsey and M.K.Simon, Telecommunications Systems Engineering. Englewood Cliffs, N.J.: Prentice-Hall, 1973.

[21] J.J.Stiffler, Theory of Synchronous Communications. Englewood Cliffs, N.J.: Prentice-Hall,1971.

References Continued

[22] A.J.Viterbi,Principles of Coherent Communication. New York: McGraw-Hill, 1966.

[23] P.Hervieux, "RD-3: an 8 Ghz digital radio system for Canada," Telesis, Bell-Northern Research, pp 53-59, Summer 1975.

[24] A.Lender," The duobinary technique for high speed data transmission," IEEE Trans. Commun.,pp 214-218, May 1963.

[25] Yamamoto,Hirade and Watanabe,"Carrier synchronizer for coherent detection of high speed 4 phase shift keyed signals," IEEE Trans. Commun., vol. COM-20, pp 803-807, August 1972.

[26] Transmission Systems for Communications, Bell telephone laboratory, pp555-565, 1969.

[27] Costas,J.P., "Sunchronous Communications," Proc. IRE, vol.44, ppl713, 1956.

[28] Proakis,J.G.,P.R.Drouilhet,Jr., and R.Price,"Performances of Coherent Detection Systems Using Decision-Directed C annel Measurement," IEEE Trans.on Comm. Syst., vol.CS-12,p.54, 1964.

[29] Gibby,R.A.,and J.W.Smith: Some Extensions of Nyquists Telegraph Transmission Theory,BSTJ, Sept., 1965.

[30] Kretzmer,E.R. : Generalization of a Technique for Binary Data Communication, IEEE Trans. on Comm.Syst.,vol.COM-14,Feb.,1966.

[31] D.P.Taylor, S.S.Haykin and H.C.Chan: Comparative Evaluation of Digital Modulation Techniques, McMaster University, CRL-18 Internal Report Series, April, 1974.

Appendix 2A

This Appendix is to show that $Q(1/\sigma)=1-Q(-1/\sigma)$.

Let $I = 1-Q(-1/\sigma)$

Therefore

$$I = \int_{-\infty}^{\infty} \frac{1}{\sqrt{2\pi}\sigma} \exp(-x^2/2\sigma^2)\,dx$$

$$= \int_{-1}^{\infty} \frac{1}{\sqrt{2\pi}\sigma} \exp(-x^2/2\sigma^2)\,dx$$

$$= \int_{-\infty}^{-1} \frac{1}{\sqrt{2\pi}\sigma} \exp(-x^2/2\sigma^2)\,dx$$

Then let $y=-x$, thus $dy=-dx$ and we obtain

$$I= -\int_{-\infty}^{1} \frac{1}{\sqrt{2\pi}\sigma} \exp(-y^2/2\sigma^2)\,dy$$

$$= \int_{1}^{\infty} \frac{1}{\sqrt{2\pi}\sigma} \exp(-y^2/2\sigma^2)\,dy$$

$$=Q(1/\sigma)$$

Appendix 3A

This Appendix is to evaluate the time averages of the duobinary signal

The duobinary filter impulse response is given as

$$h(t) = \frac{4}{\pi}\left[\frac{\cos(\pi t/2T)}{1 - t^2/T^2}\right] \qquad (3A.1)$$

Consider the pulse stream in the I-channel where h(t-2nT) (n integer) can be written as

$$h(t-2nT) = \frac{4}{\pi}\left[\frac{\cos\frac{\pi(t-2nT)}{2T}}{1 - \frac{(t-2nT)^2}{T^2}}\right] \qquad (3A.2)$$

and is illustrated below:

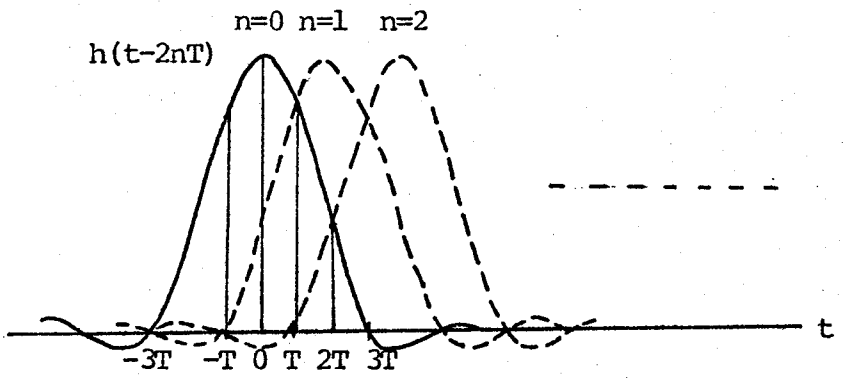

The time average of h(t-2nT) over an interval (t_1, t_2) can be written in a general expression as

$$I_n = \frac{1}{2T}\int_{t_1}^{t_2} h(t-2nT)\,dt$$

$$= \frac{1}{\pi}\left\{\left[\, si\left(\frac{\pi}{2}\left(1+\frac{t-2nT}{T}\right)\right) + si\left(\frac{\pi}{2}\left(\frac{t-2nT}{T} - 1\right)\right)\right]\Bigg|_{t_1}^{t_2}\right\}$$

where

$$si(x) \triangleq Si(x) - \frac{\pi}{2} \triangleq \int_0^x \frac{\sin t}{t}dt - \frac{\pi}{2} \qquad (3A.3)$$

For example , consider the integral $I_n'=\frac{1}{2T}\int_{-T}^{T} h(t-2nT)\,dt$. From equation (3A.3) I_n' can be evaluated as

$$I_n' = \frac{1}{\pi}\{Si[\pi(1-n)]+ Si[\pi(1+n)]\} \qquad (3A.4)$$

Carefully examined the duobinary signal as illustrated in Fig 3A, and from equation (3.11) we can see that

$$I_0' = \frac{1}{2T}\int_{2kT}^{(2k+2)T} h(t-(2k+1)T)\,dt = \frac{1}{\pi}[\,Si(\pi)+Si(\pi)\,]=1.174$$

$$I_1' = \frac{1}{2T}\int_{2kT}^{(2k+2)T} h(t-(2k+3)T)\,dt = \frac{1}{\pi}[Si(0)+Si(2\pi)\,]=0.45$$

$$I_2' = \frac{1}{2T}\int_{2kT}^{(2k+2)T} h(t-(2k+5)T)\,dt = \frac{1}{\pi}[Si(-\pi)+Si(3\pi)\,]=-0.055$$

Similarly I_3', $I_4'\cdots$ can be evaluated from equation (3A.4), but their results are so small that we are not going to present here.

Consider the integral $I_n'' =\frac{1}{2T}\int_{0}^{2T} h(t-2nT)\,dt$. From equation (3A.3) I_n'' can be evaluated as

$$I_n'' = \frac{1}{\pi}\{Si[\tfrac{\pi}{2}(3-2n)] - Si[\tfrac{\pi}{2}(-2n-1)]\} \qquad (3A.5)$$

Again we can see that

$$I_0'' = \frac{1}{2T}\int_{2kT}^{(2k+2)T} h(t-2kT)\,dt = \frac{1}{2T}\int_{2kT}^{(2k+2)T} h(t-(2k+2)T)\,dt$$

$$= \frac{1}{\pi}[\,Si(3\pi/2) - Si(-\pi/2)\,]$$

$$= \frac{1}{\pi}[\,1.608 +1.371\,]$$

$$=0.95$$

Appendix 3B

This appendix is to evaluate the infinite series S where

$$S = \sum_{n=-\infty}^{\infty} \left[\frac{4}{\pi} \frac{(-1)^{k-n}}{1 - 4(k-n)^2} \right]^2$$

The infinite series S can be written as

$$S = \sum_{n=-\infty}^{\infty} \frac{16}{\pi^2} \left[\frac{1}{4n^2-1} \right]^2$$

Thus the infinite series S can be evaluated as

$$S = \frac{16}{\pi^2} \left[1 + 2 \sum_{n=1}^{\infty} \frac{1}{(4n^2-1)^2} \right]$$

$$= \frac{16}{\pi^2} \left[1 + 2\left(\frac{\pi^2}{16} - \frac{1}{2}\right) \right]$$

$$= 2$$

Appendix 3C

This Appendix is to derive the phase error PDF.

In section 3.3, it was shown that $p(\phi)$ could be obtained by solving

$$\frac{d}{d\phi} G(\phi)p(\phi) - \frac{4}{N_0} P(\phi)p(\phi) = C \qquad (3C.1)$$

with

$$P(\phi) = - K K_0 \sin 2\phi$$

$$G(\phi) = 4K_0(2 + \sigma^2)$$

where K is found to be approximately equal 2 and $K_o = K_v(K_1K_m)^2$.

Substituting $P(\phi)$ and $G(\phi)$ in equation (3C.1) we obtain

$$\frac{d}{d\phi} p(\phi) + \frac{4 K K_0 \sin 2\phi}{N_0(8K_0+4K_0\sigma^2)} p(\phi) = \frac{C}{4K_0(2 + \sigma^2)} \qquad (3C.2)$$

Equation (3C.2) is of the form

$$\frac{dy}{dx} + R(x)y = C_1 \qquad (3C.3)$$

The solution of equation (3C.3) is

$$y(x) = [u(x)]^{-1}[\int^x u(s)C_1 ds + C_2] \qquad (3C.4)$$

where

$$[u(x)]^{-1} = \exp[-\int^x R(t)dt]$$

Let

$$U(\phi) = -\int^\phi R(t)dt$$

Comparing the equations (3C.2) and (3C.3) we can evaluate $U(\phi)$ as

$$U(\phi) = - \frac{K}{N_o(2+\sigma^2)} \int^\phi \sin 2t dt = \alpha \cos 2\phi$$

where $\alpha = \frac{K}{N_0(2+\sigma^2)}$ is the loop signal-to-noise ratio.

Using the equation (3C.4), the phase error pdf can be obtained as

$$p(\phi) = \exp[U(\phi)]\left[\int_{-\pi}^{\phi}\exp(-U(s))C_1 ds + C_2\right]$$

$$= N\exp[U(\phi)]\left[D\int_{-\pi}^{\phi}\exp(-U(s))ds + 1\right]$$

Using the boundary condition $p(\pi)=p(-\pi)$ and noting that $U(\pi)=U(-\pi)$ gives

$$p(\phi) = N\exp[U(\phi)]$$

where N is a normalization constant.

Appendix 4A

4A.1 Evaluation of $E(\hat{R}_I D_I|\phi)$ and $E(\hat{R}_Q D_Q|\phi)$.

The conditional expectation $E(\hat{R}_I D_I|\phi)$ is given by the equation (4.21) where

$$E(\hat{R}_I D_I|\phi) = 2 \sum_C D_I \left\{ \sum_D [Pr(\hat{R}_I=2|\phi,C,D) - Pr(\hat{R}_I=-2|\phi,C,D)]Pr(D) \right\} Pr(C) \tag{4A.1}$$

where $\hat{R}_I$, D_I, C, D are defined in equation (4.18).

Equation (4A.1) can be written as

$$E(\hat{R}_I D_I|\phi) = \frac{1}{4} \sum_{j=1}^{8} D_I(C_j) I(C_j) \tag{4A.2}$$

where $$I(C_j) \triangleq \sum_{m=1}^{8} [Pr(\hat{R}_I=2|\phi,C_j,D_m) - Pr(\hat{R}_I=-2|\phi,C_j,D_m)]Pr(D_m) \tag{4A.3}$$

Substitute equation (4.29) into equation (4A.3), $I(C_j)$ can then be written as

$$I(C_j) = \frac{1}{8} \sum_{m=1}^{8} \left[Q\left(\frac{1 - R_{I_j}\cos\phi + D_{Q_m}\sin\phi}{\sigma}\right) - Q\left(\frac{1+R_{I_j}\cos\phi+D_{Q_m}\sin\phi}{\sigma}\right)\right] \tag{4A.4}$$

The evaluation of the conditional expectation $E(\hat{R}_I D_I|\phi)$ in equation (4A.2) result in the expression :

$$E(\hat{R}_I D_I|\phi) = \frac{2}{3\pi}\left[Q\left(\frac{1-2\cos\phi+\frac{20}{3\pi}\sin\phi}{\sigma}\right) - Q\left(\frac{1+2\cos\phi-\frac{20}{3\pi}\sin\phi}{\sigma}\right)\right.$$
$$+ 2\,Q\left(\frac{1-2\cos\phi+\frac{4}{\pi}\sin\phi}{\sigma}\right) - 2\,Q\left(\frac{1+2\cos\phi-\frac{4}{\pi}\sin\phi}{\sigma}\right) + Q\left(\frac{1-2\cos\phi-\frac{4}{3\pi}\sin\phi}{\sigma}\right)$$
$$\left. - Q\left(\frac{1+2\cos\phi+\frac{4}{3\pi}\sin\phi}{\sigma}\right) + Q\left(\frac{1-2\cos\phi+\frac{4}{3\pi}\sin\phi}{\sigma}\right) - Q\left(\frac{1+2\cos\phi-\frac{4}{3\pi}\sin\phi}{\sigma}\right)\right]$$

$$+ 2Q\left(\frac{1-2\cos\phi-\frac{4}{\pi}\sin\phi}{\sigma}\right) - 2Q\left(\frac{1+2\cos\phi+\frac{4}{\pi}\sin\phi}{\sigma}\right) + Q\left(\frac{1-2\cos\phi-\frac{20}{3\pi}\sin\phi}{\sigma}\right)$$

$$-Q\left(\frac{1+2\cos\phi+\frac{20}{3\pi}\sin\phi}{\sigma}\right)] \qquad (4A.5)$$

The conditional expectation $E(\hat{R}_Q D_Q|\phi)$ is given by equation (4.22) where

$$E(\hat{R}_Q D_Q|\phi) = 2\sum_D D_Q \{\sum_C [Pr(\hat{R}_Q=2|\phi,C,D) - Pr(\hat{R}_Q=-2|\phi,C,D)]Pr(C)\}Pr(D) \qquad (4A.6)$$

where $\hat{R}_Q, D_Q, C, D$ are defined in equation (4.18).

Again, the equation (4A.6) can be written as

$$E(\hat{R}_Q D_Q|\phi) = \frac{1}{4}\sum_{j=1}^{8} D_Q(D_j) I(D_j) \qquad (4A.7)$$

where $I(D_j) \triangleq \sum_{m=1}^{8} [Pr(\hat{R}_Q=2|\phi,C_m,D_j) - Pr(\hat{R}_Q=-2|\phi,C_m,D_j)]Pr(C_m)$ (4A.8)

Substituting the equation (4.30) into equation (4A.8), $I(D_j)$ can be written as

$$I(D_j) = \frac{1}{8}\sum_{m=1}^{8} [Q\left(\frac{1-R_{Q_j}\cos\phi - D_{I_m}\sin\phi}{\sigma}\right) - Q\left(\frac{1+R_{Q_j}\cos\phi+D_{I_m}\sin\phi}{\sigma}\right)] \qquad (4A.9)$$

Evaluation of the equation (4A.7) yields the same result as in (4A.5). Thus it is shown in this Appendix that

$$E(\hat{R}_I D_I|\phi) = E(\hat{R}_Q D_Q|\phi)$$

4A.2 Evaluation of $E(\hat{R}_I R_Q|\phi)$ and $E(\hat{R}_Q R_I|\phi)$.

The conditional expectation $E(\hat{R}_I R_Q|\phi)$ is given by the equation (4.19) where

$$E(\hat{R}_I R_Q|\phi) = 2\sum_D R_Q \{ \sum_C [Pr(\hat{R}_I=2|\phi,C,D) - Pr(\hat{R}_I=-2|\phi,C,D)]Pr(C)\}Pr(D) \tag{4A.10}$$

where R_Q, $\hat{R}_I$, C, D are defined in equation (4.18).

Similar to the evaluation in section 4A.1, the conditional expectation $E(\hat{R}_I R_Q|\phi)$ can be written as

$$E(\hat{R}_I R_Q|\phi) = \frac{1}{4}\sum_{j=1}^{8} R_Q(D_j) I(D_j) \tag{4A.11}$$

where $I(D_j) \triangleq \frac{1}{8}\sum [Q(\frac{1-R_{I_m}\cos\phi+D_{Q_j}\sin\phi}{\sigma}) - (\frac{1+R_{I_m}\cos\phi+D_{Q_j}\sin\phi}{\sigma})]$ (4A.12)

Equation (4A.11) can be evaluated as:

$$\begin{aligned}E(\hat{R}_I R_Q|\phi) = \frac{1}{4}[&Q(\frac{1-2\cos\phi+\frac{20}{3\pi}\sin\phi}{\sigma}) - Q(\frac{1+2\cos\phi-\frac{20}{3\pi}\sin\phi}{\sigma}) \\ &+ 2Q(\frac{1+\frac{20}{3\pi}\sin\phi}{\sigma}) - 2Q(\frac{1-\frac{20}{3\pi}\sin\phi}{\sigma}) + Q(\frac{1+2\cos\phi+\frac{20}{3\pi}\sin\phi}{\sigma}) \\ &- Q(\frac{1-2\cos\phi-\frac{20}{3\pi}\sin\phi}{\sigma}) - Q(\frac{1-2\cos\phi-\frac{4}{\pi}\sin\phi}{\sigma}) + Q(\frac{1+2\cos\phi+\frac{4}{\pi}\sin\phi}{\sigma}) \\ &- 2Q(\frac{1-\frac{4}{\pi}\sin\phi}{\sigma}) + 2Q(\frac{1+\frac{4}{\pi}\sin\phi}{\sigma}) - Q(\frac{1+2\cos\phi-\frac{4}{\pi}\sin\phi}{\sigma}) \\ &+ Q(\frac{1-2\cos\phi+\frac{4}{\pi}\sin\phi}{\sigma})]\end{aligned} \tag{4A.13}$$

The evaluation of $E(\hat{R}_Q R_I|\phi)$ is similar to $E(\hat{R}_I R_Q|\phi)$ where $E(\hat{R}_Q R_I|\phi)$ is given by the equation (4.20) as

$$E(\hat{R}_Q R_I|\phi)$$

$$= 2 \sum_C R_I \{ \sum_D [Pr(\hat{R}_Q=2|\phi,C,D) - Pr(\hat{R}_Q=-2|\phi,C,D)]Pr(D)\}Pr(C)$$

where $\hat{R}_Q$, R_I, C, D are defined in equation (4.18). Thus $E(\hat{R}_Q R_I|\phi)$ can be written as

$$E(\hat{R}_Q R_I|\phi) = \frac{1}{4} \sum_{j=1}^{8} R_I(C_j) I(C_j) \qquad (4A.15)$$

where

$$I(C_j) \triangleq \frac{1}{8} \sum_{m=1}^{8} [Q(\frac{1-R_{Q_m}\cos\phi - D_{I_j}\sin\phi}{\sigma}) - Q(\frac{1+R_{Q_m}\cos\phi+D_{I_j}\sin\phi}{\sigma})]$$

Evaluation of equation (4A.15) shows that the result is the negative of the expression shown in (4A.13), thus we have shown that

$$E(\hat{R}_Q R_I|\phi) = - E(\hat{R}_I R_Q|\phi)$$

Appendix 4B

This Appendix is to evaluate the S-curve $G(\phi)$.

The loop phase detector characteristic S-curve $G(\phi)$ is defined in equation (4.13) as

$$G(\phi) = G_1(\phi)\sin\phi + G_2(\phi)\cos\phi \qquad (4B.1)$$

where

$$G_1(\phi) = E[\ (\hat{R}_I D_I + \hat{R}_Q D_Q)\,|\,\phi(t)\ ] \qquad (4B.2)$$

and

$$G_2(\phi) = E[\ (\hat{R}_I R_Q - \hat{R}_Q R_I)\,|\,\phi(t)\ ] \qquad (4B.3)$$

It was shown that $E(\hat{R}_I D_I|\phi)=E(\hat{R}_Q D_Q|\phi)$ and $E(\hat{R}_Q R_I|\phi)=-E(\hat{R}_I R_Q|\phi)$ in Appendix 4A, thus we can write

$$G_1(\phi) = 2E(\hat{R}_I D_I|\phi(t)\ ) \qquad (4B.4)$$

and

$$G_2(\phi) = 2E(\hat{R}_I R_Q|\phi(t)\ ) \qquad (4B.5)$$

Substituting the equations (4A.5) and (4A.13) into equations (4B.4) and (4B.5) respectively, and then the results are substituted into the equation (4B.1), $G(\phi)$ can be obtained as

$$\begin{aligned}
G(\phi) = \frac{4}{3\pi}\sin\phi\ \Big[\ & Q\Big(\frac{1-2\cos\phi+\frac{20}{3\pi}\sin\phi}{\sigma}\Big) - Q\Big(\frac{1+2\cos\phi-\frac{20}{3\pi}\sin\phi}{\sigma}\Big) \\
& + 2Q\Big(\frac{1-2\cos\phi+\frac{4}{\pi}\sin\phi}{\sigma}\Big) - 2Q\Big(\frac{1+2\cos\phi-\frac{4}{\pi}\sin\phi}{\sigma}\Big) + Q\Big(\frac{1-2\cos\phi-\frac{4}{3\pi}\sin\phi}{\sigma}\Big) \\
& - Q\Big(\frac{1+2\cos\phi+\frac{4}{3\pi}\sin\phi}{\sigma}\Big) + 2Q\Big(\frac{1-2\cos\phi-\frac{4}{\pi}\sin\phi}{\sigma}\Big) - 2Q\Big(\frac{1+2\cos\phi+\frac{4}{\pi}\sin\phi}{\sigma}\Big) \\
& + Q\Big(\frac{1-2\cos\phi+\frac{4}{3\pi}\sin\phi}{\sigma}\Big) - Q\Big(\frac{1+2\cos\phi-\frac{4}{3\pi}\sin\phi}{\sigma}\Big) + Q\Big(\frac{1-2\cos\phi-\frac{20}{3\pi}\sin\phi}{\sigma}\Big) \\
& - Q\Big(\frac{1+2\cos\phi+\frac{20}{3\pi}\sin\phi}{\sigma}\Big)\Big] + \frac{\cos\phi}{2}\Big[\ Q\Big(\frac{1-2\cos\phi+\frac{20}{3\pi}\sin\phi}{\sigma}\Big) \\
& - Q\Big(\frac{1+2\cos\phi-\frac{20}{3\pi}\sin\phi}{\sigma}\Big) + 2Q\Big(\frac{1+\frac{20}{3\pi}\sin\phi}{\sigma}\Big) - 2Q\Big(\frac{1-\frac{20}{3\pi}\sin\phi}{\sigma}\Big)
\end{aligned}$$

$$+ Q\left(\frac{1+2\cos\phi+ \frac{20}{3\pi}\sin\phi}{\sigma}\right) - Q\left(\frac{1-2\cos\phi- \frac{20}{3\pi}\sin\phi}{\sigma}\right)$$

$$+ Q\left(\frac{1+2\cos\phi+ \frac{4}{\pi}\sin\phi}{\sigma}\right) - Q\left(\frac{1-2\cos\phi- \frac{4}{\pi}\sin\phi}{\sigma}\right) + 2Q\left(\frac{1+ \frac{4}{\pi}\sin\phi}{\sigma}\right)$$

$$- 2Q\left(\frac{1- \frac{4}{\pi}\sin\phi}{\sigma}\right) + Q\left(\frac{1-2\cos\phi+ \frac{4}{\pi}\sin\phi}{\sigma}\right) - Q\left(\frac{1+2\cos\phi- \frac{4}{\pi}\sin\phi}{\sigma}\right)$$

(4B.6)

Appendix 4C

This Appendix is to evaluate the noise function $H(\phi)$

4C.1 Evaluation of $E(\hat{R}_I^2|\phi)$ and $E(\hat{R}_Q^2|\phi)$

The conditional expectation $E(\hat{R}_I^2|\phi)$ is given by the equation (4.23) as

$$E(\hat{R}_I^2|\phi) = 4 \sum_D \{ \sum_C [Pr(\hat{R}_I=2|\phi,C,D) + Pr(\hat{R}_I=-2|\phi,CD)]Pr(C)\} Pr(D) \tag{4C.1}$$

where $\hat{R}_I$, C and D are defined in equation (4.18).

Similar to the section 4A.2, equation (4C.1) can be written as

$$E(\hat{R}_I^2|\phi) = \frac{1}{2} \sum_{j=1}^{8} I(D_j) \tag{4C.2}$$

where $I(D_j)$ is defined in equation (4A.12) Similarly, $E(\hat{R}_Q^2|\phi)$ can be written as

$$E(\hat{R}_Q^2|\phi) = \frac{1}{2} \sum_{j=1}^{8} I(C_j) \tag{4C.3}$$

where $I(C_j)$ is defined in equation (4A.16).

Thus $E(\hat{R}_I^2|\phi)$ can be evaluated from equation (4C.2) as

$$\begin{aligned}
E(\hat{R}_I^2|\phi) = \frac{1}{4} \{ & Q\left(\frac{1-2\cos\phi+\frac{20}{3\pi}\sin\phi}{\sigma}\right) + Q\left(\frac{1+2\cos\phi+\frac{20}{3\pi}\sin\phi}{\sigma}\right) \\
& + Q\left(\frac{1-2\cos\phi-\frac{20}{3\pi}\sin\phi}{\sigma}\right) + Q\left(\frac{1+2\cos\phi+\frac{20}{3\pi}\sin\phi}{\sigma}\right) + Q\left(\frac{1-2\cos\phi-\frac{4}{3\pi}\sin\phi}{\sigma}\right) \\
& + Q\left(\frac{1+2\cos\phi+\frac{4}{3\pi}\sin\phi}{\sigma}\right) + Q\left(\frac{1-2\cos\phi+\frac{4}{3\pi}\sin\phi}{\sigma}\right) + Q\left(\frac{1+2\cos\phi-\frac{4}{3\pi}\sin\phi}{\sigma}\right) \\
& + 2\left[Q\left(\frac{1-2\cos\phi-\frac{4}{\pi}\sin\phi}{\sigma}\right) + Q\left(\frac{1+2\cos\phi+\frac{4}{\pi}\sin\phi}{\sigma}\right) + Q\left(\frac{1-2\cos\phi-\frac{4}{\pi}\sin\phi}{\sigma}\right)\right. \\
& \left. + Q\left(\frac{1+2\cos\phi+\frac{4}{\pi}\sin\phi}{\sigma}\right)\right]\} + \left[Q\left(\frac{1+\frac{20}{3\pi}\sin\phi}{\sigma}\right) + Q\left(\frac{1-\frac{20}{3\pi}\sin\phi}{\sigma}\right)\right. \\
& \left. + Q\left(\frac{1+\frac{4}{3\pi}\sin\phi}{\sigma}\right) + Q\left(\frac{1-\frac{4}{3\pi}\sin\phi}{\sigma}\right) + 2Q\left(\frac{1+\frac{4}{\pi}\sin\phi}{\sigma}\right) + 2Q\left(\frac{1-\frac{4}{\pi}\sin\phi}{\sigma}\right)\right]
\end{aligned} \tag{4C.4}$$

The conditional expectation $E(\hat{R}_Q^2|\phi)$ can be evaluated in the same manner, and the result is the same as the expression shown in equation (4C.4). Thus we have shown in this Appendix that

$$E(\hat{R}_I^2|\phi) = E(\hat{R}_Q^2|\phi)$$

4C.2 Evaluation of $H(\phi)$

$H(\phi)$ is defined in equation (4.11) as

$$H(\phi) = E(\hat{R}_I^2|\phi) + E(\hat{R}_Q^2|\phi) \qquad (4C.5)$$

Since we have shown that $E(\hat{R}_I^2|\phi)=E(\hat{R}_Q^2|\phi)$, therefore

$$H(\phi) = 2E(\hat{R}_I^2|\phi)$$

where $E(\hat{R}_I^2|\phi)$ is defined in equation (4C.4)

Appendix 5A

This Appendix is to evaluate the conditional expectations $E(\hat{c}_k c_k|\phi)$ and $E(\hat{c}_k c_{k+1}|\phi)$.

The conditional expectation $E(\hat{c}_k c_k|\phi)$ is given by equation(5.12) as

$$E(\hat{c}_k c_k|\phi) = \sum_C c_k \{ \sum_D [Pr(\hat{c}_k=1|\phi,C,D) - Pr(\hat{c}_k=-1|\phi,C,D)]Pr(D) \}Pr(C) \tag{5A.1}$$

where we defined the sets

$$D=\{d_k,\ d_{k-1}\} \qquad \text{and} \qquad C=\{c_k,\ c_{k+1},\ c_{k-1}\}$$

in section 5.1.3 . Using the result in equation (5.17) for $Pr(\hat{c}_k=1|\phi,C,D) - Pr(\hat{c}_k=-1|\phi,C,D)$, and similar to the evaluation procedure as shown in Appendix 4A, $E(\hat{c}_k c_k|\phi)$ is found as

$$\begin{aligned} E(\hat{c}_k c_k|\phi) = \frac{1}{8}[\ 8 &- Q\left(\frac{\frac{20}{3\pi}\cos\phi - 2\sin\phi}{\sigma}\right) - Q\left(\frac{\frac{20}{3\pi}\cos\phi}{\sigma}\right) - Q\left(\frac{\frac{20}{3\pi}\cos\phi+2\sin\phi}{\sigma}\right) \\ &- 2Q\left(\frac{\frac{4}{\pi}\cos\phi - 2\sin\phi}{\sigma}\right) - 2Q\left(\frac{\frac{4}{\pi}\cos\phi}{\sigma}\right) - 2Q\left(\frac{\frac{4}{\pi}\cos\phi+2\sin\phi}{\sigma}\right) \\ &- Q\left(\frac{\frac{4}{3\pi}\cos\phi-2\sin\phi}{\sigma}\right) - 2Q\left(\frac{\frac{4}{3\pi}\cos\phi}{\sigma}\right) - Q\left(\frac{\frac{4}{3\pi}\cos\phi+2\sin\phi}{\sigma}\right)\ ] \end{aligned} \tag{5A.2}$$

Similarly, we can evlauate the conditional expectation $E(\hat{c}_k c_{k+1}|\phi)$ as

$$E(\hat{c}_k c_{k+1}|\phi) = \sum_C c_{k+1} \{ \sum_D [Pr(\hat{c}_k=1|\phi,C,D) - Pr(\hat{c}_k=-1|\phi,C,D)]Pr(D) \}Pr(C)$$

$$= \frac{1}{8}\left[-Q\left(\frac{\frac{20}{3\pi}\cos\phi-2\sin\phi}{\sigma}\right) - 2Q\left(\frac{\frac{20}{3\pi}\cos\phi}{\sigma}\right) - Q\left(\frac{\frac{20}{3\pi}\cos\phi+2\sin\phi}{\sigma}\right)\right.$$

$$\left. + Q\left(\frac{\frac{4}{3\pi}\cos\phi-2\sin\phi}{\sigma}\right) + Q\left(\frac{\frac{4}{3\pi}\cos\phi}{\sigma}\right) + Q\left(\frac{\frac{4}{3\pi}\cos\phi+2\sin\phi}{\sigma}\right)\right]$$

(5A.3)

Therefore the summation of equations(5A.2) and (5A.3) can be shown as

$$E(\hat{c}_k c_k|\phi)+E(\hat{c}_k c_{k+1}|\phi)$$

$$= 1 - \frac{1}{4}Q\left(\frac{\frac{20}{3\pi}\cos\phi-2\sin\phi}{\sigma}\right) - \frac{1}{2}Q\left(\frac{\frac{20}{3\pi}\cos\phi}{\sigma}\right) - \frac{1}{4}Q\left(\frac{\frac{20}{3\pi}\cos\phi+2\sin\phi}{\sigma}\right)$$

$$- \frac{1}{4}Q\left(\frac{\frac{4}{\pi}\cos\phi-2\sin\phi}{\sigma}\right) - \frac{1}{2}Q\left(\frac{\frac{4}{\pi}\cos\phi}{\sigma}\right) - \frac{1}{4}Q\left(\frac{\frac{4}{\pi}\cos\phi+2\sin\phi}{\sigma}\right)$$

(5A.4)

Appendix 5B

5B.1 Show that $E[\hat{c}_k(c_k+c_{k+1})|\phi] = E[\hat{d}_k(d_k+d_{k-1})|\phi]$.

The conditional expectation $E(\hat{c}_k c_k|\phi)$, similar to the evaluation in Appendix 4A, can be expressed as

$$E(\hat{c}_k c_k|\phi) = \frac{1}{8}\sum_{j=1}^{8} c_k(j)I(j) \tag{5B.1}$$

where $I(j) \triangleq \frac{1}{2}\sum_{m=1}^{2}[\Pr(\hat{c}_k=1|\phi,C_j,D_m) - \Pr(\hat{c}_k=-1|\phi,C_j,D_m)]$ (5B.2)

Simlarly, we obtain

$$E(\hat{c}_k c_{k+1}|\phi) = \frac{1}{8}\sum_{j=1}^{8} c_{k+1}(j)I(j) \tag{5B.3}$$

where I(j) is defined in equation (5B.2), and the sets C and D are defined in section 5.1.3.

From equation (5.18), $E(\hat{d}_k d_k|\phi)$ can be evaluated as

$$E(\hat{d}_k d_k|\phi) = \frac{1}{8}\sum_{j=1}^{8} d_k(j)I'(j) \tag{5B.4}$$

where $I'(j) \triangleq \frac{1}{2}\sum_{m=1}^{2}[\Pr(\hat{d}_k=1|\phi,C'_m,D'_j) - \Pr(\hat{d}_k=-1|\phi,C'_m,D'_j)]$ (5B.5)

Similarly, we obtain

$$E(\hat{d}_k d_{k-1}|\phi) = \frac{1}{8}\sum_{j=1}^{8} d_{k-1}(j)I'(j) \tag{5B.6}$$

where I'(j) is defined in equation (5B.5) and the sets C' and D' are defined in section 5.1.3.

Comparing the results as evaluated from equations (5B.1), (5B.3), (5B.4), and (5B.6), we can see that

$$E(\hat{c}_k c_k|\phi) = E(\hat{d}_k d_k|\phi)$$

and

$$E(\hat{c}_k c_{k+1}|\phi) = E(\hat{d}_k d_{k-1}|\phi)$$

Thus we have shown in this Appendix that $E[\hat{c}_k(c_k+c_{k+1})|\phi] = E[\hat{d}_k(d_k+d_{k-1})|\phi]$

5B.2 This section is to show that $E[(\hat{c}_k d_k + \hat{c}_k d_{k-1})|\phi] = -E[(c_k \hat{d}_k + c_{k+1}\hat{d}_k)|\phi]$

From equation (5.24), the conditional expectation $E(\hat{c}_k d_k|\phi)$ can be obtained as

$$E(\hat{c}_k d_k|\phi) = \frac{1}{2}\sum_{j=1}^{2} d_k(j)M(j) \tag{5B.7}$$

where $M(j) \triangleq \frac{1}{8}\sum_{m=1}^{8}[\Pr(\hat{c}_k=1|\phi,C_m,D_j) - \Pr(\hat{c}_k=-1|\phi,C_m,D_j)]$ (5B.8)

Similarly, the conditional expectation $E(\hat{c}_k d_{k-1}|\phi)$ can be obtained from equation (5.25) as

$$E(\hat{c}_k d_{k-1}|\phi) = \frac{1}{2}\sum_{j=1}^{2} d_{k-1}(j)M(j) \tag{5B.9}$$

where M(j) is defined in equation (5B.8).

From equations (5.26) and (5.27), the conditional expectations $E(c_k\hat{d}_k|\phi)$ and $E(c_{k+1}\hat{d}_k|\phi)$ can be expressed as follows:

$$E(c_k\hat{d}_k|\phi) = \frac{1}{2}\sum_{j=1}^{2} c_k(j)M'(j) \tag{5B.10}$$

and

$$E(c_{k+1}\hat{d}_k|\phi) = \frac{1}{2}\sum_{j=1}^{2} c_{k+1}(j)M'(j) \tag{5B.11}$$

where $M'(j) = \frac{1}{8}\sum_{m=1}^{8}[\Pr(\hat{d}_k=1|\phi,C'_j,D'_m) - \Pr(\hat{d}_k=-1|\phi,C'_j,D'_m)]$ (5B.12)

Again, the results show that

$$E(\hat{c}_k d_k|\phi) = -E(c_k\hat{d}_k|\phi) \quad \text{and} \quad E(\hat{c}_k d_{k-1}|\phi) = -E(c_{k+1}\hat{d}_k|\phi)$$

Thus we have shown in this section that

$$E[(\hat{c}_k d_k + \hat{c}_k d_{k-1})|\phi] = -E[(c_k\hat{d}_k + c_{k+1}\hat{d}_k)|\phi]$$

Appendix 5C

This Appendix is to evaluate $G_1(\phi)$, $G_2(\phi)$ and $G(\phi)$.

5C.1 Evaluation of $G_1(\phi)$.

From equation (5.11), $G_1(\phi)$ is defined as

$$G_1(\phi) = E[\hat{c}_k(c_k+c_{k+1}) + \hat{d}_k(d_k+d_{k-1})\,|\,\phi]$$

Since we have shown that $E[\hat{c}_k(c_k+c_{k+1})\,|\,\phi]$ is equal to $E[\hat{d}_k(d_k+d_{k-1})\,|\,\phi]$, thus $G_1(\phi)$ can be evaluated as

$$\begin{aligned} G_1(\phi) &= 2\,E[(\hat{c}_k c_k+\hat{c}_k c_{k+1})\,|\,\phi] \\ &= 2 - \frac{1}{2}Q\left(\frac{\frac{20}{3\pi}\cos\phi-2\sin\phi}{\sigma}\right) - Q\left(\frac{\frac{20}{3\pi}\cos\phi}{\sigma}\right) + \frac{1}{2}Q\left(\frac{\frac{20}{3\pi}\cos\phi+2\sin\phi}{\sigma}\right) \\ &\quad - \frac{1}{2}Q\left(\frac{\frac{4}{\pi}\cos\phi-2\sin\phi}{\sigma}\right) - Q\left(\frac{\frac{4}{\pi}\cos\phi}{\sigma}\right) - \frac{1}{2}Q\left(\frac{\frac{4}{\pi}\cos\phi+2\sin\phi}{\sigma}\right) \end{aligned} \tag{5C.1}$$

5C.2 Evaluation of $G_2(\phi)$.

From equation (5.13), $G_2(\phi)$ is defined as

$$G_2(\phi) = \frac{4}{\pi}[E(\hat{c}_k d_k\,|\,\phi) + \frac{1}{3}E(\hat{c}_k d_{k-1}\,|\,\phi) - E(c_k\hat{d}_k\,|\,\phi) - \frac{1}{3}E(\hat{d}_k c_{k+1}\,|\,\phi)]$$

Since $E(\hat{c}_k d_k\,|\,\phi) = -E(c_k\hat{d}_k\,|\,\phi)$ and $E(\hat{c}_k d_{k-1}\,|\,\phi) = -E(c_{k+1}\hat{d}_k\,|\,\phi)$, which have been shown in Appendix 5B.2, thus $G_2(\phi)$ can be evaluated as

$$\begin{aligned} G_2(\phi) &= \frac{8}{\pi}[\,E(\hat{c}_k d_k\,|\,\phi) + \frac{1}{3}E(\hat{c}_k d_{k-1}\,|\,\phi) \\ &= \frac{4}{3\pi}[\,Q\left(\frac{\frac{20}{3\pi}\cos\phi+2\sin\phi}{\sigma}\right) + 2Q\left(\frac{\frac{4}{\pi}\cos\phi+2\sin\phi}{\sigma}\right) + Q\left(\frac{\frac{4}{3\pi}\cos\phi+2\sin\phi}{\sigma}\right) \\ &\quad - Q\left(\frac{\frac{20}{3\pi}\cos\phi-2\sin\phi}{\sigma}\right) - 2Q\left(\frac{\frac{4}{\pi}\cos\phi-2\sin\phi}{\sigma}\right) - Q\left(\frac{\frac{4}{3\pi}\cos\phi-2\sin\phi}{\sigma}\right)] \end{aligned} \tag{5C.2}$$

5C.3 Evaluation of $G(\phi)$.

From equation (5.10), $G(\phi)$ is defined as

$$G(\phi) = G_1(\phi)\sin\phi + G_2(\phi)\cos\phi \tag{5C.3}$$

Substituting the equations (5C.1) and (5C.2) into (5C.4), we obtain

$$\begin{aligned} G(\phi) &= \sin\phi\Big[\, 2 - \frac{1}{2}Q\Big(\frac{\frac{20}{3\pi}\cos\phi - 2\sin\phi}{\sigma}\Big) - Q\Big(\frac{\frac{20}{3\pi}\cos\phi}{\sigma}\Big) - \frac{1}{2}Q\Big(\frac{\frac{20}{3\pi}\cos\phi + 2\sin\phi}{\sigma}\Big) \\ &\quad - \frac{1}{2}Q\Big(\frac{\frac{4}{\pi}\cos\phi + 2\sin\phi}{\sigma}\Big) - \frac{1}{2}Q\Big(\frac{\frac{4}{\pi}\cos\phi - 2\sin\phi}{\sigma}\Big) - Q\Big(\frac{\frac{4}{\pi}\cos\phi}{\sigma}\Big)\Big] \\ &\quad + \frac{4}{3}\cos\Big[Q\Big(\frac{\frac{20}{3\pi}\cos\phi + 2\sin\phi}{\sigma}\Big) + 2Q\Big(\frac{\frac{4}{\pi}\cos\phi + 2\sin\phi}{\sigma}\Big) + Q\Big(\frac{\frac{4}{3\pi}\cos\phi + 2\sin\phi}{\sigma}\Big) \\ &\quad - Q\Big(\frac{\frac{20}{3\pi}\cos\phi - 2\sin\phi}{\sigma}\Big) - 2Q\Big(\frac{\frac{4}{\pi}\cos\phi - 2\sin\phi}{\sigma}\Big) - Q\Big(\frac{\frac{4}{3\pi}\cos\phi - 2\sin\phi}{\sigma}\Big)\Big] \end{aligned} \tag{5C.4}$$

Appendix 5D

This Appendix is to evaluate the conditional expectation $E(\hat{R}_I R_I|\phi)$ and to show that $E(\hat{R}_I R_I|\phi) = E(\hat{R}_Q R_Q|\phi)$.

5D.1 Evaluation of $E(\hat{R}_I R_I|\phi)$

From equation (5.28), the conditional expectation $E(\hat{R}_I R_I|\phi)$ is given as

$$E(\hat{R}_I R_I|\phi) = 2 \sum_C R_I \{ \sum_D [Pr(\hat{R}_I=2|\phi,C,D) - Pr(\hat{R}_I=-2|\phi,C,D)]Pr(D) \}Pr(C) \tag{5D.1}$$

where C, D, R_I and $\hat{R}_I$ are defined in equation (4.18).

Equation (5D.1) can be written as

$$E(\hat{R}_I R_I|\phi) = \frac{1}{4} \sum_{j=1}^{8} R_I(C_j) I(C_j) \tag{5D.2}$$

where $I(C_j)$ is defined in equation (4A.3).

Evaluation of the equation (5D.2) yields

$$\begin{aligned} E(\hat{R}_I R_I|\phi) = \frac{1}{4} [& Q\left(\frac{1-2\cos\phi+\frac{20}{3\pi}\sin\phi}{\sigma}\right) - Q\left(\frac{1+2\cos\phi-\frac{20}{3\pi}\sin\phi}{\sigma}\right) + Q\left(\frac{1-2\cos\phi+\frac{4}{\pi}\sin\phi}{\sigma}\right) \\ & - 2Q\left(\frac{1+2\cos\phi-\frac{4}{\pi}\sin\phi}{\sigma}\right) + Q\left(\frac{1-2\cos\phi+\frac{4}{3\pi}\sin\phi}{\sigma}\right) - Q\left(\frac{1+2\cos\phi-\frac{4}{3\pi}\sin\phi}{\sigma}\right) \\ & + Q\left(\frac{-2\cos\phi-\frac{20}{3\pi}\sin\phi}{\sigma}\right) - Q\left(\frac{1+2\cos\phi+\frac{20}{3\pi}\sin\phi}{\sigma}\right) + 2Q\left(\frac{1-2\cos\phi-\frac{4}{\pi}\sin\phi}{\sigma}\right) \\ & - 2Q\left(\frac{1+2\cos\phi+\frac{4}{\pi}\sin\phi}{\sigma}\right) + Q\left(\frac{1-2\cos\phi-\frac{4}{3\pi}\sin\phi}{\sigma}\right) - Q\left(\frac{1+2\cos\phi+\frac{4}{3\pi}\sin\phi}{\sigma}\right)] \end{aligned} \tag{5D.3}$$

5D.2 Show that $E(\hat{R}_I R_I|\phi) = E(\hat{R}_Q R_Q|\phi)$

From equation (5.29), the conditional expectation $E(\hat{R}_Q R_Q|\phi)$ is given as

$$E(\hat{R}_Q R_Q|\phi)$$
$$= 2 \sum_D R_Q \{ \sum_C [Pr(\hat{R}_Q=2|\phi,C,D) - Pr(\hat{R}_Q=-2|\phi,C,D)]Pr(C)\}Pr(D) \tag{5D.4}$$

where C,D,R_Q, and R_Q are defined in equation (4.18).

Again, Equation (5D.4) can be written as

$$E(\hat{R}_Q R_Q|\phi) = \frac{1}{4} \sum_{j=1}^{8} R_Q(D_j) I(D_j) \tag{5D.5}$$

where $I(D_j)$ is defined in equation (4A.9). The evaluation of (5D.5) thus shows that

$$E(\hat{R}_I R_I|\phi) = E(\hat{R}_Q R_Q|\phi)$$

Appendix 5E.

This Appendix is to evaluate $E(\hat{R}_I D_Q|\phi)$ and to show that $E(\hat{R}_Q D_I|\phi) = -E(\hat{R}_I D_Q|\phi)$

5E.1 Evaluation of $E(\hat{R}_I D_Q|\phi)$

From equation (5.30), The conditional expectation $E(\hat{R}_I D_Q|\phi)$ can be written as

$$E(\hat{R}_I D_Q|\phi) = 2\sum_{j=1}^{8} D_Q(D_j) I(D_j) \qquad (5E.1)$$

where $I(D_j)$ is defined in equation (4A.9).

Thus, from equation (5E.1), $E(\hat{R}_I D_Q|\phi)$ can be evaluated as

$$\begin{aligned}
&E(\hat{R}_I D_Q|\phi) \\
&= \frac{4}{32}\Bigg\{ \frac{20}{3\pi}\Bigg[Q\left(\frac{1-2\cos\phi+\frac{20}{3\pi}\sin\phi}{\sigma}\right) - Q\left(\frac{1+2\cos\phi-\frac{20}{3\pi}\sin\phi}{\sigma}\right) \\
&+ Q\left(\frac{1+2\cos\phi+\frac{20}{3\pi}\sin\phi}{\sigma}\right) - Q\left(\frac{1-2\cos\phi-\frac{20}{3\pi}\sin\phi}{\sigma}\right)\Bigg] + \frac{8}{\pi}\Bigg[Q\left(\frac{1-2\cos\phi+\frac{4}{\pi}\sin\phi}{\sigma}\right) \\
&- Q\left(\frac{1+2\cos\phi-\frac{4}{\pi}\sin\phi}{\sigma}\right) + Q\left(\frac{1+2\cos\phi+\frac{4}{\pi}\sin\phi}{\sigma}\right) - Q\left(\frac{1-2\cos\phi-\frac{4}{\pi}\sin\phi}{\sigma}\right)\Bigg] \\
&+ \frac{4}{3\pi}\Bigg[Q\left(\frac{1-2\cos\phi+\frac{4}{3\pi}\sin\phi}{\sigma}\right) - Q\left(\frac{1+2\cos\phi-\frac{4}{3\pi}\sin\phi}{\sigma}\right) \\
&+ Q\left(\frac{1+2\cos\phi+\frac{4}{3\pi}\sin\phi}{\sigma}\right) \quad Q\left(\frac{1-2\cos\phi-\frac{4}{3\pi}\sin\phi}{\sigma}\right)\Bigg]
\end{aligned} \qquad (5E.2)$$

5E.2 Show that $E(\hat{R}_Q D_I|\phi) = -E(\hat{R}_I D_Q|\phi)$

The conditional expectation $E(\hat{R}_Q D_I|\phi)$ given in equation (5.31) can be written as

$$E(\hat{R}_Q D_I|\phi) = 2\sum_{j=1}^{8} D_I(C_j) I(C_j) \qquad (5E.3)$$

where $I(C_j)$ is defined in equation (4A.3). The result of evaluating the equation (5E.3) shows that $E(\hat{R}_Q D_I|\phi)$ is equal to $-E(\hat{R}_I D_Q|\phi)$

Appendix 5F

This Appendix is to evaluate $G(\phi)$ for the half-shifted loop structure.

From Equation (5.25), $G(\phi)$ is given as

$$G(\phi) \triangleq G_1(\phi)\sin\phi + G_2(\phi)\cos\phi \tag{5F.1}$$

where

$$G_1(\phi) \triangleq E[(\hat{R}_I R_I + \hat{R}_Q R_Q)|\phi] \tag{5F.2}$$

and

$$G_2(\phi) \triangleq E[(\hat{R}_I D_Q - \hat{R}_Q D_I)|\phi] \tag{5F.3}$$

Since we have shown that $D(\hat{R}_I R_I|\phi) = E(\hat{R}_Q R_Q|\phi)$ as in Appendix 5D, thus $G_1(\phi)$ can be evaluated as

$$\begin{aligned} G_1(\phi) &= 2E(\hat{R}_I R_I|\phi) \\ &= 0.5\ [\ Q\left(\frac{1-2\cos\phi+\frac{20}{3\pi}\sin\phi}{\sigma}\right) - Q\left(\frac{1+2\cos\phi-\frac{20}{3\pi}\sin\phi}{\sigma}\right) \\ &\quad +2Q\left(\frac{1-2\cos\phi+\frac{4}{\pi}\sin\phi}{\sigma}\right) -2Q\left(\frac{1+2\cos\phi-\frac{4}{\pi}\sin\phi}{\sigma}\right)+Q\left(\frac{1-2\cos\phi+\frac{4}{3\pi}\sin\phi}{\sigma}\right) \\ &\quad - Q\left(\frac{1+2\cos\phi+\frac{20}{3\pi}\sin\phi}{\sigma}\right)+ Q\left(\frac{1-2\cos\phi-\frac{20}{3\pi}\sin\phi}{\sigma}\right) \\ &\quad -Q\left(\frac{1+2\cos\phi+\frac{20}{3\pi}\sin\phi}{\sigma}\right) + 2Q\left(\frac{1-2\cos\phi-\frac{4}{\pi}\sin\phi}{\sigma}\right) \\ &\quad - 2Q\left(\frac{1+\cos\phi+\frac{4}{\pi}\sin\phi}{\sigma}\right) + Q\left(\frac{1-2\cos\phi-\frac{4}{3\pi}\sin\phi}{\sigma}\right) \\ &\quad - Q\left(\frac{1+2\cos\phi+\frac{4}{3\pi}\sin\phi}{\sigma}\right)\ ] \end{aligned} \tag{5F.4}$$

In Appendix 5E, we have shown that $E(\hat{R}_I D_Q|\phi) = -E(\hat{R}_Q D_I|\phi)$, therefore $G_2(\phi)$ can be evaluated as

$$\begin{aligned} G_2(\phi) &= 2E(\hat{R}_I D_Q|\phi) \\ &= 0.25\ \{\ \ \frac{20}{3\pi}\ [\ Q\left(\frac{1-2\cos\phi+\frac{20}{3\pi}\sin\phi}{\sigma}\right) - Q\left(\frac{1+2\cos\phi-\frac{20}{3\pi}\sin\phi}{\sigma}\right) \end{aligned}$$

$$+ Q\left(\frac{1+2\cos\phi+ \frac{20}{3\pi}\sin\phi}{\sigma}\right) - Q\left(\frac{1-2\cos\phi- \frac{20}{3\pi}\sin\phi}{\sigma}\right)]$$

$$+ \frac{8}{\pi}\left[Q\left(\frac{1-2\cos\phi+ \frac{4}{\pi}\sin\phi}{\sigma}\right) - Q\left(\frac{1-2\cos\phi- \frac{4}{\pi}\sin\phi}{\sigma}\right)\right.$$

$$\left. + Q\left(\frac{1+2\cos\phi+ \frac{4}{\pi}\sin\phi}{\sigma}\right) - Q\left(\frac{1-2\cos\phi- \frac{4}{\pi}\sin\phi}{\sigma}\right)\right]$$

$$+ \frac{4}{3\pi}\left[Q\left(\frac{1-2\cos\phi+ \frac{4}{3\pi}\sin\phi}{\sigma}\right) - Q\left(\frac{1+2\cos\phi- \frac{4}{3\pi}\sin\phi}{\sigma}\right)\right.$$

$$\left. +Q\left(\frac{1+2\cos\phi+ \frac{4}{3\pi}\sin\phi}{\sigma}\right) - Q\left(\frac{1-2\cos\phi- \frac{4}{3\pi}\sin\phi}{\sigma}\right)\right]\}$$

(5F.5)

Therefore

$$G(\phi) = G_1(\phi)\sin\phi + G_2(\phi)\cos\phi$$

where $G_1(\phi)$ is defined in equation (5F.4) and $G_2(\phi)$ is defined in equation (5F.5).